Theses and Dissertations   Graduate School

2014

Platinum Complexes and Zinc Finger Proteins: From Target Recognition to Fixation

Samantha Tsotsoros
Virginia Commonwealth University

Platinum Complexes and Zinc Finger Proteins: From Target Recognition to Fixation

A Dissertation submitted in partial fulfillment of the requirements for the degree of Ph.D.
at Virginia Commonwealth University

by

Samantha D. Tsotsoros
B.Sc. in Chemistry, Christopher Newport University, 2009

Advisor: Dr. Nicholas P. Farrell
Professor, Department of Chemistry, College of Humanities and Sciences,
Virginia Commonwealth University

Virginia Commonwealth University
Richmond, Virginia
May 2014

Acknowledgments

The work that comprises this dissertation is the direct result of the contributions of many individuals. To my family, I can never express enough gratitude for their love and support throughout the years. I would not have been able to acomplish what I have without them. To my best friend and partner, Rachel, there are no words. You got me through even the most difficult days bearable. My best childhood friend, Christina, for the many phone calls and encouragement that helped keep me going. I give a special thanks to Dr. Nicholas Farrell for giving me the opportunity to grow and learn while working on an interesting project and for being patient with me throughout the process. My committee members for their time and input. Dr. Yun Qu for all of her guidance and assistance with NMR projects. Dr. Turner for all of his help with the various instruments in the department, but especially for his help with the ICP-MS. Past and present group members of the Farrell Lab; Sarah Spell, Daniel Lee, Ralph Kipping, Queite dePaula and Erica Peterson for their guidance and assistance. I would also like to thank the National Science Foundation and Altria for providing the financial means to complete my work.

Contents

List of Figures

List of Tables

List of Schemes

List of Abbreviations

1MeCyt	1-methylcytosine
4-pic	4-picoline
5'-GMP	5'-guanosine monophosphate
9-EtGua	9-ethylguanine
9-MeGua	9-methylguanine
A	adenine
A2780	human ovarian carcinoma
ADA	azodicarbonamide
AgCl	silver chloride
$AgNO_3$	silver nitrate
AIDS	Acquired Immunodeficiency Syndrome
Ala	alanine
Arg	arginine
As	arsenic
Au	gold
bipy	2,2'-bipyridine
bme-dach	N,N'-bis(2-mercaptoethyl)-1,4-diazocycloheptane
bpy	2,2'-bipyridine
bztz	benzothiazole
C	carbon
C	cytosine

C_2H_2	cysteine$_2$histidine$_2$
C_3H	cysteine$_3$histidine
C_4	cysteine$_4$
CACG	N-acetyl-glycine-alanine-cysteine-glycine
CC$_{50}$	dose necessary to kill 50% of cells
CCHC	cysteine, cysteine, histidine, cysteine
Cd	cadmium
CD	circular dichroism
CD4	cluster of differentiation 4
cDDP	*cis*-diamminodichloroplatinum(II)
CID	Collision Induced Dissociation
Cl	chloride
CMP	5'-cytosine monophosphate
CNpyr	cyanopyridine
Co	cobalt
Co-sb	cobalt Schiff base
COD	cyclooctadiene
CT	Calf Thymus
CWCK	cysteine-tryptophan-cysteine-lysine
Cys	cysteine
Cyt	cytosine
D_2O	deuterium oxide
DFT	Density Functional Theory
DIBA-1	2,2'-dithiobenzamide-1
dien	diethylenetriamine
DMAP	4-dimethylaminopyridine

DMF	dimethyl formamide
DNA	deoxyribonucleic acid
ds	double-stranded
EC_{50}	dose necessary to inhibit 50% of viral activity
EMT	epitheial-to-mesenchymal transitions
en	ethylenediamine
EPV	Epstein-Barr virus
ESI	electrospray ionization
Et	ethyl
EtBr	ethidium bromide
F	apo-NCp7
FDA	Food and Drug Administration
Flc	fluoroscein
FTICRMS	Fourier Transform Ion Cyclotron Mass Spectrometry
G	glycine
G	guanine
GAG	group-specific antigen
GAMG	N-acetyl-glycine-alanine-methionine-glycine
Gln	glutamine
Glu	glutamic acid
Gly	glycine
GS	glutathione
GSH	glutathione
Gua	guanine
GWCG	N-acetyl-glycine-tryptophan-cysteine-glycine
GWMG	N-acetyl-glycine-tryptophan-methionine-glycine

H	hydrogen
H_2O	water
HAART	Highly Active Antiretroviral Therapy
HBr	hydrobromic acid
HCl	hydrochloric acid
HCMV	human cytomegalo virus
HCT-116	human colon carcinoma
His	histidine
HIV1	Human Immunodeficiency Virus Type 1
HMG	high mobility group proteins
HOMO	Highest Occupied Molecular Orbital
HSA	human serum albumin
HSQC	heteronuclear single quantum coherence
HSV-1	herpes simplex virus-1
HSV-2	herpes simplex virus-2
K	lysine
K_2PtCl_4	potassium tetrachloroplatinate(II)
K_2PtCl_6	potassium hexachloroplatinate(IV)
Ka	association constant
KCl	potassium chloride
L	ligand
LUMO	Lowest Unoccupied Molecular Orbital
Lys	lysine
M	metal
MALDI-TOF	Maxtrix Assisted Laser Desorption Ionization- Time of Flight
MCF7	human breast carcinoma

MDA-MB-231	human breast carcinoma
Me	methyl
MeOH	methanol
MeOpyr	4-methoxypyridine
Met	methionine
MPNs	monofunctional *trans*-platinum-nucleobase complexes
MS	mass spectrometry
MTT	3-(4,5-dimethylthiazol-2-yl)-2,5-diphenyltetrazolium bromide
N	nitrogen
N-AcCys	N-acetylcysteine
N-AcMet	N-acetylmethionine
N_2	nitrogen gas
NaCl	sodium chloride
$NaClO_4$	sodium perchlorate
NaH	sodium hydride
$NaNO_3$	sodium nitrate
NaOAc	sodium acetate
NaOH	sodium hydroxide
NC	nucleocapsid protein 7
NCI	National Cancer Institute
NCp7	nucleocapsid protein 7
NER	Nuclear Excision Repair
NH_4NO_3	ammonium nitrate
NH_4OH	ammonium hydroxide
Ni	nickle

NIH	National Institute of Health
NOBA	4-nitrosobenzamide
NSF	National Science Foundation
PAR	4-(2-pridylazo)resorcinol
PBMCs	peripheral blood mononuclear cells
Pd	palladium
Phe	phenylalanine
pKa	acid dissociation constant
Pro	proline
Pt	platinum
Pt-BCH	exo-[N-2-methyamino-2,2,1-bicycloheptane]dichloroplatinum(II)
py	pyridine
pyr	pyridine
QTOF	quadrupole time of flight
quin	quinoline
RNA	ribonucleic acid
RPA	replication protein A
S	sulfur
SAMTs	S-acyl-2-mercaptobenzamide thioester
Sb	antimony
SI	ratio of EC50 to IC50
SIV	simian immunodeficiency virus
SL	stem loop
SR	alkanethiolates
ss	single-stranded
tDDP	*trans*-diamminodichloroplatinum(II)

terpy	2,2';6',2"-tepyridine
Thr	threonine
TPAs	*trans*-platinum planar amine compounds
Tris	tris(hydroxymethyl)aminomethane
Trp	tryptophan
Ts	p-toluenesulfonylchloride
TSP	trimethylsilyl propionate
TSQ	N-(6-methoxy-8-quinolyl)-p-toluenesulfonamide
tz	thiazole
VCV	varcella virus
W	tryptophan
WST	(4-[3-(4-iodophenyl)-2-(4-nitrophenyl)-2H-5-tetrazolio]-1,3-benzene disulfonate
Xnt	xanthine
XPA	xeroderma pigmentosum complementation group A
ZF	zinc finger
ZF2	C-terminal zinc finger of NCp7
Zn	zinc

Abstract

Platinum Complexes and Zinc Finger Proteins: From Target Recognition to Fixation

A Dissertation submitted in partial fulfillment of the requirements for the degree of Ph.D. at Virginia Commonwealth University

by

Samantha D. Tsotsoros

B.Sc. in Chemistry, Christopher Newport University, 2009

Advisor: Dr. Nicholas P. Farrell

Professor, Department of Chemistry

Bioinorganic chemistry strives to understand the roles of metals in biological systems, whether in the form of naturally occurring or addition of non-essential metals to natural systems. Metal ions play vital roles in many cellular functions such as gene expression/regulation and DNA transcription and repair. The study of metal-protein-DNA/RNA interactions has been relatively unexplored. It is important to understand the role of metalloprotein interactions with DNA/RNA as this enhanced knowledge may lead to better understanding of diseases and therefore more effective treatments.

A major milestone in the development of this field was the discovery of the cytotoxic properties of cisplatin in 1965 and its FDA approval in 1978. Since then, two other chemotherapeutic drugs containing platinum, carboplatin and oxaliplatin, have been used in the clinic. These three compounds are all bifunctional with the ligands surrounding platinum

in the *cis* conformation and rearrangement of the ligands to the *trans* orientation results in a loss of cytotoxic properties due to rapid deactivation through binding to S-containing proteins. This enhanced reactivity yields new opportunities to study the reactions between proteins and DNA.

One of the first crosslinking experiments used transplatin to crosslink NCp7 to viral RNA in order to understand how/where the protein bound to RNA. We have studied the interaction between *cis* and *trans* dinuclear platinum complexes and the C-terminal zinc finger (ZF). The *trans* complex reacts at a faster rate than the *cis* isomer and causes N-terminal specific cleavage of the ZF. The dinuclear structure plays a critical role in the peptide cleavage as studies with transplatin (the mononuclear derivative) does not result in cleavage.

Monofunctional *trans* platinum-nucleobase complexes (MPNs) serve as a model for the binding of transplatin to DNA. This provides an interesting opportunity to study their reactions with S-containing proteins, such as HIV1 NCp7. MPNs have been shown to bind to the C-terminal ZF of HIV1 NCp7, resulting in zinc ejection. This occurs through a two-step process where the nucleobase π-stacks with Trp37 on the ZF, followed by covalent binding at the labile Cl site to Cys. MPNs have also shown antiviral activity *in vitro*.

The labile Cl on MPNs reduces specificity of these compounds, as it leaves an available coordination site on the platinum center for binding to other S-proteins or DNA. Therefore, we have moved to an inert PtN_4 coordination sphere, $[Pt(dien)L]^{2+}$ (dien= diethylenetriamine). Due to the strong bond between platinum and nitrogen, covalent reactions are highly unlikely to occur at rapid rates. The strength of the π-stacking interaction between nucleobases (free and platinated) and the aromatic amino acid, tryptophan (Trp), showed an enhanced binding constant for platinated nucleobases. This was confirmed by density functional theory (DFT) calculations as the difference in energy between the HOMO of Trp and the LUMO of the nucleobase was smaller for the platinum complex. The studies were

extended to the Trp-containing C-terminal ZF of HIV1 NCp7 and an increase in association constant was seen compared to free Trp.

Reaction of PtN_4 nucleobases compounds with a short amino acid sequence containing either Ala (no π-stacking capabilities) or Trp (π-stacking interactions) revealed an enhanced rate of reactivity for the Trp-containing peptide. This result supports the theory of a two-step reaction mechanism where the platinum-nucleobase complex recognizes the peptide through a π-stacking interaction with Trp followed by covalent binding to the platinum center.

The $[Pt(dien)L]^{2+}$ motif allows for systematic modification of the structural elements surrounding platinum in a search for the most effective compound. Methylation of the dien ligand should, in theory, increase lipophilicity of the compounds, however, due to 2+ charge of the compounds, this simple association does not hold true. Analysis of the cellular accumulation profiles showed little change in the uptake with the addition of methyl groups to the dien ligand, in agreement with the non-linear change in lipophilicity.

Modification of L using different nucleobases allows for the tuning of the strength of the π-stacking interaction between Trp and the platinum complex. The addition of inosine (which lacks a H-bonding donor/acceptor at the C2 position) resulted in a lower association constant with both N-AcTrp and the C-terminal zinc finger of HIV1 NCp7. Interestingly, the addition of xanthosine resulted in an ehanced π-stacking interaction with the C-terminal zinc finger of HIV1 NCp7; likely as a results of the addition of a H-bonding donor (double-bonded O) at the C2 position.

The ability of PtN_4 nucleobase complexes to inhibit formation of the NCp7 complexation with viral RNA was studied by mass spectrometry and gel electrophoresis. Dissociation of the NCp7-RNA complex was seen upon addition of PtN_4 compounds. These compounds were also able to retard formation of the NCp7-RNA complex when pre-incubated with the protein. These results have important implications as inhibition of complex formation

between NCp7 and viral RNA has negative implications for viral replication.

Despite the success of platinum-nucleobase compounds, it is important to evaluate all potential π-stacking ligands. A series of pyridine- and thiazole-based compounds were evaluated for the strength of the π-stacking interaction with N-AcTrp and the C-terminal ZF of HIV1 NCp7. There was notable increase in association constant for the platinum-DMAP (4-dimethylaminopyridine) complex compared to other ligands studied. This result highlights the importance of exploring multiple avenues for the design of specifically targeted inhibitors and further confirms the viability of the medicinal chemistry dual approach of target recognition (non-covalent) followed by target fixation (covalent).

Chapter 1

Introduction

1.1   General Overview
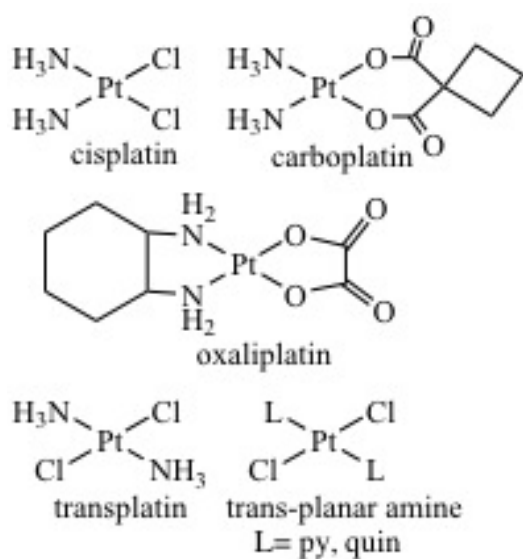
Figure 1.1: Structures of traditional platinum complexes used in the development of anti-cancer agents.

Bioinorganic chemistry strives to understand the roles of metals in biological systems, whether in the form of naturally occurring or non-essential metal addition to natural systems. Metal ions play vital roles in many cellular functions such as gene expression/regulation and DNA transcription and repair[1,2]. The study of metal-protein-DNA/RNA interactions has been relatively unexplored[3,4]. It is important to understand the role of metalloprotein interactions with DNA/RNA as this enhanced knowledge may lead to better understanding of diseases and therefore more effective treatments.

One of the major milestones in the development of this field was the discovery of cisplatin.

Cisplatin is a remarkable compound that has improved the odds of survival for nearly all cancer patients that receive it as treatment. Since the discovery of its cytotoxic properties in 1965[5] and FDA approval in 1978, cisplatin has become a regular part of the chemotherapy cocktail used to treat testicular, ovarian, head and neck, bladder and cervical cancer, among others. In more recent years, carboplatin and oxaliplatin have been approved for use in the clinic, Figure 1.1. Together, the three platinum compounds make up a multi-billion dollar drug industry and have significantly improved survival rates for cancer patients[6].
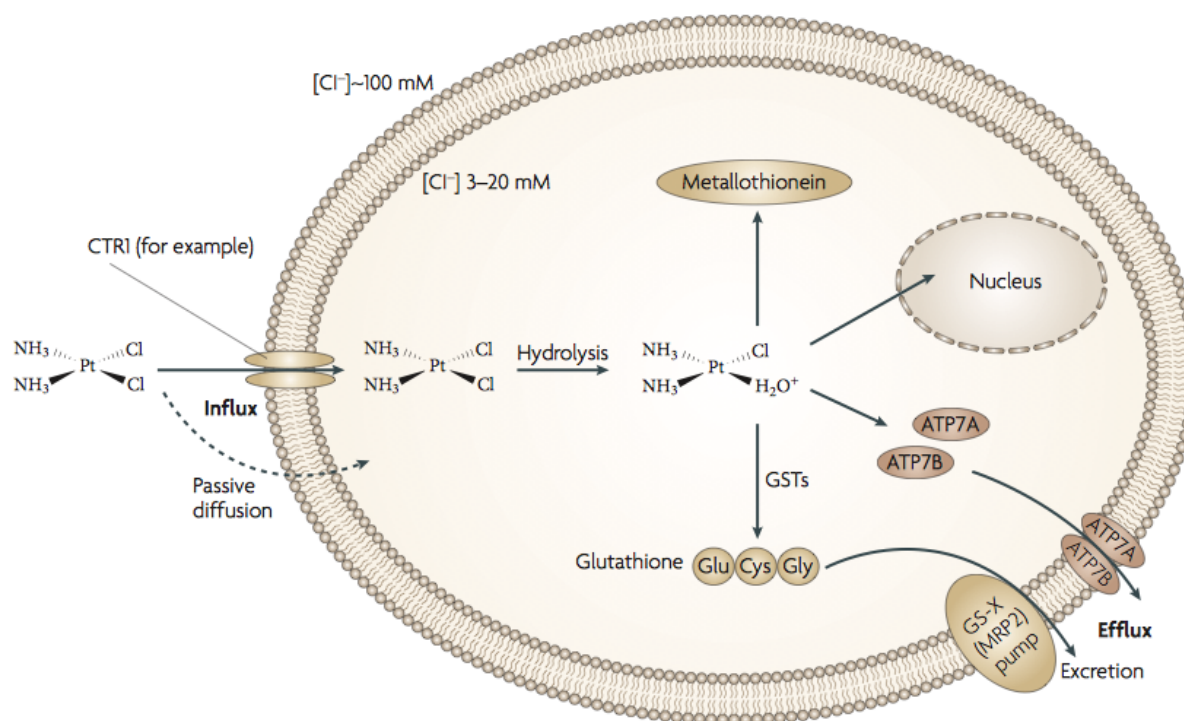
Figure 1.2: Cellular processing of cisplatin is a multistep process in which cisplatin enters the cell, undergoes hydrolysis and binds to proteins (results in deactivation of compound) and DNA (results in apoptosis).

Due to its success, there has been an extensive amount of research aimed at discovering the mechanism of action for cisplatin in the hopes of improving upon the drug. While all of the molecular details have not been obtained, it is clear that cisplatin, oxaliplatin

and carboplatin exert cytotoxicity through loss of the labile chloride (cisplatin) or oxygen (oxaliplatin and carboplatin) ligands upon cell uptake and binding to the N7 of guanine in DNA, causing a distortion in the DNA structure, Figures 1.2 and 1.3[6].
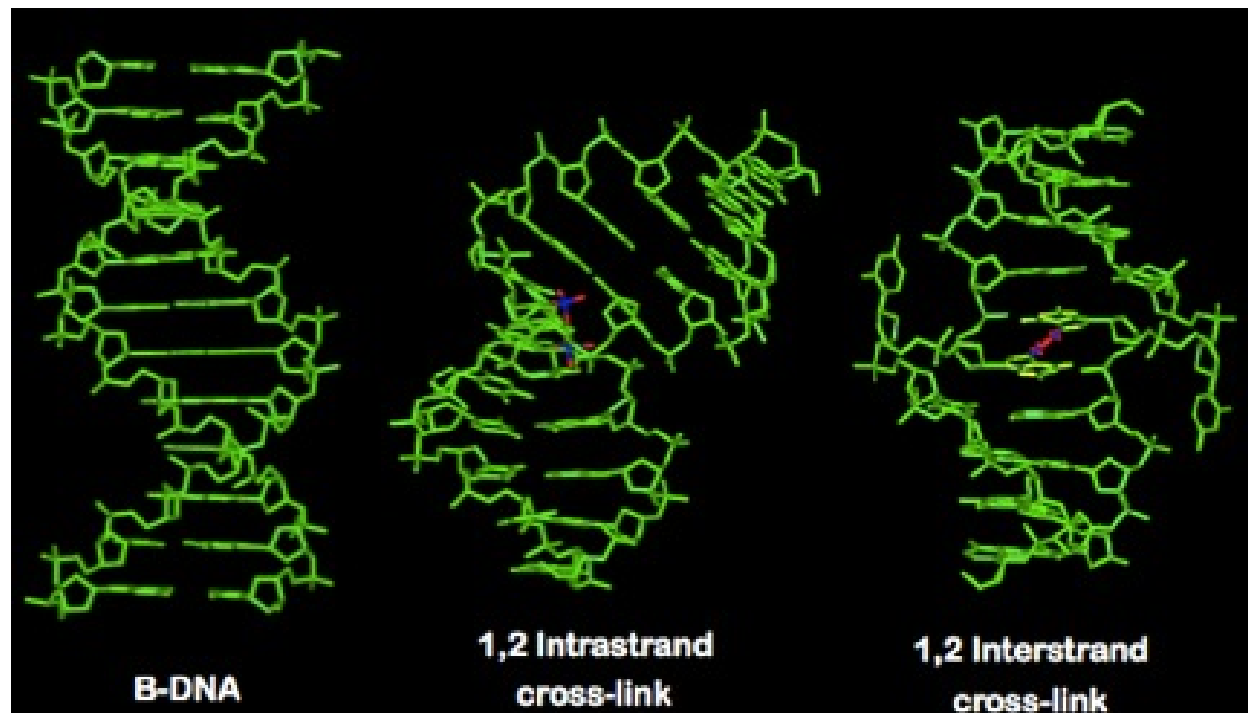
Figure 1.3: Left: structure of B-DNA, Center: DNA bend caused by a 1,2-intrastrand crosslink by cisplatin, and Right: DNA Bend caused by a 1,2-interstrand crosslink by cisplatin.

This distortion is recognized by high mobility group proteins (HMG) and TATA-binding proteins, and eventually induces apoptosis unless the cells have developed resistance[7,8]. Cisplatin resistant cell lines have been shown to recognize the cisplatin-DNA adduct, remove it and repair the DNA using nuclear excision repair (NER). Two proteins involved in the repair of cisplatin-DNA adducts are replication protein A (RPA) and xeroderma pigmentosum group A (XPA) have been shown to have different affinities to cisplatin- and oxaliplatin-DNA adducts, which may explain the lack of cross-resistance between the compounds[9,10]. Resistance can also be enhanced through reduced cellular accumulation[11,12] and rapid detox-

3

ification of the system (glutathione-binding)[13-15].

Treatment with platinum chemotherapeutic agents also results in severe side effects such as kidney and nervous system toxicity, nausea, vomiting, etc. This toxicity has been accepted as a function of the non-specific reaction between cisplatin and S-containing residues (Cys, Met) in proteins[16]. For reasons of resistance and non-specificity, it is important to continue to probe the activity of cytotoxic platinum agents and develop new structurally distinct compounds.

The *cis* orientation has proven to be crucial for the clinical success of platinum agents. When oriented in *trans* geometry, the labile Cl ligands are aquated rapidly due to the *trans* effect. This rapid aquation allows for reactions with proteins, such as human serum albumin and glutathione, resulting in deactivation of the compounds and removal from the system[6]. However, the addition of a planar amine (pyridine, quinoline, etc) ligand in place of ammonia enhances cytotoxic properties in both cisplatin sensitive and resistant cell lines[17,18]. Mechanistic studies on these compounds have shown that the additional steric hindrance of the planar amine results in a somewhat slower rate of aquation, which leads to long-lived mono-adducts on DNA. Compared to cisplatin, which is 70% bound to DNA in a bifunctional intrastrand adduct (either G,G or A,G), *trans*-planar amine complexes (TPAs) bind to DNA in a mixture of interstrand, intrastrand and monofunctional adducts[19-21]. The planar amine in the *cis* position on TPA complexes has also been found to intercalate DNA, creating a bend similar to cisplatin. Due to this similarity, monofunctional adducts of *trans*-[PtCl$_2$(NH$_3$)(quin)] and *trans*-[PtCl$_2$(NH$_3$)(thiazole)] are recognized by HMG proteins and repaired by NER, Table 1.1[21]. This novel DNA-binding motif may help to explain the unique cytotoxic properties of these compounds when compared to other platinum agents.

Trans-platinum complexes have also been used as probes for DNA-protein reactions. One of the first experiments used transplatin as a crosslinking agent for NCp7 with HIV1 RNA. NCp7 was shown to catalyze the formation of the RNA dimer and a crosslinking ex-

Table 1.1: Summary and comparison of basic characteristics of the monofunctional adduct of *trans*-PtTz with 1,2-GG intrastrand crosslink (CL) of cisplatin and the monofunctional adduct of [PtCl(dien)]Cl

	monofunctional adduct of *trans*-PtTz	1,2-GG intrastrand CL of cisplatin	monofunctional adduct of [PtCl(dien)]
termination of DNA synthesis	yes	yes	no
DNA bending	34°	$32\text{-}34^o$	no
$K_{D(app)}$ (HMGB1a recognition)	38.5 nM	30.8 nM	no
$K_{D(app)}$ (HMGB1a recognition)	2.05 μM	1.85 μM	no
NER by eukaryotic excinuclease	yes	yes	no

periment determined that the location of the Pt-RNA-NCp7 crosslink was between positions 315 and 324 of the RNA[22]. It has since been discovered that the binding of NCp7 occurs at the Ψ-RNA site. This binding has been studied in depth, allowing for analysis of the structure of the adduct. The binding affinities for different stem loop regions 1-4 of Ψ-RNA have been determined and it was found that the NCp7 binds the tightest to SL2 and SL3[23,24].

1.2 Zinc Finger Proteins

Zinc finger proteins constitute 2-3% of the human genome and play a diverse role in many cell processes, such as transcription, DNA repair, cellular signaling and apoptosis. The role of zinc in zinc finger proteins is a structural one and zinc fingers play an important role in the three-dimensional folding of the protein of which it is a part[25]. Loss of zinc from ZF proteins causes a loss of structure and often this leads to loss of the protein's function[26].
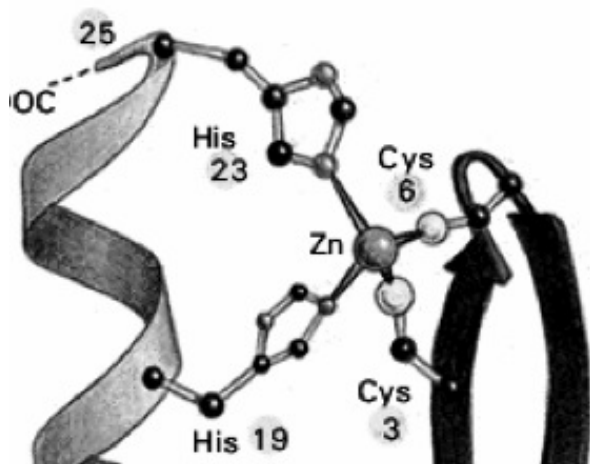
Figure 1.4: Structural zinc is coordinated to four amino acids in a tetrahedral arrangement.

Zinc fingers (ZFs) are classified by the number and type of amino acids that make up the Zn(II) coordination sphere, Figure 1.5. Zinc is an intermediate hard/soft acid and is most commonly coordinated to histidine and cysteine residues in a tetrahedral geometry when in a strucutral role, Figure 1.4. Therefore, the classifications of zinc fingers include C_2H_2, C_3H, and C_4. Of the three types of zinc fingers, C_2H_2 fingers are the most common and are present in many human transcription factors[27]. The different types of zinc fingers often have different functions and the examples shown in Figure 1.5 will be discussed briefly.
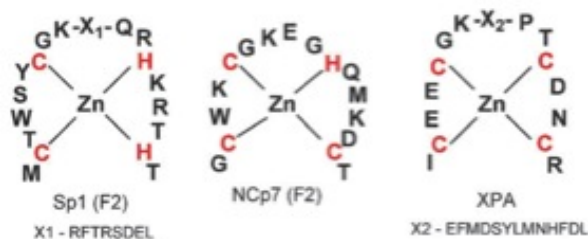
Figure 1.5: Examples of the three zinc coordination spheres found in zinc finger proteins.

C_2H_2 zinc finger proteins are commonly part of transcription factors. One example of a C_2H_2 zinc finger is the human transcription factor Sp1, which contains three C_2H_2 zinc finger domains. Sp1 functions by recognizing DNA through hydrogen bonding with nucleotides in the major groove and by interaction of amino acids with the DNA nucleotides. Because this protein does not use the symmetry of DNA to recognize it, a series of zinc fingers is linked together in order to be specific to a long sequence[26].

6

C_4 zinc finger proteins are common in DNA repair enzymes and nuclear localized systems, e.g. XPA. As discussed earlier, XPA plays a critical role in the recognition of damaged DNA and signaling for other proteins the NER complex, such as RPA[28].

C_3H ZF proteins are much less common than C_2H_2 and C_4 and are involved in the binding of RNA and ss or dsDNA through the interaction of aromatic amino acids with nucleotides. They are found in nearly all retroviruses. One example of a C_3H ZF is the HIV-1 NCp7, which interacts with ssRNA through the π-stacking interaction of Phe/Trp and G/C. This protein is critically involved in the HIV viral life cycle by playing roles in RNA packaging, reverse transcription and integration[26].

1.3 HIV1 NCp7

NCp7 is a basic 55-amino acid protein containing two C_3H zinc fingers. The basicity of this protein is highlighted by the presence of 15 Lys and Arg residues, Figure 1.6. NCp7 binds Zn with very high affinity, with K_a values between 10^{12}-10^{14} M^{-1} [29]. The C-terminal,
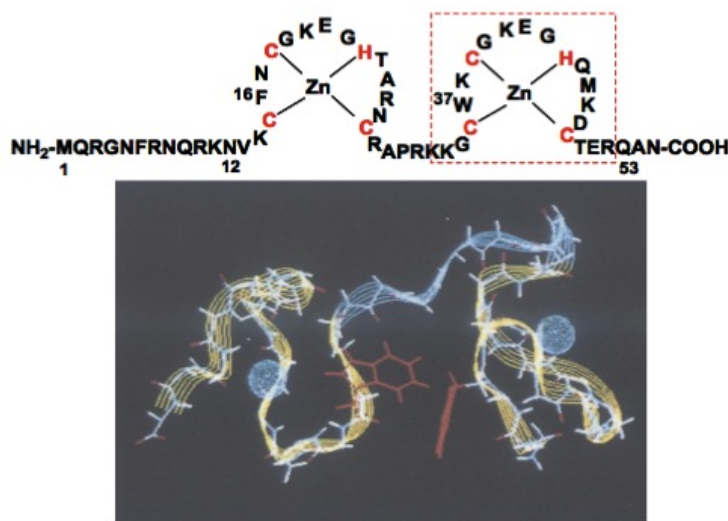
Figure 1.6: Top- Sequence of HIV1 NCp7 and Bottom- NMR strucutre of the three-dimension folding of the peptide.

N-terminal and zinc finger linker sequences provide no secondary structure; therefore, the zinc fingers are the most important structural elements. It has also been found that the C-terminal zinc finger is more reactive than the N-terminal zinc finger[30−32], with Cys49 being the most reactive site on NCp7[33]. As part of the viral packaging process, NCp7 binds to Ψ-RNA through π-stacking interactions of the aromatic amino acid residues, Phe and Trp, with nucleotides on the RNA (Cyt, Gua)[23,24,34]. This π-stacking recognition element is unique to NCp7 when compared to cellular C_2H_2 and C_4 zinc fingers and provides a starting point for the development of specific inhibitors[35].
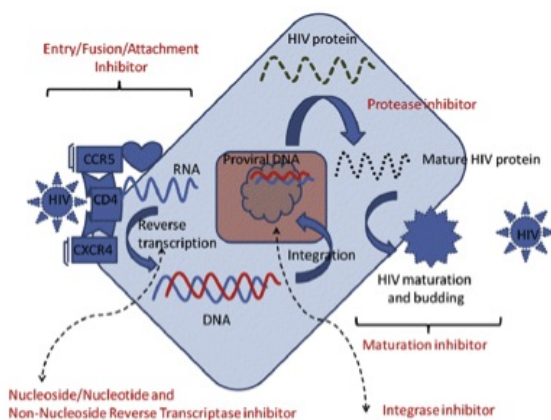
Figure 1.7: HIV life cycle highlighted by the various steps in which current HIV therapies interrupt.

HIV1 NCp7 has become an attractive drug target in recent years for several reasons. Current therapies include a combination of drugs that inhibit reverse transcriptase and protease, Figure 1.7. While this approach has been successful in reducing the viral loads of many patients, there are problems of resistance, drug toxicity and latent viral reservoirs that are contained in long-lived cell populations. The development of resistance is enhanced by the ability of the viral enzymes to efficiently carry out their functions despite mutations. This ability to easily mutate while retaining viral function is a major limiting factor of drug regimens. NCp7 is an attractive target because it is highly conserved in all viral strains and mutations in the zinc-binding sequence have been shown to render the virus non-infectious[36].
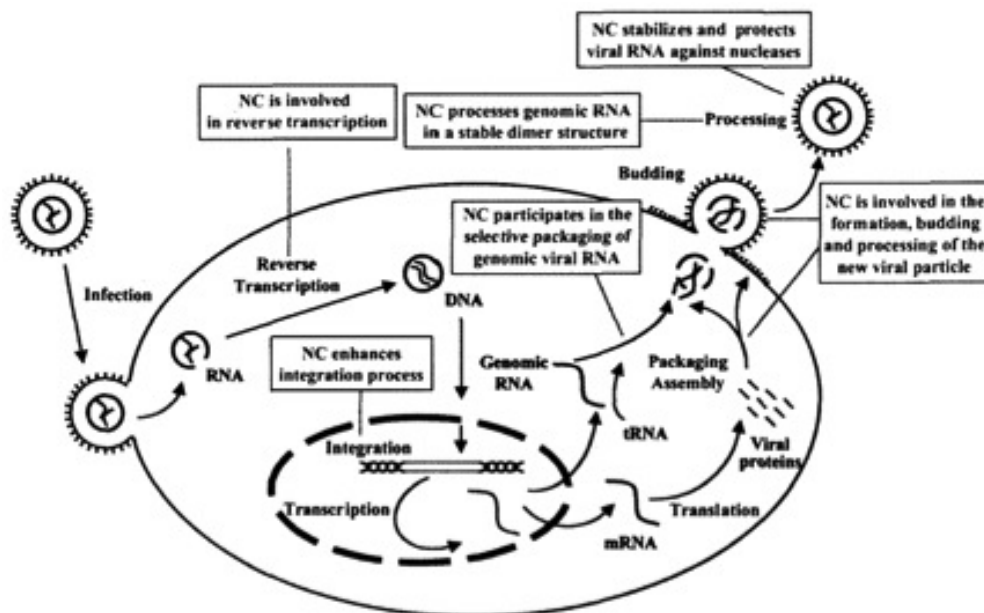
Figure 1.8: The various roles of NCp7 in the HIV life cycle are highlighted. NCp7 participates in nearly all steps of the life cycle, with the exception of cell entry.

NCp7 is cleaved from the parent GAG protein which encodes for proteins that play a role in compartmentalization of viral components and maintenance of the structural integrity of the virus. The roles of NCp7 are complex and numerous; this protein plays a role in reverse transcription, integration of viral components into the host cell, and viral packaging, Figure 1.8[36,37]. A major difficulty in targeting NCp7, as with any target, is specificity. The use of zinc fingers in normal cellular functions means that the drugs have to be able to only react with the NCp7 and not just the zinc finger motif. The C_3H motif of NCp7 provides a starting point due to the rarity of such zinc finger coordination spheres.

According to previous studies, C_4 should be more reactive than C_3H, which should be more reactive than C_2H_2. The inherent difference in reactivity is due to an increase in the number of nucleophilic cysteine residues and may provide a starting point for the rational design of inhibitory agents. To date, many types of inhibitors have been tested with NCp7 and few have yielded the specificity needed to successfully inhibit HIV without affecting

9

cellular functions[26,36].

A successful approach to targeting NCp7 and inhibiting viral activity is through modification of the Cys residues coordinating zinc. While zinc fingers contain redox inert d^{10} structural Zn(II) ions, the coordinated Cys residues are highly nucleophilic and are susceptible to electrophilic attack by small molecules. The first inhibitor of NCp7 was 3-nitrosobenzamide (NOBA)(Figure 1.9), which ejected zinc from the protein and inhibited its function. The compound was highly reactive and its toxic properties stalled further development[38].
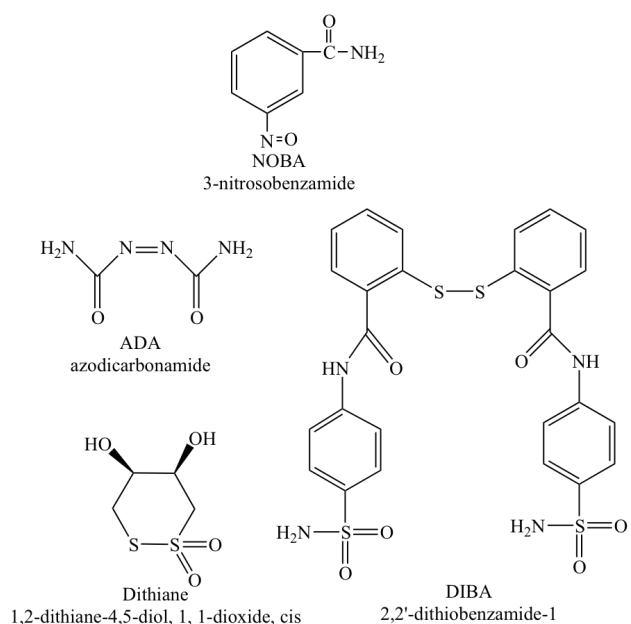
Figure 1.9: Structures of well-studied compounds designed to target NCp7.

Compounds have since been developed that can selectively target HIV NCp7 through electrophilic attack with lower toxicity profiles[39]. The effectiveness and mechanism of action of the disulfide drugs pictured in Figure 1.9 were evaluated through a number of biochemical techniques. A dose and time dependent increase in the fluorescence of the Zn-(TSQ)$_2$ (TSQ= N-(6-methoxy-8-quinolyl)-p-toluenesulfonamide) complex was seen upon incubation of NOBA, DIBA-1, ADA and dithiane was seen, with DIBA-1 causing the most rapid zinc ejection. Capillary zone electrophoresis showed that upon incubation with the electrophilic agents the peak for NCp7 shifted, broadened and formed multiple peaks indicating reaction of the compounds with the protein. Gel electrophoretic studies showed that incubation of these four compounds with NCp7 at 1 μM for 2-3 hours completely inhibited binding with DNA.

When these compounds were tested with Sp1 (C_2H_2) and GATA (C_4), only NOBA showed inhibition of the binding properties with DNA. These data suggest that ADA, dithiane and DIBA-1 are selective inhibitors for NCp7 interactions with DNA. The idea of specificity for these compounds is also supported by the fact that they do not inhibit the spumavirus, which does not have a zinc finger protein, but do inhibit all other retroviruses tested[39]. The proposed mechanism for the disulfide compounds, DIBA-1 and dithiane, can be found in Figure 1.10, where binding of the compound induces cleavage of the disulfide bond which is followed by subsequent binding to another zinc finger, creating inactive ZF protein polymers[40].

DIBA-1 is part of a family of DIBA compounds that contain various changes on the disulfide-linked aromatic structure. These compounds were found to inactivate cell-free virions, inhibit acute and chronic infections, exhibiting broad antiviral activity. They were also found to be synergistic with current HIV therapies and no resistance was detected[41]. This class of compounds is not without problems, as the disulfide bond can be easily reduced, limiting the effective half-life of the compound[32].

The success of this class of compounds is illustrated by the clinical trial of ADA in advanced AIDS patients with resistant strains. The trial found that 27% of patients
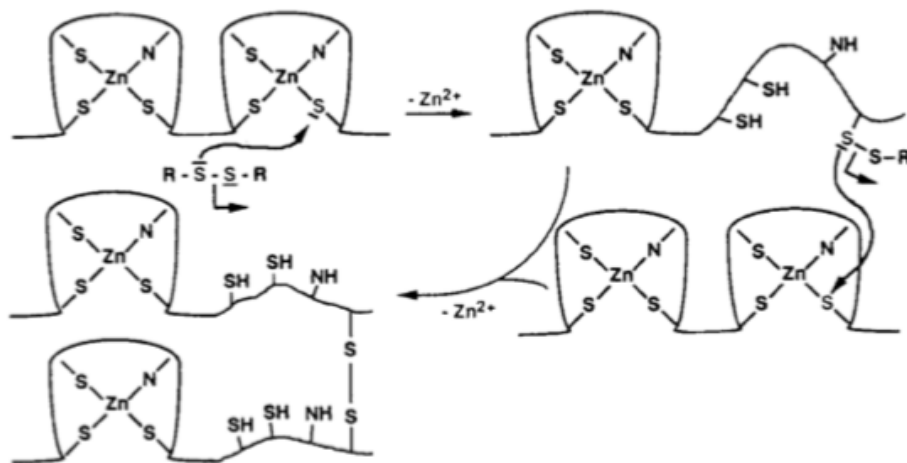
Figure 1.10: Mechanism of action for disulfide complexes designed to target NCp7.

had a reduction in viral load when treated with ADA in conjunction with other approved treatments and 45% showed a recovery in CD4 cells. No evidence of resistance to ADA was seen. The apparently disappointing results
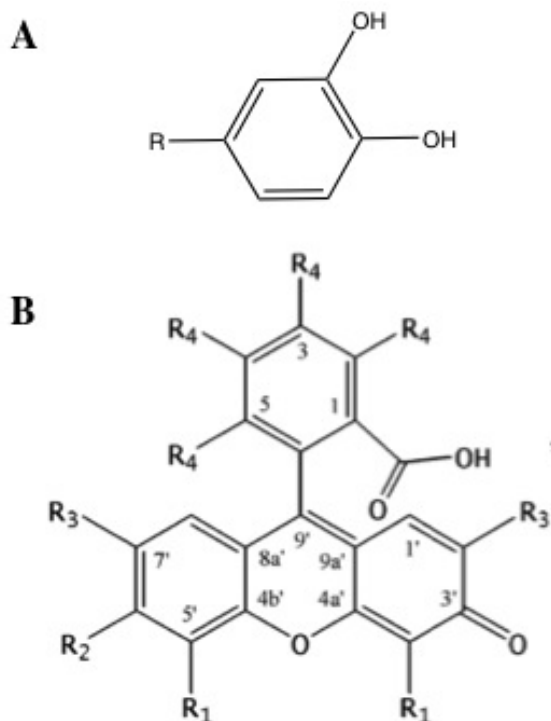
Figure 1.11: A- Structural motif of compounds found to inhibit function of NCp7 from a high throughput screen of 4800 compounds and B- Fluoroscein-based structure of compound identified as inhibitors of NCp7.

of a low rate of decrease in viral load may not be a good indicator of the compound's success because of the way in which it targets HIV. By inhibiting NCp7, the virus is rendered non-infectious, but may still be present in the body. While the study had a small sample size (n=11), it showed the relevance of NCp7 and these electrophilic compounds as a strategy to combat HIV[42].

Other strategies have been used to target and inactivate NCp7, such as peptidomimetics, nucleomimetics, use of actinomycin D to prevent RNA synthesis, and vaccinations[40], as well as a different class of compounds called SAMTs (S-acyl-2-mercaptobenzamide thioester)[43] which modify the NCp7 portion of the GAG precursor protein thereby blocking GAG processing. A library of approximately 2,000 small molecules from the NCI Diversity Set suggested a good correlation between trytpophan quenching and inhbition of NCp7-nucleic acid binding for fluorescein-based compounds[44]. A second high-throughput screening revealed 5 hits out of 4800 compounds. The ability of these compouds to inhibit the NCp7-mediated destabi-

lization of cTAR DNA was correlated with their ability to compete with nucleic acid binding to NCp7[45], Figure 1.11.

1.4   Use of Platinum Complexes to Target NCp7

1.4.1   Interactions of monofunctional Pt complexes with S-donors

While bifunctional platinum compounds are known to exhibit cytotoxic properties, monofunctional complexes, such as [PtCl(dien)]Cl (dien=diethylenetriamine) do not have the same cellular effects[46]. In order to study the effect of the "carrier" dien ligand, [PtCl(terpy)]Cl (terpy= 2,2';6',2"-terpyridine) was also studied, Figure 1.12. [PtCl(terpy)]$^+$ also provides the possibility of π-stacking interactions with aromatic amino acids and has, in fact, been shown to exhibit some selectivity towards amino acids; specifically the SH in cysteine and N in histidine and arginine[47].

The reaction of [PtCl(dien)]$^+$ with the C-terminal zinc finger of HIV1 NCp7 by ESI-MS yielded three main adducts immediately upon incubation; {ZF/[Pt(dien)]}$^+$, {ZF/[PtCl(dien)]}$^+$, and {ZF/[Pt(dien)]/Na}$^+$. Further incubation (up to 48 hrs) did not result in any additional adducts. The adducts seen by MS display displacement of Cl by S, most likely from Cys49 as it has been shown to be the most nucleophilic site on the C-terminal ZF[48,49]. Of special interest is the peak corresponding to {ZF/[PtCl(dien)]}$^+$. Redox reactions
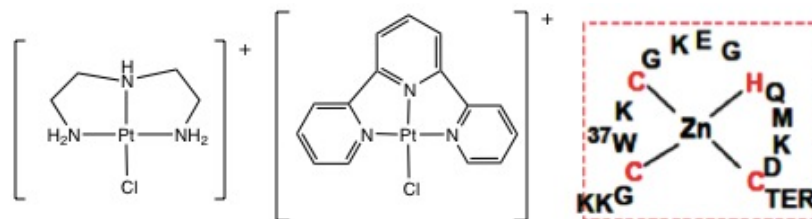
Figure 1.12: Left- Structure of [PtCl(dien)]$^+$, Center- Structure of [PtCl(terpy)]$^+$ and Right- Sequence of NCp7 C-terminal zinc finger.

are unlikely for platinum and it is likely that 4-coordinate square planar coordination will remain intact. Therefore, it is possible that the Cl is displaced from platinum by a Cys S and the zinc coordination sphere is expanded to 5-coordinate (Figure 1.13B).

The rigid aromatic chelating ring of terpy and electron-withdrawing effect through π-backbonding to Pt suggest that $[PtCl(terpy)]^+$ will be more reactive than $[PtCl(dien)]^+$. Immediately upon addition of $[PtCl(terpy)]^+$ to the C-terminal ZF of HIV1 NCp7, four new peaks were seen in the mass spectrum. No simple stoichiometry could account for the new species, but it is likely that extensive platination of the peptide is seen. Deconvolution of the spectrum supports this as $[Pt(terpy)]_3$/peptide is seen. MS2 of this peak shows loss of $[Pt(terpy)]$ indicating that at least one $[Pt(terpy)]$ species remains intact upon binding to the ZF. Interestingly, $[ZnCl(terpy)]^+$ is seen suggesting "metal scrambling" between the two species. No such event is seen for $[PtCl(dien)]^+$.

The circular dichroism (CD) spectrum of the C-terminal ZF of HIV1 NCp7 is charac-
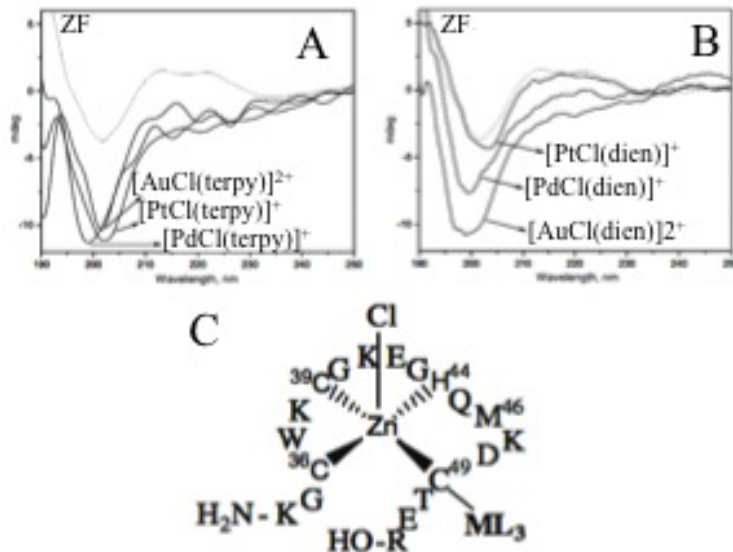
Figure 1.13: CD spectra for the reaction between the (A) $[MCl(terpy)]^+$ (M = Pt(II), Pd(II), Au(III)) complexes and (B) $[MCl(dien)]^+$ (M = Pt(II) or Pd(II), Au(III)) with the C-terminal ZF of HIV1 NCp7 after 15 min of incubation. (C) Proposed structure of 5-coordinate zinc.

terized by a slightly positive maximum centered at 210 nm and a stronger negative minimum centered between 190-200 nm. Loss of zinc from the ZF results in a decrease in the positive band and a significant increase in the intensity of the negative band as well as a slight red shift. These changes are indicative of a random coil[49]. Incubation of $[PtCl(dien)]^+$ and $[PtCl(terpy)]^+$ contrasts the reactivity of the species. There is very little change in the spectrum for $[PtCl(dien)]^+$ after 15 minutes of incubation, while $[PtCl(terpy)]^+$ induces are large conformational change, Fig 1.13.
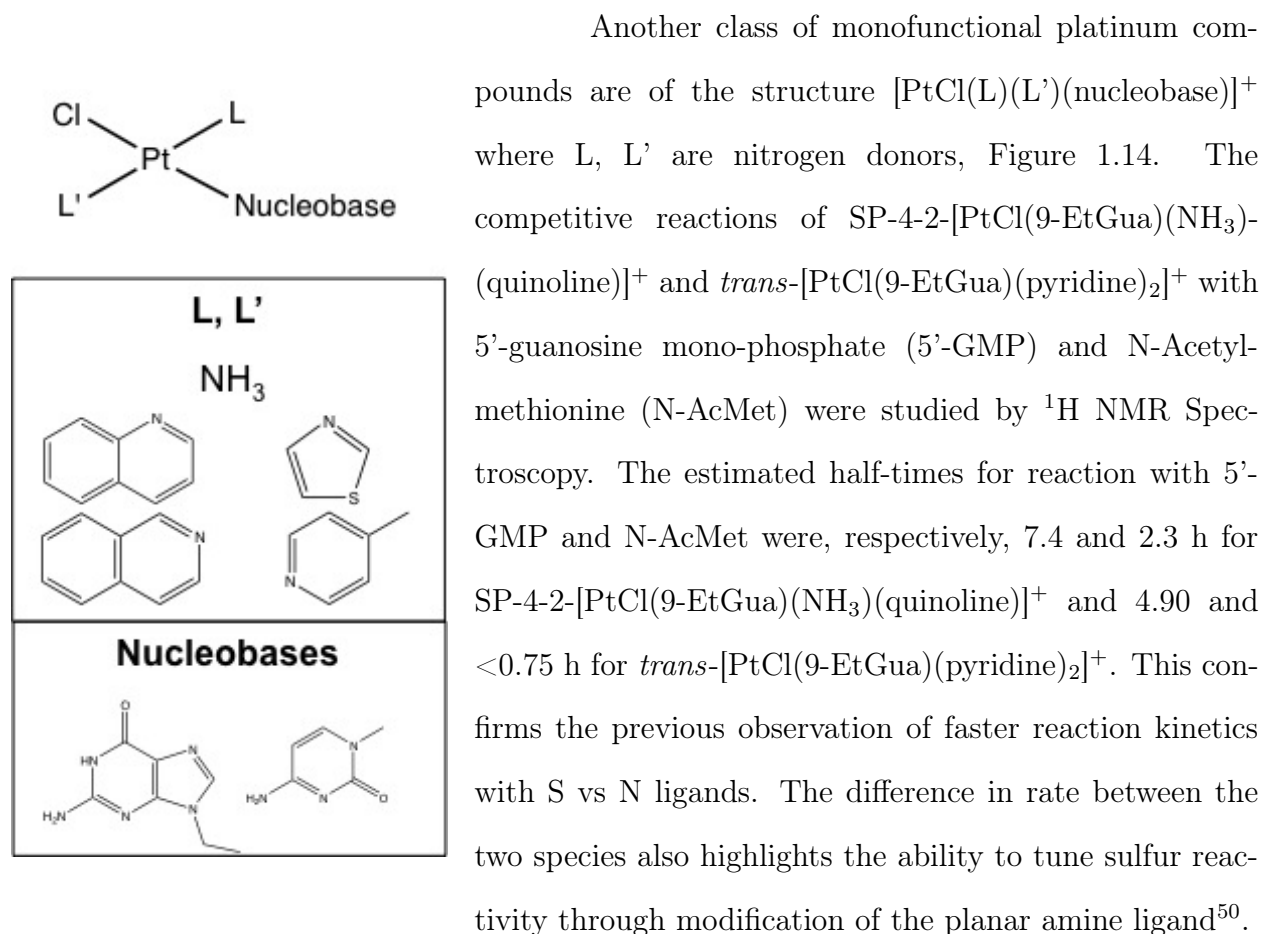
Figure 1.14: Structure of *trans*-platinum mononucleobase complexes.

Another class of monofunctional platinum compounds are of the structure $[PtCl(L)(L')(nucleobase)]^+$ where L, L' are nitrogen donors, Figure 1.14. The competitive reactions of SP-4-2-$[PtCl(9\text{-}EtGua)(NH_3)$-(quinoline)$]^+$ and *trans*-$[PtCl(9\text{-}EtGua)(pyridine)_2]^+$ with 5'-guanosine mono-phosphate (5'-GMP) and N-Acetyl-methionine (N-AcMet) were studied by ^{1}H NMR Spectroscopy. The estimated half-times for reaction with 5'-GMP and N-AcMet were, respectively, 7.4 and 2.3 h for SP-4-2-$[PtCl(9\text{-}EtGua)(NH_3)(quinoline)]^+$ and 4.90 and <0.75 h for *trans*-$[PtCl(9\text{-}EtGua)(pyridine)_2]^+$. This confirms the previous observation of faster reaction kinetics with S vs N ligands. The difference in rate between the two species also highlights the ability to tune sulfur reactivity through modification of the planar amine ligand[50].

Based on this ability to control reactivity, a series of compounds following the same structural motif, $[PtCl(L)(L')(nucleobase)]^+$ using 9-EtGua and 1MeCyt as the nucleobase, were studied. As seen in Table 1.2, com-

Table 1.2: *In vitro* cytotoxicities and antiviral infectivity results for [SP-4-2]-[PtCl(nucleobase)(L)(L')](NO$_3$) [b]For details see www.niaid.nih.gov/dmid/apdsame.htm. [c]The parent dichloride compound *trans*-Pt-Cl$_2$(NH$_3$)(quinoline). EC$_{50}$ is dose to inhibit viral infectivity while CC$_{50}$ is cytotoxic dose in cell carriers. HCMV, human cytomegalo virus; VCV, varicella virus; HIV-1, human immunodeficiency virus type 1; HSV-1, herpes simplex virus-1; HSV-2, herpes simplex virus-2; EPV, Epstein-Barr virus.

					In Vitro data		
Cpd	Nucleobase	L	L'	Virus[b]	EC$_{50}$ (μg/mL)	CC$_{50}$ (μg/mL)	SI (CC$_{50}$/IC$_{50}$)
1	9-EtGua	NH$_3$	NH$_3$	HCMV	>20	73	<3.7
3	9-EtGua	NH$_3$	Quinoline	VCV	51	>100	>1.9
				HIV-1	41.9	>200	>47.5
4	1-MeCyt	NH$_3$	Quinoline	VCV	>20	94.4	<4.7
5	9-EtGua	NH$_3$	Isoquinoline	HSV-1	>20	81.8	<4.1
				HSV-2	>20	81.8	<4.1
6	1-MeCyt	NH$_3$	Isoquinoline	EBV	25.1	>50	>2
				VCV	>20	82.2	>4.1
7	9-EtG	NH$_3$	Thiazole	VCV	>20	94.8	>4.7
10	9-EtGua	4-Mepy	4-Mepy	EBV	42	>50	>1.2
I[c]		NH$_3$	Quinoline			2.98	

pounds of this structure show some antiviral activity *in vitro*. These platinum agents react through displacement of the labile chloride leaving group and an important factor is the change from two chlorides (cytotoxic agents) to one chloride (antiviral agents). Thus, structural features enhancing antiviral selectivity are recognizable[51].

It is plausible that the antiviral activity of these compounds may be a result of zinc ejection from zinc finger proteins. When the C-terminal ZF of HIV1 NCp7 was incubated with SP-4-2-[PtCl(nucleobase)(NH$_3$)(L)]$^+$ in the presence of 4-(2-pyridylazo)resorcinol (PAR) the absorbance at 500 nm attributed to Zn(PAR)$_2$ increases while that of free PAR at 420 nm decreases. This ZF binding is supported by the kinetic preference for N-AcMet over 5'-GMP for SP-4-2-[PtCl(9-EtGua)(NH$_3$)(L)]$^+$ compounds[51].

Of a similar structure, $[PtCl(9\text{-}EtGua)(pyr)_2]^+$ shows nearly identical reactivity with the C-terminal ZF of HIV1 NCp7 as SP-4-2-$[PtCl(9\text{-}EtGua)(NH_3)(quinoline)]^+$ by mass spectrometry. In both cases, intact compound, free 9-EtGua and 9-EtGua associated with the ZF are seen in the mass spectrum. There are also a number of platinum adducts such as, ZF + $[Pt(pyr)_2]$ and apo-ZF + $2[Pt(pyr)_2]$. Study of the reaction by circular dichroism show a decrease in ordered structure, indicative of zinc ejection. Therefore, the proposed mechanism of action for these compounds is two steps- first, the compounds π-stack with Trp37, which brings the platinum center close to S-containing amino acids, such as Cys, after which covalent binding occurs. Finally, *trans*-labilization of 9-EtGua creates a secondary binding site on Pt and Zn is released from the peptide, Scheme 1.1[49].
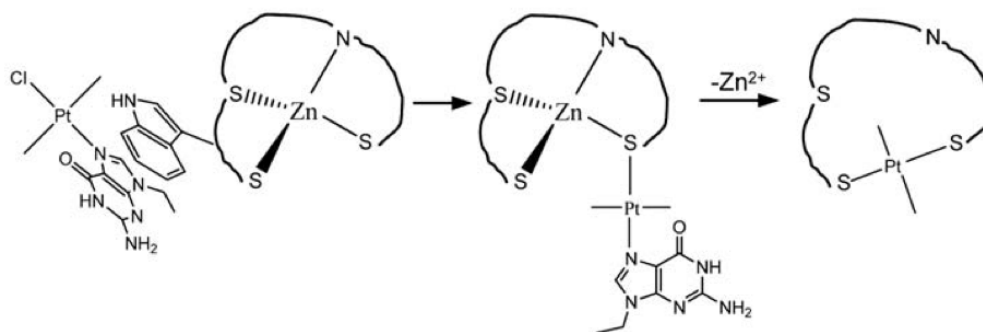
Scheme 1.1: A proposed chemical mechanism for zinc ejection from the C-terminal ZF of HIV1 NCp7 using platinum-nucleobase electrophiles. The specific nature of the coordination site for the $[Pt(py)_2]$ unit remains to be determined.

1.5   Reactions with Zn Model Chelates

Zinc model chelates have been used as a examples for reactions of Zn-containing proteins upon methylation[52]. Therefore, the reactions between three platinum complexes; $[Pt(pyridine)_2(9\text{-}EtGua)Cl]^+$; $[PtCl(dien)]^+$; and $[PtCl(terpy)]^+$; and $[Zn(bme\text{-}dach)]_2$ have been studied to model the interaction between platinum complexes and the C-terminal ZF of HIV1-NCp7[53,54]. For the reaction of $[Zn(bme\text{-}dach)]_2$ and $[Pt(pyridine)_2(9\text{-}EtGua)Cl]$ (1:1

ratio) an intermediate Pt-Zn species is seen in the mass spectrum corresponding to [Zn(bme-dach){Pt(pyr)$_2$(9-EtGua)}]. This is supported by splitting of the H8 signal of 9-EtGua in ^{1}H NMR, indicating a sterically hindered species. One product species is [{Zn(bme-dach)}{Pt(9-EtGua)}], which upon subsequent MS, yields a final product of [Pt(bme-dach)]. The same result is achieved upon MS3 of [Zn(bme-dach)-PtCl]. This indicates that platinum binding induces zinc ejection after which, platinum can be incorporated into the macrocycle[53].

The same zinc model was used to study the reactions of [PtCl(dien)]$^+$ and [PtCl(terpy)]$^+$, Figure 1.15. For the reaction of [PtCl(dien)]$^+$ with the model chelate, mass spectrometry shows the formation of two major peaks ([Zn(bme-dach)(Pt(dien))]$^{2+}$ and [Zn(bme-dach)Cl-(Pt(dien))]$^+$) and two minor peaks ([(Zn(bme-dach)$_2$)Pt(dien)] and [(Zn(bme-dach)$_3$)Pt-
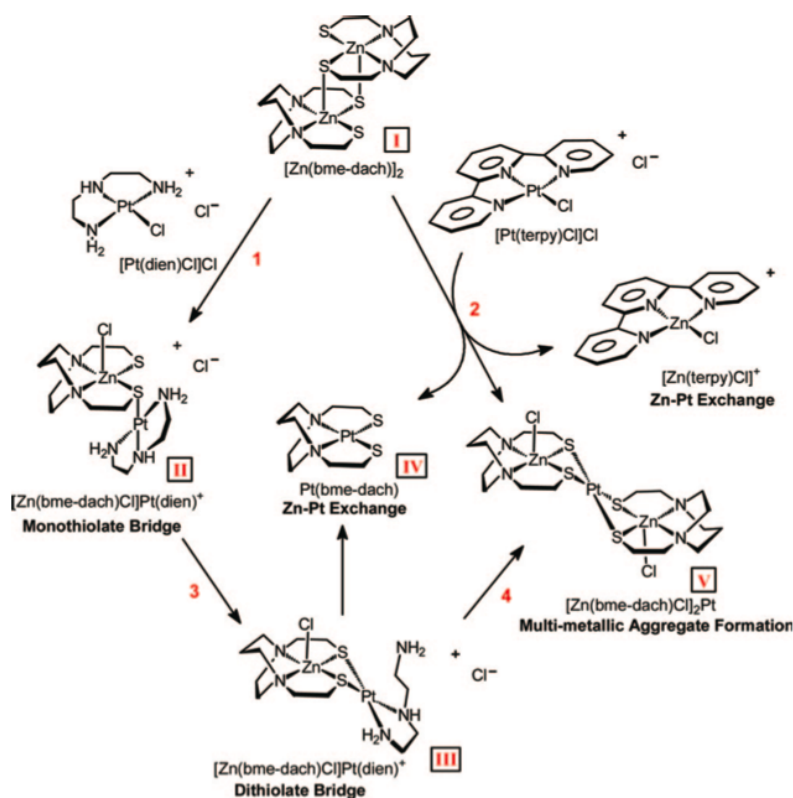
Figure 1.15: Reaction pathways of the reaction of [Zn(bme-dach)]$_2$ with [PtCl(dien)]Cl and [PtCl(terpy)]Cl showing the formation of thiolate-bridged, metal-exchanged, and multimetallic aggregate species.

18

(dien)]); the products do not change with time. MS2 of [Zn(bme-dach)Cl(Pt(dien))]$^+$ shows loss of Cl and MS3 yields [PtCl(dien)]$^+$ and [[Zn(bme-dach))Pt]$^+$. ^{195}Pt NMR of the reaction shows the reaction from PtN$_3$S to PtS$_4$ over time and a yellow precipitate was isolated and identified by crystallography as [Zn(bme-dach)]$_2$Pt. The opening of the dien chelate ring displays the strong *trans* influence of the cysteinate[54].

The reaction of [PtCl(terpy)]$^+$ with [Zn(bme-dach)]$_2$ was studied at a ratio of 1:1 (Zn:Pt) and 2:1 (Zn:Pt). At a 1:1 ratio, the mass spectrum showed a series of ligand-scrambled species at 5 minutes. Peaks were seen for [ZnCl(terpy)]$^+$, [Pt(bme-dach)]$^+$, and {[Zn- (bme-dach)]$_2$PtCl]}$^+$. The major peak for 1:2 ratio corresponds to [(Zn(bme-dach)-Pt(terpy)]$^+$ and minor peaks are seen for [Zn$_3$(bme-dach)$_2$(terpy)Cl$_3$], [Zn(bme-dach)]$_3$PtCl]$^+$, and [Zn(bme-dach)]$_4$PtCl]$^+$ [54].

The model chelate studies correlate well with experimental data, as ligand scrambling was also seen for the reaction of [PtCl(terpy)]$^+$ with the C-terminal ZF of HIV1 NCp7. These studies further exemplified the ability to change the reactivity profile of platinum complexes with Zn-containing nucleophiles.

1.6 Non-covalently-interacting PtN$_4$ complexes as selective agents for targeting NCp7

While the monofunctional platinum complexes exhibit some antiviral activity, the labile chloro group allows for non-specific reactions between the platinum center and sulfur-containing proteins, such as human serum albumin (HSA) or glutathione. Therefore, we have moved to a non-covalent approach, in which platinum is bound to four substitution inert N-containing ligands. Compounds of the structure [Pt(dien)(L)]$^{n+}$ where L is a nucleobase have been evaluated for their π-stacking interactions with Trp and the C-terminal ZF of HIV1 NCp7, Figure 1.16. We have used the analogy of a "weak electrophile" for these substitution-

inert complexes compared to other organic weak electrophiles that have been used to target NCp7.
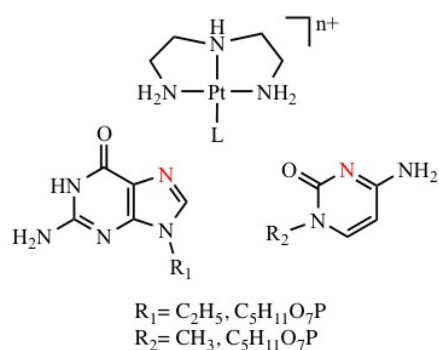
Figure 1.16: Structure of $[Pt(dien)L]^{n+}$ complexes with the platinum binding site highlighted in red.

The π-stacking interaction between aromatic amino acids, such as Trp, and a nucleobase is a defining characteristic of protein/DNA recognition. It has been shown that N-quaternization of nucleobases enhances the stacking interaction by lowering the energy of the LUMO of the nucleobase, making it closer in energy to the HOMO of Trp. The change in the energy of the LUMO may be due to the removal of the lone pair of electrons on the nitrogen of the nucleobase[55]. Another way to remove the lone pair is through coordination to a metal. In this way, metalation and alkylation can be directly compared as a way to modify nucleobases to increase the stacking interaction with aromatic amino acids. Assessment of the HOMO/LUMO energies can be a simple way to compare alkylation and metallation and predict their effects on π-stacking with Trp. DFT calculations have shown that coordination of the nucleobase derivatives 1MeCyt and 9-EtGua to Pt or Pd results in a lowering of the HOMO and LUMO, similar to that seen upon protonation and methylation[56]. The energy of the LUMO of the Pt complexes are closer to the HOMO of Trp than for Pd, which is in agreement with higher K_a values that have been published for Pt[57,58].

Fluorescence quenching of Trp is measured in the presence of a nucleobase or platinum-nucleobase complex in order to calculate an association constant. Due to an electron transfer from the Trp indole ring to the nucleobase in the excited state, a quenching of Trp fluorescence is seen and can therefore be considered a good indicator of the strength of the interaction[55]. Our group has published studies of platinum and palladium nucleobase/nucleotide complexes

with N-AcTrp compared to free nucleobase/nucleotide. On average, free 9-EtGua, GMP, and CMP have K_a values of 3×10^3 M^{-1} while platination increases the K_a for all nucleobases to 6.8, 6.9, and 7.0 $\times10^3$ M^{-1}, respectively. 1MeCyt has a K_a value higher than the other free nucleobases/nucleotide at 6.0×10^3 M^{-1} and upon platination sees a slightly smaller increase to 8.8×10^3 M^{-1}. This increase is associated with the above-mentioned lowering of the LUMO of the nucleobase[57]. These studies show that platinum nucleobase complexes have the potential to be used as probes for protein/DNA interaction through their ability to π-stack with Trp.
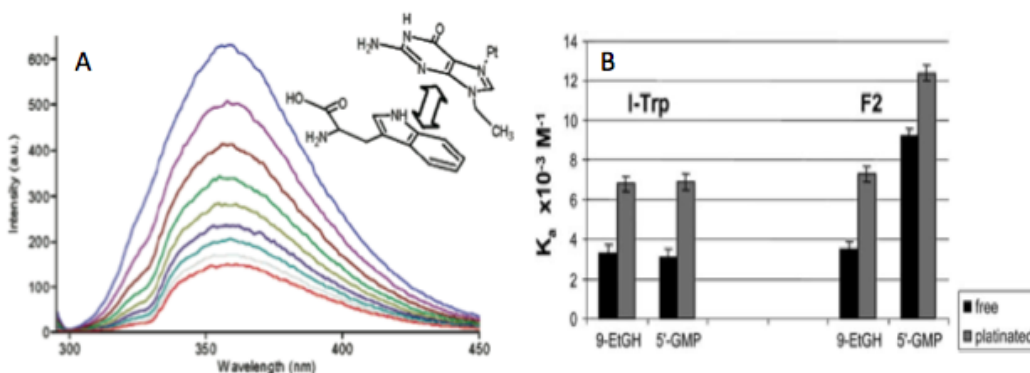
Figure 1.17: (A) Fluorescence quenching of L-Trp in the presence of $[Pt(dien)L]^{2+}$ (B) Calculated K_a values for free and $[Pt(dien)L]^{2+}$ nucleobases with L-Trp and the C-terminal ZF of HIV1 NCp7.

The studies to determine the K_a of platinum complexes with Trp in solution can be extended to short peptide sequences. Electrophilic compounds that modify the Cys residues and subsequently eject zinc have been identified (8). Our group has extended the concept of electrophilic attack to PtN_4 species. The Trp stacking interaction with the C-terminal ZF of HIV1 NCp7 for $[Pt(dien)(9-EtGua)]^{2+}$ and $[Pt(dien)(GMP)]$ was studied and the K_a values were found to be 7.5 and 12.4 $\times10^3$ M^{-1}, respectively (Figure 1.17)[49]. While the phosphate group of the GMP does not have a strong effect on the stacking interaction with free Trp, it enhances the stacking with ZF. This may be due to an extra recognition feature (Lys-phosphate) that has been previously reported for NCp7 with dACGCC[49,59]. The CD

spectrum of the ZF does not change in the presence of $[Pt(dien)(9\text{-}EtGua)]^{2+}$ which suggests that the stacking interaction does not disrupt the three-dimensional structure. Analysis by ESI-MS shows an adduct corresponding to $[Pt(dien)(9\text{-}EtGua)]/ZF$ and upon MS2 of the parent ion, peaks corresponding to $[Pt(dien)(9\text{-}EtGua)]$, ZF, $[Pt(dien)(9\text{-}EtGua)]/ZF$, and $[Pt(dien)]/ZF$ were seen indicating that non-covalent and covalent complexes form between ZF and $[Pt(dien)(9\text{-}EtGua)]^{2+}$ [49].

1.7 Interaction of Platinated DNA with the C-terminal ZF of HIV1 NCp7
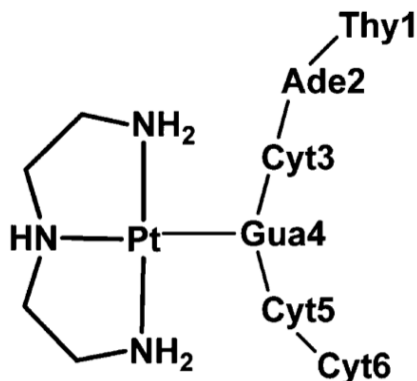
Figure 1.18: Structure of [Pt(dien)6-mer].

The interaction of Pt(dien)(6-mer) (6-mer = d'(5'-TACGCC-3') with the C-terminal finger of the HIV NCp7 zinc finger was studied by NMR Spectroscopy, Figure 1.18. Upon coordination to platinum, significant structural changes were seen compared to the uncoordinated 6-mer, Figure 1.19. The tryptophan resonances were shifted upfield and broadened, while the H8 of Gua4 remained downfield, confirming platination. Both cytosines remained in the same environment upon platination. Other major shifts were seen for Gln45, Met46, Lys47, and Glu50. The Zn-Cys/His chemical shifts show only minor changes[60].

The solution structures of the ZF, 6-mer/ZF, and Pt(dien)6mer/ZF adducts were calculated from NOESY-derived distance constraints. An interaction between Trp37 and the ribose protons of Gua4 of the hexanucleotide was observed. Metallation of Gua4 results in a change of orientation of the aromatic ring of tryptophan (Figure 1.19B), a result of which
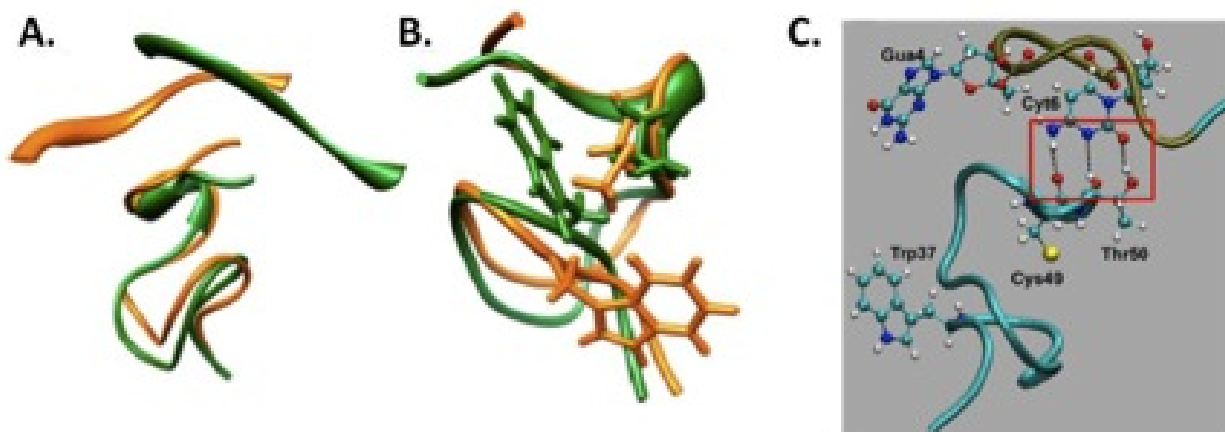
Figure 1.19: (A) Superposition of the minimized structures of the 6-mer/F2 adduct (green) and the Pt(dien)(6-mer)/F2 adduct (orange). (B) Change in conformation of Trp37 upon platination of Gua4. (C) Stabilizing interactions of Cyt6 with the protein residues, Cys49 and Thr50, in the Pt(dien)(6-mer)/F2 adduct (hydrogen bonding highlighted in red box).

is a conformational change in the overall DNA structure. This is reflected in the weakening of the Trp37-Gua4 contact for Pt(dien)(6-mer) when compared with unbound 6-mer. These conformational changes can be attributed to the steric effects caused by platination of Gua4[60].

Molecular dynamics calculations of the DNA-protein interactions showed that the π-stacking between Trp37 and Gua4 as well as the hydrogen bonding between the ribose and phosphate oxygen(s) of Cyt5 and Gua4 help stabilize the interactions between the 6-mer and ZF. Once platinum is bound, the 6-mer is less flexible and stays in one stable conformation on the surface of the zinc finger. The Gua4-Trp37 interaction is disrupted, resulting in hydrogen bonding interactions between Cyt6 and Cys49 and Thr50. Additionally, the backbone CH group is close to N3 of Cyt6. With the addition of this third hydrogen bond, the bonding mode imitates the three intermolecular Cyt-Gua base pair hydrongen bonds (Figure 1.19C)[60].

These results are the first example of structural characterization of platinated single-stranded DNA interacting with a zinc finger protein, resulting in conformational change of

the peptide. The studies performed show the feasibility of using DNA-tethered coordination compounds to target zinc finger proteins[60].

1.8   References

1. Finney, L. A.; O'Hallaran, T. V. Transition metal speciation in the cell: insights from the chemistry of metal ion receptors. Science **2003**, *300*, 931-936.

2. Silver, S.; Walden, W. Overview of cellular inorganic metabolism and the need for gene regulation. In Metal Ions in Gene Regulation; Silver, S., Walden, W., Eds.; Springer-Science+Business Media, B.V., **1998**; pp 1-10.

3. Sabat, M. Ternary metal ion-nucleic acid base-protein complexes. Met. Ions Biol. Syst. **1996**, *32*, 522-555.

4. Reynolds, M.; Peterson, E.; Quievryn, G.; Zhitkovich, A. Human nucleotide excision repair efficiently removes chromium-DNA phosphate adducts and protects cells against chromate toxicity. J. Biol. Chem. **2004**, *279*, 30419-30424.

5. Rosenburg, B.; Van Camp, L.; Krigas, T. Inhibition of cell division in Escherichia coli by electrolysis products from a platinum electrode. Nature **1965**, *205*, 698-699.

6. Alderen, R. A.; Hall, M. D.; Hambley, T. W. The discovery of cisplatin. J. Chem. Ed. **2006**, *83*, 728-734.

7. Jung, Y.; Mikata, Y.; Lippard, S. J. Kinetic studies of the TATA-binding protein interaction with cisplatin-modified DNA. J. Biol. Chem. **2001**, *276*, 43589-43596.

8. Kasparkova, J.; Farrell, N.; Brabec, V. Sequence specificity, conformation, and recognition by HMG1 protein of major DNA interstrand cross-links of antitumor dinuclear platinum complexes. J. Biol. Inorg. Chem. **2000**, *75*, 15789-15798.

9. Farrell, N. Preclinical perspectives on the use of platinum compounds in cancer chemotherapy. Semin. Oncol. **2004**, *31*, 1-9.

10. Kartalou, M.; Essigmann, J. M. Mechanisms of resistance to cisplatin. Mutat. Res. **2001**, *478*, 23-43.

11. Samimi, G.; Safaei, R.; Katano, K.; Holzer, A.; Rochdi, M.; Tomioka, M.; Goodman, M.; Howell, S. B. Increased Expression of the Copper Efflux Transporter ATP7A Mediates Resistance to Cisplatin, Carboplatin, and Oxaliplatin in Ovarian Cancer Cells. Clin. Cancer Res. **2004**, *10*, 4661-4669.

12. Song, I. M.; Savaraj, N.; Siddik, Z. H.; Liu, P.; Wei, Y.; Wu, C. J.; Kuo, M. T. Role of human copper transporter Ctr1 in the transport of platinum-based antitumor agents in cisplatin-sensitive and cisplatin-resistant cells. Mol. Cancer Ther. **2004**, *3*, 1543-1549.

13. Timerbaev, A. R.; Aleksenko, S. S.; Polec-Powlak, K.; Ruzik, R.; Semenova, O.; Hartinger, C. G.; Oszwalkdowski, S.; Galanski, M.; Jarosz, M.; Keppler, B. K. Platinum metallodrug-protein binding studies by capillary electrophoresis-inductively coupled plasma-mass spectrometry: Characterization of interactions between Pt(II) complexes and human serum albumin. Electrophoresis **2004**, *25*, 1988-1995.

14. Peleg-Shulma, T.; Gibson, D. Cisplatin-protein adducts are efficiently removed by glutathione but not by 5'-guanosine monophosphate. J. Am. Chem. Soc. **2001**, *123*, 3171-3172.

15. Masters, J. R.; Thomas, R.; Hall, A. G.; Hogarth, L.; Matheson, E. C.; Cattan, A. R.; Lohrer, H. Sensitivity of testis tumour cells to chemotherapeutic drugs: Role of detoxifying pathways. Eur. J. Cancer **1996**, *7*, 1248-1253.

16. Montine, T. J.; Borcch, R. F. Role of endogenous sulfur-containing nucleophiles in an

in vitro model of *cis*-diamminedichloroplatinum(II)-induced nephrotoxicity. Biochem. Pharmacol. **1990**, *39*, 1751-1757.

17. Farrell, N.; Ha, T. T. B.; Souchard, J. P.; Wimmer, F. L.; Cros, S.; Johnson, N. P. Cytostatic *trans*-platinum(II) complexes. J. Med. Chem. **1989**, *32*, 2240-2241.

18. Farrell, N.; Kelland, L. R.; Roberts, J. D.; Van Beusichem, M. Activation of the *trans* geometry in platinum antitumor complexes: a survey of the cytotoxicity of *trans* complexes containing planar ligands in murine L1210 and human tumor panels and studies on their mechanism of action. Cancer Res. **1992**, *52*, 5065-5072.

19. Zakovska, A.; Novakova, O.; Balcarova, Z.; Bierbach, U.; Farrell, N.; Brabec, V. DNA interactions of antitumor *trans*-[PtCl$_2$(NH$_3$)(quinoline)]. Eur. J. Biochem. **1998**, *254*, 547-557.

20. Brabec, V.; Neplechova, K.; Kasparkova, J.; Farrell, N. Steric control of DNA interstrand cross-link sites of *trans* platinum complexes: specificity can be dictated by planar nonleaving groups. J. Biol. Inorg. Chem. **2000**, *5*, 364-368.

21. Kasparkova, J.; Novakova, O.; Farrell, N.; Brabec, V. DNA binding by antitumor *trans*-[PtCl$_2$(NH$_3$)(thiazole)]. Protein recognition and nucleotide excision repair of monofunctional adducts. Biochem. **2003**, *42*, 792-800.

22. Darlix, J. L.; Gabus, C.; Nugeyere, M. T.; Clave, F.; Barre-Sinoussi, F. *Cis* elements and *trans*-acting factors involved in the RNA dimerization of the human immunodeficiency virus HIV-1. J. Mol. Biol. **1990**, *216*, 689-699.

23. Amarasinghe, G. K.; de Guzman, R. N.; Turner, R. B.; Chancellor, K. J.; Wu, Z. R.; Summers, M. F. NMR Structure of the HIV-1 Nucleocapsid Protein Bound to Stem-Loop SL2 of the Psi-RNA Packaging Signal. Implications for Genome Recognition. J. Mol. Biol. **2000**, *301*, 491-511.

24. de Guzman, R. N.; Wu, Z. R.; Stalling, C. C.; Pappalardo, L.; Borer, P. N.; Summers, M. F. Structure of the HIV-1 Nucleocapsid Protein Bound to the SL3 Ψ-RNA Recognition Element. Science **1998**, *279*, 384-388.

25. Klug, A. The Discovery of Zinc Fingers and Their Applications in Gene Regulation and Genome Manipulation. Ann. Rev. Biochem. **2010**, *79*, 213-231.

26. Anzellotti, A. I.; Farrell, N. P. Zinc metalloproteins as medicinal targets. Chem. Soc. Rev. **2008**, *37*, 1629-1651.

27. Quintal, S. M.; de Paula, Q. A.; Farrell, N. P. Zinc finger proteins as templates for metal ion exchange and ligand reactivity. Chemical and biological consequences. Metallomics **2010**,*3*, 121-139.

28. Li, L.; Lu, X.; Peterson, C. A.; Legerski, R. J. An interaction between the DNA repair factor XPA and replication protein A appears essential for nucleotide excision repair. Mol. Cell Biol. **1995**, *15*, 5396-5402.

29. Mely, Y.; De Rocquigny, H.; Morellet, N.; Roques, B. P.; Gerard, D. Zinc binding to the HIV-1 nucleocapsid protein: a thermodynamic investigation by fluorescence spectroscopy. Biochem. **1996**, *35*, 5175-5182.

30. Chertova, E. N.; Kane, B. P.; McGrath, C.; Johnson, D. G.; Sowder II, R. C.; Arthur, L. O.; Henderson, L. E. Proping the topography of HIV-1 nucleocapsid protein with the alkylating agent N-ethylmalemide. Biochem. **1998**, *37*, 17890-17897.

31. Hathout, Y.; Fabris, D.; Han, M. S.; Sowder II, R. C.; Henderson, L. E.; Fenselau, C. Characterization of intermediates in the oxidation of zinc fingers in Human Immunodeficiency Virus Type 1 nucleocapsid protein P7. Drug Metab. Dispos. **1996**, *24*, 1395-1400.

32. Tummino, P. J.; Scholten, J. D.; Harvey, P. J.; Holler, T. P.; Maloney, L.; Gogliotti, R.; Domagala, J.; Hupe, D. The *in vitro* ejection of zinc from human immunodeficiency virus (HIV) type 1 nucleocapsid protein by disulfide benzamides with cellular anti-HIV activity. PNAS **1996**, *93*, 969-973.

33. Maynard, A. T.; Covell, D. G. Reactivity of Zinc Finger Cores: Analysis of Protein Packing and Electrostatic Screening. J. Am. Chem. Soc. **2001**, *123*, 1047-1058.

34. Morellet, N.; Demene, H.; Teilleux, V.; Huynh-Dinh, T.; Roques, M. C.; Fournie-Zaluski, M. C.; Roques, B. P. Structure of the complex between the HIV-1 nucleocapsid protein NCp7 and the single-stranded pentanucleotide d(ACGCC). J. Mol. Biol. **1998**, *283*, 419-434.

35. Andreini, C.; Banci, L.; Bertini, I.; Rosato, A. Counting the zinc-proteins encoded in the human genome. J. Proteosome Res. **2006**, *5*, 196-201.

36. Musah, R. A. The HIV nucleocapsid zinc finger protein as a target of antiretroviral therapy. Curr. Topics in Med. Chem. **2004**, *4*, 1605-1622.

37. Freed, E. O. HIV-1 GAG proteins: diverse fuctions in the virus life cycle. Virology **1998**, *251*, 1-15.

38. Rice, W. G.; Schaeffer, C. A.; Graham, L.; Bu, M.; McDougal, J. S.; Orloss, S. L.; Villinger, F.; Young, M.; Oroszlan, S.; Fesen, M. R.; Pommier, Y.; Mendeleyev, J.; Kun, E. The site of antiviral action of 3-nitrosobenzamide on the infectivity process of human immunodeficiency virus in human lymphocytes. PNAS **1993**, *90*, 9721-9724.

39. Huang, M.; Maynard, A.; Turpin, J. A.; Graham, L.; Janini, G. M.; Covell, D. G.; Rice, W. G. Anti-HIV agents that selectively target retroviral nucleocapsid protein zinc fingers without affecting cellular zinc finger proteins. J. Med. Chem. **1998**, *41*, 1371-1381.

40. Druillennec, S.; Roques, B. P. HIV-1 NCp7 as a target for the design of novel antiviral agents. Drugs News Perspect. **2000**, *13*, 337-349.

41. Rice , W. G.; Supko, J. G.; Malspeis, L.; Buckheit, jr., R. W.; Clanton, D.; Bu, M.; Graham, L.; Schaeffer, C. A.; Turpin, J. A.; Domagala, J. Inhibitors of HIV nucleocapsid protein zinc fingers as candidates for the treatment of AIDS. Science **1995**, *270*, 1194-1197.

42. Goebel, F. D.; Hemmer, R.; Schmit, J. C.; Bogner, J. R.; de Clercq, E.; M.; Pannecouque, C.; Valeyev, R.; Vandevelde, M.; Margery, H.; Tassignon, J. P. Phase I/II dose escalation and randomized withdrawal study with add-on azodicarbonamide in patients failing on current antiretroviral therapy. AIDS **2001**, *15*, 33-45.

43. Miller Jenkins, L. M.; Ott, D. E.; Hayashi, R.; Coren, L. V.; Wang, D.; Xu, Q.; Schito, M. L.; Inman, J. K.; Appella, D. H.; Appella, E. Small molecule inactivation of HIV-1 NCp7 by repetitive intracellular acyl transfer. Nat. Chem. Biol. **2010**, *6*, 887-889.

44. Stephen, A.G.; Worthy, K.M.; Towler, E.; Mikovits, J.A.; Sei, S.; Roberts, P.; Yang, Q.E.; Akee, R.K.; Klausmeyer, P.; McCloud, T.G.; Henderson, L.; Rein, A.; Covell, D.G.; Currens, M.; Shoemaker, R.H.; Fisher, R.J. Identification of HIV-1 nucleocapsid protein:nucleic acid antagonists with cellular anti-HIV activity. Biochem. Biophys. Res. Comm. **2002**, *296*, 1228-1237.

45. Shvadchak, V.; Sanglier, S.; Rocle, S.; Villa, P.; Haiech, J.; Hibert, M.; Van Dorsselar, A.; Mely, Y.; de Rocquigny, H. Identification by high throughput screening of small compounds inhibiting the nucleic acid destabilization of the HIV-1 nucleocapsid protein. Biochimie **2009**, *91*, 916-923.

46. Cleare, M. J.; Hoeschele, J. D. Studies on the antitumor activity of Group VIII transition metal complexes. Part I. Platinum (II) complexes. Bioinorg. Chem. **1973**, *2*,

187-210.

47. Ratilla, E. M. A.; Scott, B. K.; Moxness, M. S.; Kostic, N. M. Terminal and new bridging coordination of methylguanidine, arginine, and canavanine to platinum(II). The first crystallographic study of bonding between a transition metal and a guanidine ligand. Inorg. Chem. **1990**, *29*, 918-926.

48. Bombarda, E.; Cherrade, H.; Morellet, N.; Roques, B. P.; Mely, Y. Zn2+ Binding properties of single-point mutants of the C-terminal zinc finger of the HIV-1 nucleocapsid protein:âĂĽ evidence of a critical role of cysteine 49 in Zn^{2+} dissociation. Biochem. **2002**, *41*, 4312-4320.

49. Anzellotti A.I.; Liu Q.; Bloemink M.J.; Scarsdale J.N.; Farrell N. Targeting retroviral Zn finger-DNA interactions: a small-molecule approach using the electrophilic nature of *trans*-platinum-nucleobase compounds. Chem. Biol. **2006**, *13*, 539-548.

50. Anzellotti, A.; Stefan, S.; Gibson, D.; Farrell, N. Donor atom preferences in substitution reactions of trans-platinum mononucleobase compounds: Implications for DNAâĂŞprotein selectivity. Inorg. Chim. Acta **2006**, *339*, 3014-3019.

51. Sartori, D. A.; Miller, B.; Bierbach, U.; Farrell, N. Modulation of the chemical and biological properties of trans platinum complexes: monofunctional platinum complexes containing one nucleobase as potential antiviral chemotypes. J. Bio. Inorg. Chem. **2000**, *5*, 575-583.

52. Grapperhaus, C. A.; Tuntulani, T.; Reibenspies, J. H.; Darensbourg, D. Y. Methylation of tethered thiolates in [(bme-daco)Zn]$_2$ and [(bme-daco)Cd]$_2$ as a model of zinc sulfur-methylation proteins. Inorg. Chem. **1998**, *37*, 4052-4058.

53. Liu, Q.; Golden, M.; Darensbourg, M. Y.; Farrell, N. Thiolate-bridged heterodinuclear platinumâĂŞzinc chelates as models for ternary platinumâĂŞDNAâĂŞprotein

complexes and zinc ejection from zinc fingers. Evidence from studies using ESI-mass spectrometry. Chem. Comm. **2005**, 4360-4362.

54. Almaraz, E.; de Paula, Q. A.; Liu, Q.; Reibenspies, J. H.; Darensbourg, M. Y.; Farrell, N. P. Thiolate bridging and metal exchange in adducts of a zinc finger model and Pt(II) complexes: biomimetic studies of protein/Pt/DNA interactions. J. Am. Chem. Soc. **2008**, *130*, 6272-6280.

55. Kawai, H.; Tarui, M.; Doi, M.; Ishida, T. Enhancement of aromatic amino acid-nucleic acid base stacking interaction by metal coordination to base: fluorescence study on a tryptophan-Pt(II)-guanine ternary complex. FEBS Letters **1995**, *370*, 193-196.

56. Anzelloti, A. I.; Bayse, C. A.; Farrell, N. P. Effects of nucleobase metalation on frontier molecular orbitals: potential implications for ÏĂ-stacking interactions with tryptophan. Inorg. Chem. **2008**, *47*, 10425-10431.

57. Anzellotti, A. I.; Ma, E. S.; Farrell, N. P. Platination of nucleobases to enhance noncovalent recognition in protein-DNA/RNA complexes. Inorg. Chem. **2005**, *44*, 483-485.

58. Anzellotti, A. I.; Sabat, M.; Farrell, N. Covalent and noncovalent interactions for [Metal(dien)nucleobase]$^{2+}$ complexes with L-tryptophan derivatives: formation of palladiumâĹŠtryptophan species by nucleobase substitution under biologically relevant conditions. Inorg. Chem. **2006**, *45*, 1638-1645.

59. Venter, J. C.; Adams, M. D.; Myers, E. W.; Li, P. W.; Mural, R. J.; Sutton, G. G.; Smith, H. O.; Yandell, M.; Evans, C. A.; Holt, R. A.; al., e. The sequence of the human genome. Science **2001**, *291*, 1304-1313.

60. Quintal, S. M.; dePaula, Q. P.; Farrell, N. P. Zinc finger proteins as templates for metal ion exchange and ligand reactivity. Chemical and biological consequences. Metallomics **2011**, *3*, 121-139.

Dissertation Outline

The work presented in this dissertation is a continuation of the previously published work designing platinum agents selective for HIV1 NCp7. Targeting of NCp7 is of particular interest due to its intolerance to mutation and importance in the viral life cycle. The success of our work to develop anti-HIV platinum complexes is highlighted by the fact that some of the previous $[\text{PtCl(L)(L')(nucleobase)}]^+$ compounds show anti-viral activity *in vitro*. It is important to understand how platinum complexes interact with proteins and what enhances these reactions. The effect of the presence of a tryptophan residue in a short peptide sequence on the reactivity of the platinum-nucleobase compound $[\text{Pt(dien)(9-EtGua)}]^{2+}$ was evaluated using ^{195}Pt, ^{1}H NMR and mass spectrometry in Appendix A.

Previous studies have used the C-terminal ZF of HIV1 NCp7 as a model for the full two-zinc finger peptide, NCp7. NCp7 plays a critical role in nearly all steps of the HIV1 viral life cycle. Therefore, the ability of $[\text{Pt(dien)(9-EtGua)}]^{2+}$ to interrupt the binding of NCp7 and viral RNA was evaluated using mass spectrometry and gel electrophoresis. These results are reported in Chapter 2. Chapters 3 and 4 explore modulation of the interaction of PtN$_4$ complexes with N-AcTrp and the C-terminal ZF of HIV1 NCp7. It is important to optimize this interaction as it may have important implications for the efficacy of the platinum drug in a larger biological role (interruption of the HIV life cycle).

Chapter 5 and Appendix B evaluate the use of covalently-binding platinum drugs to target NCp7. Other unpublished work related to the development of antiviral platinum agents is discussed in Chapter 6. A review of the importance of metal compounds in the study of the interactions of proteins and DNA/RNA can be found in Appendix C.

Published work will be included in a format as close as possible to that in which it was published.

Chapter 2

A new class of HIV nucleocapsid protein (NCp7)-nucleic acid antagonists

Sarah R. Spell[a], Samantha D. Tsotsoros[a], John B. Mangrum[b], Erica J. Peterson[a], Daniele Fabris[b], and Nicholas P. Farrell[a*]

[a]Department of Chemistry, Virginia Commonwealth University, 1001 W. Main Street, Richmond, VA 23284-2006 USA

[b]The RNA Institute, University at Albany, State University of New York, 1400 Washington Avenue, Albany NY 12222, USA In preparation for submission to J. Inorg. Biochem.

2.1 Contribution

S.D.T.'s contributions include synthesis of $[Pt(dien)(9\text{-}EtGua)]^{2+}$ following literature methods, fluorescence studies, circular dichroism studies and mass spectrometry studies for the platinum complex. S.R.S. contribrutions include synthesis of $[Au(dien)(9\text{-}EtGua)]^{3+}$, circular dichroism and mass spectrometry studies for the gold complex. S.D.T. and S.R.S. were responsible for preparation of the figures. J.B.M.'s contribution inlcudes assistance with mass spectrometry experiments. S.R.S. also contributed to the preparation of the

manuscript.

2.2 Introduction

Assessment of protein packing, steric accessibility and electrostatic screening of zinc finger cores has recognized the enhanced reactivity of Zn-Cys$_3$His coordination spheres over their Cys$_2$His$_2$ counterparts[1,2]. Selectivity for the former, and the ability to distinguish between different zinc finger-coordination spheres, can be found in nucleophilic discrimination through reaction of weak "organic" electrophiles with the highly nucleophilic zinc-cysteine residues[1,2]. In coordination chemistry the equivalent of weak "inorganic" electrophiles has been suggested by us to be <u>formally substitution-inert</u> MN$_4$ compounds with four strong M-N bonds typical of the quintessential soft electrophiles Pt(II) and Au(III)[3]. Compounds containing a Pt(Au)-Cl bond are likely to be far too reactive for <u>protein</u> selectivity - exemplified by the often quoted statement that $< 5\%$ of the administered dose of the anticancer drug cisplatin, cis-[PtCl$_2$(NH$_3$)$_2$], is considered to get to its cellular target DNA.

A significant source of selectivity for HIV-1 inhibition lies in identification of nucleocapsid NC-nucleic acid antagonists[4–6]. Agents which interrupt the interaction with "natural" substrate combined with either electrophilic attack or covalent modification may be classed as a discrete approach to zinc finger inhibition. The aromatic amino acids tryptophan (Trp) and phenylalanine (Phe) are critical for the NC-nucleic acid molecular recognition. The mutation of even one of these residues significantly decreases NC's nucleic acid chaperone activity, and correlates with inhibition of viral replication[7]. Trp interacts with nucleobases through both H-bonding and π-stacking with the indole ring of the W37 residue inserted between adjacent C and G bases and stacked on the latter[8–11]. Metallation of nucleobases, as with protonation and alkylation, enhances π-π stacking interactions with tryptophan, in part due to lowering of the HOMO-LUMO gap[12]. Using the C-terminal finger of the HIVNCp7 (F2, residues 34-52) we have demonstrated the targeting of the critical tryptophan residue

with metallated nucleobases[13,14].

We have now extended these studies to the "full" two-zinc finger NC and its complex with SL2 RNA (SL2). In the presence of the metallated nucleobases $[M(dien)(9\text{-}EtGua)]^{n+}$ (M=Au, n=3, I; M=Pt, n=2, II); 9-EtGua = 9-ethylguanine) the NC-SL2 interaction is inhibited in an antagonist fashion and expands the chemistry of this important HIV target in hitherto unrecognized directions. Incorporation of a functionalized nucleobase within the MN_4 structure as in $[M(dien)(Nucleobase)]^{n+}$ gives agents capable in principle of (i) molecular recognition through the non-covalent tryptophan-nucleobase interaction and (ii) subsequent peptide covalent bond formation through manipulation of the reactivity of the coordination

Figure 2.1: Structures of A) $[M(dien)(9\text{-}EtGua)]^{n+}$ (M=Au, n= 3, I ; Pt, n=2, II), B) SL2 RNA (SL2) and C) HIVNCp7 (NC).

sphere. The contrast in substitution kinetics between the isoelectronic and isostructural Au(III) and Pt(II) compounds provides valuable insights into the antagonist mechanism, allowing for further systematic enhancement of this new biological role for platinum metal complexes. The proposed chemistry represents the first class of inorganic molecules capable of systematic study on the HIV zinc finger with the potential for intrinsic selectivity. The structures of the complexes and biomolecules are shown in Figure 2.1.

2.3   Results and Discussion

Incubation of $[Au(dien)(9\text{-}EtGua)]^{3+}$ (I) with intact NC resulted in the detection of species produced by ejection of both Zn^{2+} ions and incorporation of up to 3 Au ions - AuF, Au_2F and Au_3F, Figure 2.2. There was no evidence for intermediate Au-ligand-peptide

Figure 2.2: ESI-FTICRMS spectra (positive ion mode) of a 1:1 reaction of NC:[Au(dien)(9-EtGua)]$^{3+}$.

species, in contrast to the reaction of the C-terminal finger of NC with [Au(I)(PPh$_3$)(L)]$^{+15}$.

The CD spectrum of NC is characterized by a positive maximum observed at 215 nm. The Au compound caused a decrease in intensity of this band and a significant increase in the negative ellipticity with a slight blue shift of the 195-200 nm band, which are indicative of conformational changes from ordered structure to random coil, Figure 2.3A[16,17]. The pronounced changes are consistent with a loss of structural integrity in NC upon treatment with I.

The effects of these conformational changes on the NC-SL2 interaction were investigated by FT-ICRMS by adding SL2 to an NC sample that was pre-incubated with I for 30 min, or by adding I to preformed NC-SL2 complex. In the former case, only free unbound SL2 was observed, thus indicating that the major structural changes induced by Zn^{2+}-Au^{3+} replacement abrogated the binding capabilities of NC (Figure 2.4). In the latter case, a direct comparison of data obtained from NC-SL2 in the presence/absence of I showed a significant increase of free SL2 in solution (Figure 2.5 and Figure 2.6), thus suggesting that the gold compound is capable of inducing dissociation of the peptide from its cognate RNA. In addition,

36
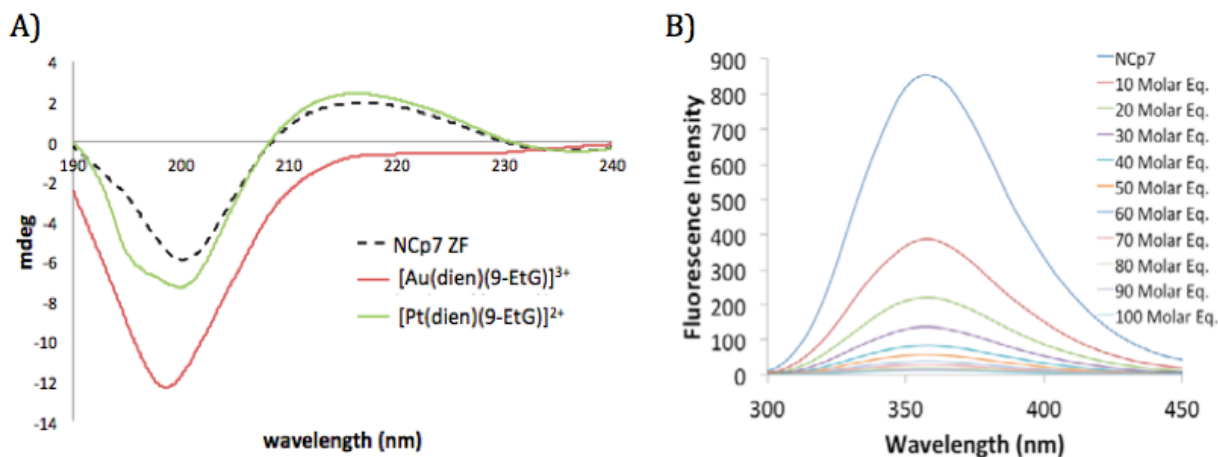
Figure 2.3: A. CD spectra of the reaction of NC and $[M(dien)(9\text{-}EtGua)]^{n+}$ at 15 minutes incubation. B. NC Fluorescence quenching upon addition of $[Pt(dien)(9\text{-}EtGua)]^{2+}$ from 10-100 molar ratios (Pt:Trp).

minor signals corresponding to $[(Au,ZnNC)\text{-}SL2]$ and $[(Au2NC)\text{-}SL2]$ were detected, which are consistent with direct displacement of Zn^{2+} from the intact NC-SL2complex (Figure 2.7).

An advantage of the $[M(dien)(9\text{-}EtGua)]^{n+}$ system is that both isostructural and isoelectronic systems can be studied. The CD spectrum in the presence of $[Pt(dien)(9\text{-}EtGua)]^{2+}$ (II) case shows that there is little disruption of the 3D structure in the presence of the Pt(II) complex, as evidenced by the maintenance of the positive ellipticity, (Figure 2.3A). Incubation of the intact NC with II results in a concentration-dependent decrease in fluorescence from which an association constant (K_a) of 2.0 x 10^4 M^{-1} was calculated, compared to 7.5 x 10^3 M^{-1} for the C-terminal finger alone, [24], Figure 2.3B.

In the case of the Pt complex, analysis under identical experimental conditions as the Au(III) case revealed only weak association between II and NC. Nevertheless, pre-incubation significantly retarded the kinetics of formation of the NC-SL2 complex. Furthermore, addition of II to preformed NC-SL2 complex induced the release of free SL2, similar to the observations afforded by the gold compound, Figure 2.8. In this case, the release of nucleic acid was also accompanied by the detection of a relatively abundant species corresponding
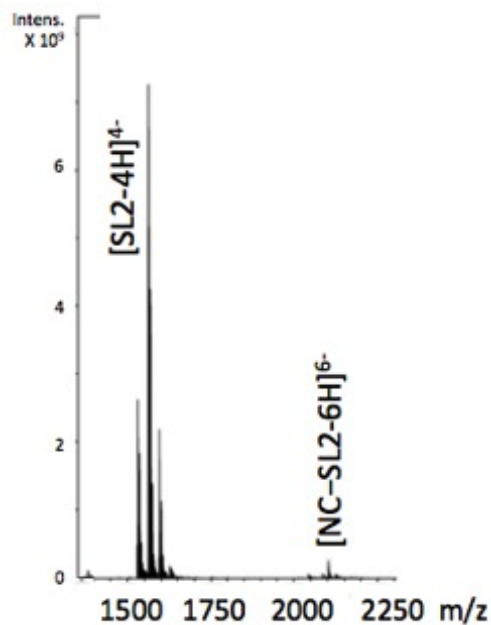
Figure 2.4: FT-ICRMS spectrum (negative ion mode) of 1:1 [Au(dien)(9-EtGua)]$^{3+}$/NC (incubated for 30 minutes) followed by addition of SL2 RNA.
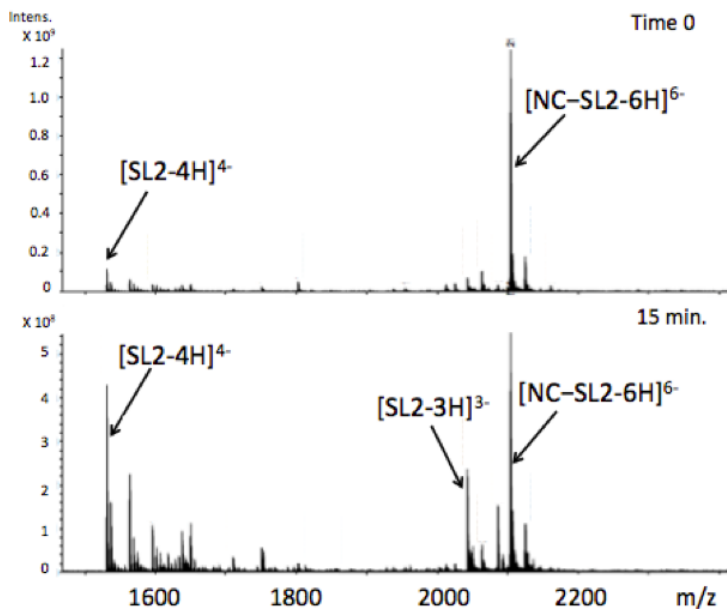
Figure 2.5: FT-ICRMS spectra (negative ion mode) of 2:1 NC-SL2 complex upon addition of 1 eq. [Au(dien)(9-EtGua)]$^{3+}$ (top t=0, run immediately; bottom after 15 mins reaction)
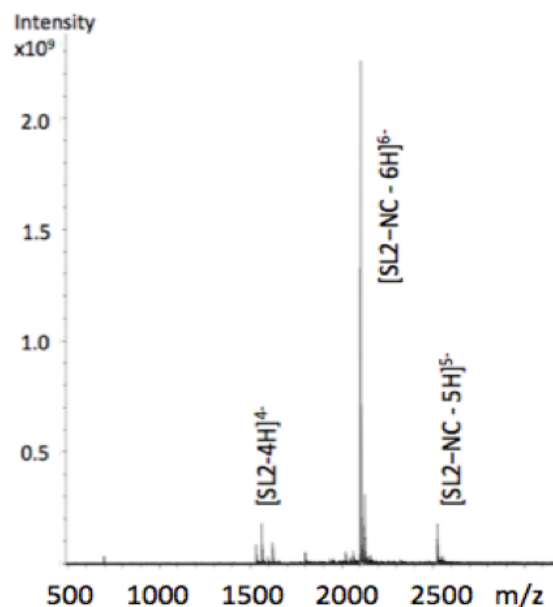
Figure 2.6: FT-ICRMS spectrum (negative ion mode) of NC:SL2 RNA complex in a 2:1 ratio. Note that under these MS conditions, the complex remains intact. These conditions were used before addition of any metallated nucleobase.
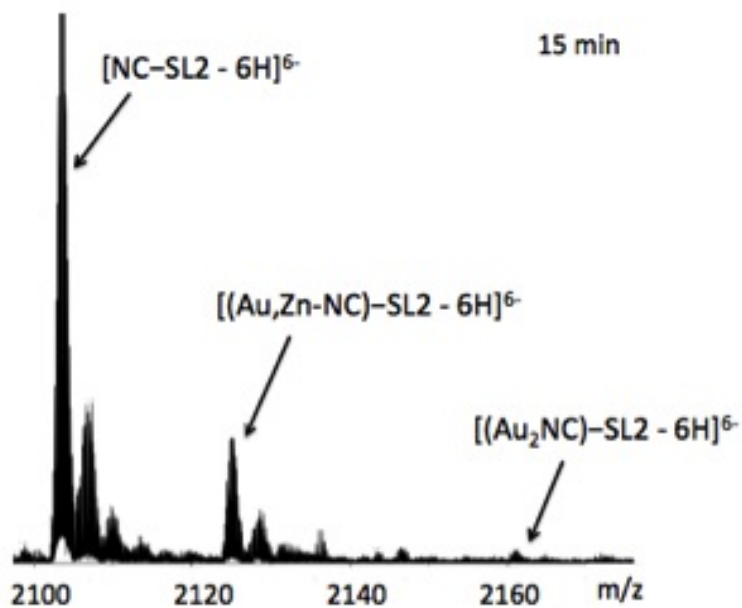
Figure 2.7: Expanded region of 2:1 NC/RNA complex reacted with 1 eq. [Au(dien)(9-EtGua)]$^{3+}$ showing presence of possible RNA-Au-NC crosslinking.

to a [Pt(dien)(9-EtGua)]$^{2+}$-SL2 adduct. Biophysical studies on the interaction of II with Calf Thymus DNA indicated little or no reaction [15], but the tertiary structure of RNA may enhance association.
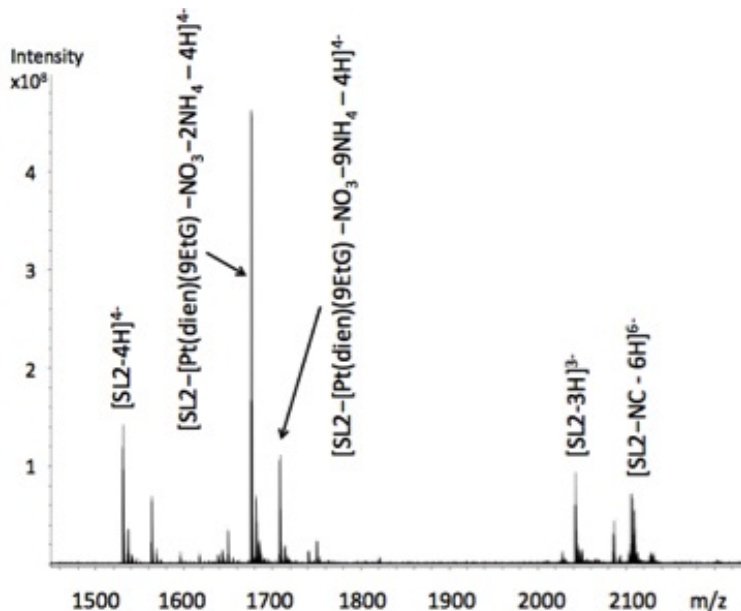
Figure 2.8: ESI-MS Spectrum (negative ion mode) of NC-SL2 (2:1) in presence of 2.5 eq. of [Pt(dien)(9-EtGua)]$^{2+}$ showing liberation of SL2 with decrease in intensity of NC-SL2 species and observation of SL2-[Pt(dien)(9-EtGua)] species.

Electrophoretic mobility shift assays (EMSA) confirm the general trend of these results, Figure 2.9. Increasing concentrations of [Pt(dien)(9-EtGua)]$^{2+}$ results in a decrease in intensity of the NC-SL2 band. Concomitantly, the free SL2 band changes to an upward smear, which again may indicate interaction of the compound itself with the RNA. In contrast, there is no diminution of the NC-SL2 band in the presence of the Au compound, which could be explained by the absence of any interaction, in contradiction to the MS and CD results. An alternative explanation is the possible cross-linking of the two biomolecules by the gold compound, or metabolite or substitution product thereof. In this case, EMSA analysis may be precluded from properly resolving the cross-linked adduct by the large size of the NC-SL2 complex

The cross-linking hypothesis was further investigated by fluorescence polarization experiments using labelled SL2-[Flc]. A control sample consisting of NC and SL2-[Flc] afforded results consistent with formation of the NC-SL2 complex, Table 2.1. Upon incubation of NC for 1 h with increasing concentrations of $[Au(dien)(9-EtGua)]^{3+}$ addition of SL2-RNA-[Flc] gave polarization values that were higher than those obtained from the control sample. Although it would be tempting to explain the strengthening of the RNA-protein interaction with the formation of a stable [NC-Au-SL2] species, the fluorescent anisotropy experiments cannot per se provide direct proof of its formation. Nevertheless, the minor products observed in the MS spectra, Figure 2.7, are consistent with such a hypothesis. The gold compound does not interact with RNA itself, as indicated by the values of polarization afforded by this control, Table 2.1. In agreement, no $[Au(dien)(9-EtGua)]$-SL2 adducts were observed from the MS analysis of Figure 2.5. The "parent" $[AuCl(dien)]^{2+}$ also has only weak affinity for DNA[18]. These results can be rationalized by considering that upon NC interaction,
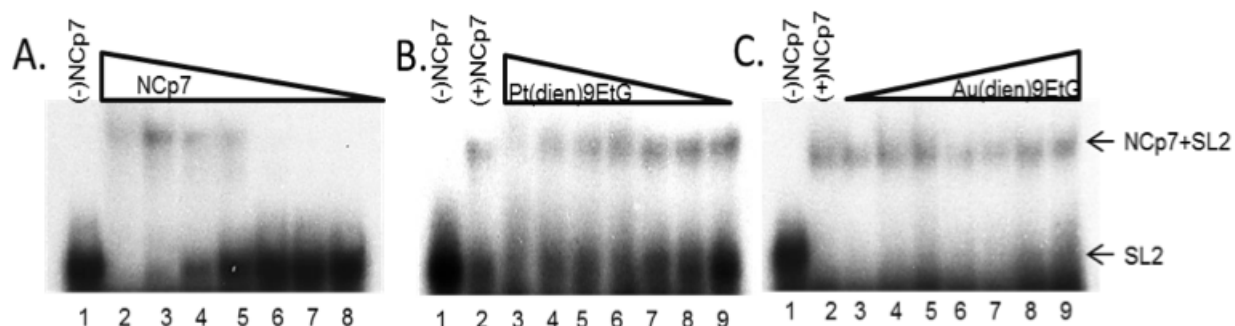
Figure 2.9: Effect of Metal-Nucleobase Compounds on SL2 RNA -NCp7 protein interaction. A: Control Experiment. ^{32}P end-labeled SL2 RNA (2nM) incubated with varying concentrations of NCp7 in binding buffer. Lane 1 contains SL2; Lanes 2-8 1μM, 500, 250, 125, 62.5, 31.3, and 15.6 nM NCp7 respectively. B: Incubation of NC (250nM) with $[Pt(dien)(9-EtGua)]^{2+}$ for 1hr followed by addition of SL2 (2nM) in binding buffer and further incubation for 1 h. Lane 1 contains SL2 only, Lane 2 SL2 and NCp7 only; Lanes 3-9 contain NC, SL2 and 500, 250, 125, 62.5, 31.3, 15.6, and 7.8 μM of I respectively. C: Identical to B in all respects but Lanes 3-9 contain 7.8, 15.6, 31.3, 62.5, 125, 250, and 500 μM $[Au(dien)(9-EtGua)]^{3+}$ respectively.

41

the Au ligands are lost (confirmed by MS and CD studies, Figures 2.2 and 2.3A) and it is possible that coordinatively unsaturated Au-S or Au-OH(H_2O) species could then bind to nucleotides. Of relevance, *trans*-[PtCl$_2$(NH$_3$)$_2$] (tDDP) produces cross-links between NC and HIV-1 RNA[19], presumably by taking advantage of the long-lived nature of monofunctional tDDP-biomolecule adducts[20].

Table 2.1: Fluorescence Polarization (mP) of NC (100 nM) incubated with indicated concentrations of [Au(dien)(9-EtGua)]$^{3+}$ (I) followed by addition of SL2-[Flc] (10nM). See Materials and Methods.

SL2 (-)I	SL2 (+I)I	SL2+NC (-1)I	SL2+NC (+)0.01μM I	SL2+NC (+)0.08μM I	SL2+NC (+)1.25μM I	SL2+NC (+)10μM I
106	101	173.5	169	175	191.5	203

In summary, the results are consistent with the ability of the chemotype [M(dien)(9-EtGua)]$^{n+}$ to act as antagonist of the NC-SL2 interaction, with significant potential for optimization as a structurally discrete new class of agents capable of disrupting the chaperone activity of NC, Scheme 2.1. The differences in profile between the two metallated nucleobases reflect the different substitution kinetics of the central metal ions. Thus, we see immediate displacement of Zn^{2+} by Au^{3+} (MS, CD) whereas with the kinetically inert Pt^{2+} an association constant can be measured and there is no evidence of Zn^{2+} dislocation from the NC under these conditions - the stacking reaction is observed by fluorescence and CD. In this case, purely "non-covalent" approaches appear to allow physical blocking of the interaction. It is reasonable to expect the Au compound to react in the same way - the subsequent loss of ligands upon covalent reaction with peptide is just too fast. Model studies with N-AcTrp confirm the greater stacking of the Au(III) species relative to Pt(II)[21]. Thus, a classical "two-step" approach of molecular recognition followed by target fixation (electrophilic attack on the zinc finger core) is suggested[13]. The greater reactivity of the Au(III) species is also reflected in the possible formation of the higher-order aggregates.

Both components of the NC-nucleic acid chaperone activity have been targeted[22−26].
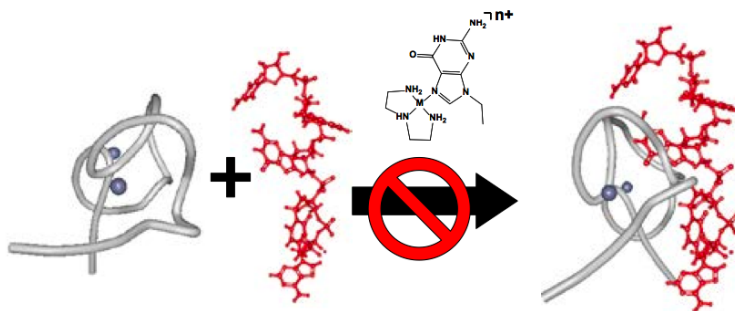
Scheme 2.1: HIV Nucleocapsid-Nucleic Acid Antagonism based on metallated nucleobases.

A study of approximately 2,000 small molecules from the NCI Diversity Set suggested a possible fluoroscein-based pharmacore with a good correlation between tryptophan quenching and inhibition of NC-nucleic acid binding[22]. A second high-throughput screening of small molecules for inhibition of NC-mediated destabilization of the stem-loop structure of cTAR DNA (a sequence complementary to the transactivation response element) produced five selected hits from a total of 4800 compounds[23]. The inhibitory activity of 4 of the 5 correlated with their ability to compete with the nucleic acid for binding to NC[13]. Along with platinum compounds[1,13], gold drug binding to single zinc fingers has been reported by a number of authors[15,27−28], but this report is the first of coordination compounds reacting on a "multiple (>1)" zinc finger peptide. The chemotype has the potential for intrinsic selectivity for this important target over other zinc fingers - the formally substitution-inert species are the equivalent of "weak" electrophiles proposed as one approach to selectivity[3,4].

2.4 Materials and Methods

2.4.1 Synthesis and Biomolecule Preparation

The Pt and Au compounds were prepared as described previously[3,11]. For the MS studies the NC was prepared in the Fabris lab. Briefly, Nucleocapsid (NC) protein of HIV-1 was obtained by *in vitro* expression in E. coli, subsequently purified under non-denaturing con-

ditions to preserve the coordination of Zn^{2+} by its characteristic zinc-finger domains. For the gel shift and biophysical studies, the NC (identical sequence) was a generous gift of Dr. R.J. Gorelick, NIH. RNA oligonucleotides corresponding to the SL2 stem loop domain of the HIV-1 genome packaging signal (Ψ-RNA) were purchased from IDT (Coralville, IA) and desalted using ultrafiltration against 150 mM ammonium acetate.

2.4.2 Mass Spectrometry

Experiments were conducted on a modified Bruker Daltonics (Billerica, MA) SolariX FTICR-MS equipped with a 12T superconducting magnet. Analyses were carried out by direct infusion using tapered quartz nanospray emitters loaded with 5-10 μL of sample with a spray voltage between 800-1100 V relative to the capillary inlet supplied by an inserted stainless steel wire.

Solutions were prepared as follows:

A. 1:1 reaction of NC with $[Au(dien)(9\text{-}EtGua)]^{3+}$

A solution of $[Au(dien)(9\text{-}EtGua)]^{3+}$ (7.5 μM in 1 μL H_2O) was added to a solution of NC (7.5 μM in 1 μL H_2O) and volume was brought up to 10 μL with 7μL 150 μM ammonium acetate and 1 μL isopropyl alcohol. The solution was analyzed immediately in positive ion mode.

B. 1:1:1 reaction of NCp7/$[Au(dien)(9\text{-}EtGua)]^{3+}$ with SL2-RNA, Figure S1.

A solution of NC (7.5 μM in 1 μL H_2O) and $[Au(dien)(9\text{-}EtGua)]^{3+}$ (7.5 μM in 1 μL) was incubated for 30 minutes at room temperature. SL2-RNA (7.5 μM in 1 μL), 6 μL 150 mM ammonium acetate, and 1 μL isopropyl alcohol were added and the mixture was analyzed immediately in negative ion mode.

C. Control experiment showing formation of NC/SL2 (2:1) complex, Figure S2

A solution of NC (7.5 μM in 4 μL H_2O) was added to a solution of SL2 (7.5 μM in 2 μL H_2O) and volume was brought up to 10 μL with 3 μL 150 mM ammonium acetate, and 1

μL isopropyl alcohol. The solution was analyzed immediately. No significant incubation was necessary.

D. 2:1:1 reaction of NC/RNA complex with [Au(dien)(9-EtGua)]$^{3+}$

A solution of NC (7.5 μM in 4 μL H$_2$O) was added to a solution of SL2 (7.5 μM in 2 μL H$_2$O) to form the 2:1 NC/RNA complex. The complex formed immediately; no significant incubation was necessary. A solution of [Au(dien)(9-EtGua)]$^{3+}$ (7.5 μM in 2 μL) was added and volume was brought up to 10 μL with 1 μL 150 mM ammonium acetate and 1 μL isopropyl alcohol. The mixture was analyzed in negative ion mode immediately (time = 0) and after 15 minutes incubation.

E. 2:1:2.5 reaction of NCp7/RNA complex with [Pt(dien)(9-EtGua)]$^{2+}$, Figure S4.

A solution of NC (7.5 μM in 4 μL H$_2$O) was added to a solution of SL2 (7.5 μM in 2 μL H$_2$O) to form the 2:1 NC/RNA complex. Complex formed immediately; no significant incubation was necessary. A solution of [Pt(dien)(9-EtGua)]$^{2+}$ (37.5 μM in 1 μL) was added and volume was brought up to 10 μL with 2 μL 150 mM ammonium acetate and 1 μL isopropyl alcohol. The mixture was analyzed immediately in negative ion mode.

2.4.3 Circular Dichroism

Methods were adapted from those previously published[3,18].

2.4.4 Fluorescence Spectroscopy

Methods were adapted from those previously published[3]. A 3 mL solution of NC (5 μM) in water was titrated with aliquots of the corresponding quenching compound (7.5 mM) in the range [quencher]/[N-AcTrp]) 10-100.

2.4.5   Gel Shift Assays

As a control experiment, ^{32}P end-labeled SL2 RNA (2 nM) was incubated with varying concentrations of NC in binding buffer (50 mM Tris-HCl, 40 mM MgCl$_2$, 200 mM NaCl, 0.1 mM ZnCl$_2$, 5% glycerol, and 1% BME) for 1 hr at 30°C. In all subsequent reactions, 250 nM NC was incubated with increasing concentrations of [Au(dien)(9-EtGua)]$^{3+}$ or [Pt(dien)(9-EtGua)]$^{2+}$ for 1 hr in binding buffer. Subsequently, 2 nM SL2 was added to the buffer and the mixture incubated for an additional hour.

2.4.6   Fluorescence Polarization

In 250 μL total volume, increasing concentrations of NC were incubated with 10 nM fluorescein-labeled SL2 RNA for 4 hrs in minimal buffer (25 μM phosphate buffer, pH 7.2 and 225 mM NaCl) at room temperature to afford control values. In all subsequent experiments, in 250 μL total volume, 100 nM of NC was incubated in minimal Buffer (25 μM phosphate buffer, pH 7.2 and 225 mM NaCl) with varying concentration of drug before addition of 10 nM SL2-RNA[Flc]. The reactions were incubated 4hrs at room temperature and analyzed on a SynergyTM NEO HTS multi-mode microplate reader system.

2.5 References

1. Maynard A.T.; Huang M.; Rice W.G.; Covell D.G. Reactivity of the HIV-1 nucleocapsid protein p7 zinc finger domains from the perspective of density-functional theory. Proc. Natl. Acad. Sci. USA **1998**, *95*, 11578-11583.

2. Maynard A.T.; Covell D.G. Reactivity of Zinc Finger Cores: Analysis of Protein Packing and Electrostatic Screening. J. Am. Chem. Soc. **2001**, *123*, 1047-1058.

3. Quintal S.M.; dePaula Q.A.; Farrell N.P. Zinc finger proteins as templates for metal ion exchange and ligand reactivity. Chemical and biological consequences. Metallomics **2011**, *3*, 121-139.

4. de Paula Q.A.; Tsotsoros S.D.; Qu Y.; Bayse C.A.; Farrell, N.P. Platinum-Nucleobase PtN$_4$ Complexes as Chemotypes for Selective Peptide Reactions with Biomolecules. Inorg. Chim. Acta **2012**, *393*, 222-229.

5. Fisher R.J.; Fivash, M.J.; Stephen, A.G.; Hagan, N.A.; Shenoy, S.R.; Medaglia, M.V.; Smith, L.R.; Worthy, K.M.; Simpson, J.M.; Shoemaker, R.; McNitt, K.L.; Johnson, D.G.; Hixson, C.V.; Gorelick, R.J.; Fabris, D.; Henderson, L.E.; Rein, A. Complex interaction of HIV-1 nucleocapsid protein with oligonucleotides. Nuc. Acids Res. **2006**, *34*, 472-484.

6. Stephen A.G.; Worthy, K.M.; Towler, E.; Mikovitz, K.A.; Sei, S.; Roberts, P.; Yang, Q.; Akee, R.K.; Klausmeyer, P.; McCloud, T.G.; Henderson, L.; Rein, A.; Covell, D.G.; Currens, M.; Shoemaker, R.H.; Fisher, R.J. Identification of HIV-1 nucleocapsid protein:nucleic acid antagonists with cellular anti-HIV activity. Biochem. Biophys. Res. Comm. **2002**, *296*, 1228-1237.

7. Wu, H.; Mitra, M.; McCauley, M.J.; Thomas, J.A.; Rouzina, I.; Musier-Forsyth, K.;

Williams, M.C.; Gorelick, R.J. Aromatic residue mutations reveal direct correlation between HIV-1 nucleocapsid protein's nucleic acid chaperone activity and retroviral replication. Virus Res. **2013** *171*, 263-277.

8. De Guzman, R.N.; Wu, R.; Stalling, C.C.; Pappalardo, L.; Borer, P.N.; Summers, M.F. Structure of the HIV-1 nucleocapsid protein bound to the SL3 Ψ-RNA recognition element. Science **1998** *279*, 384-388.

9. Morellet, N,; Demene, H.; Teilleux, V.; Huynh-Dinh, T.; De Rocquigny, H.; Fournie-Zaluski, M.C.; Roques, B.P. Structure of the complex between the HIV-1 nucleocapsid protein NCp7 and the single-stranded pentanucleotide d(ACGCC). J. Mol. Biol. **1998**, *283*, 419-434.

10. Bourbigot, S.; Ramalanjaona, N.; Boudier, C.; Salgado, G.F.; Roques, B.P.; Mely, Y.; Bouaziz, S.; Morellet, N. How the HIV-1 nucleocapsid protein binds and destabilises the (-) primer binding site during reverse transcription. J. Mol. Biol. **2008**, *383*, 1112-1128.

11. Bazzi, A.; Zargarian, L.; Chaminade, F.; Boudier, C.; De Rocquigny, H.; Rene, B.; Mely, Y.; Fosse, P.; Mauffret, O. Structural insights into the cTAR DNA recognition by the HIV-1 nucleocapsid protein: role of sugar deoxyriboses in the binding polarity of NC. Nuc. Acid Res. **2011**, *39*, 3903-3916.

12. Anzellotti A.I.; Bayse C.A.; Farrell N.P. Effects of nucleobase metalation on frontier moleculear orbitals: Potential implications for π-stacking interactions with tryptophan. Inorg. Chem. **2008**, *47*, 10425-10431.

13. Anzellotti A.I.; Liu Q.; Bloemink M.J.; Scarsdale J.N.; Farrell N. Targeting retroviral Zn finger-DNA interactions: a small-molecule approach using the electrophilic nature of *trans*-platinum-nucleobase compounds. Chem. Biol. **2006**, *13*, 539-548.

14. Anzellotti A.I.; Sabat M.; Farrell N.P. Covalent and noncovalent interactions for [Metal (dien)nucleobase]$^{2+}$ complexes with L-tryptophan derivatives: formation of palladium-tryptophan species by nucleobase substitution under biologically relevant conditions. Inorg. Chem. **2006**, *45*, 1638-1645.

15. Abbehausen, C.; Peterson, E.J.; de Paiva, R.E.F.; Corbi, P.P.; Formiga, A.L.B.; Qu, Y.; Farrell, N.P. Gold(I)-phosphine-N-heterocycles: biological activity and specific (ligand) interactions on the C-terminal HIVNCp7 zinc finger. Inorg. Chem. **2013**, *52*, 11280-11287.

16. Loo, J. A.; Holler, T.P.; Sanchez, J.; Gogliotti, R.; Maloney, L.; Reily, M.D. Biophysical characterization of zinc ejection form HIV nucleocapsid protine by anti-HIV 2,2'-dithiobis[benzamides] and benzisothiazolones. J. Med. Chem. **1996**, *39*, 4313-4320.

17. Omichinski J.G.; Clore G.M.; Sakaguchi K.; Appella E.; Gronenborn A.M. Structural characterization of a 39-residue synthetic peptide contaiing the two zinc bindng domains from the HIV-1 p7 nucleocapsid protein by CD and NMR spectroscopy. FEBS Letters **1991** *292*, 25-30.

18. Messori L.; Orioli P.; Tempi C.; Marcon G. Interactions of Selected Gold(III) Complexes with Calf Thymus DNA. Biochem. Biophys. Res. Commun. **2001**, *281*, 352-360.

19. Darlix J.L.; Gabus C.; Nugeyre M.T.; Clavel F.; Barre-Sinoussi F. *Cis* elements and *trans*-acting factors involved in the RNA dimerization of the human immunodeficiency virus HIV-1. J. Mol. Biol. **1990**, *216*, 689-99.

20. Marini, V.; Christofis, P.; Novakova, O.; Kasparkova, J.; Farrell, N.P.; Brabec, V. Conformation, protein recognition and repair of DNA interstrand and intrastrand cross-

links of Antitumor *trans*-[PtCl$_2$(NH$_3$)(thiazole)]. Nuc. Acids Res. **2005**, *33*, 5819-5828.

21. Spell S.R.; Farrell N.P. Synthesis and properties of the first [Au(dien)(N-heterocycle)]$^{3+}$ compounds. Inorg. Chem. **2014**, *53*, 30-32.

22. Stephen, A.G.; Worthy, K.M.; Towler, E.; Mikovits, J.A.; Sei, S.; Roberts, P.; Yang, Q.E.; Akee, R.K.; Klausmeyer, P.; McCloud, T.G.; Henderson, L.; Rein, A.; Covell, D.G.; Currens, M.; Shoemaker, R.H.; Fisher, R.J. Identification of HIV-1 nucleocapsid protein:nucleic acid antagonists with cellular anti-HIV activity. Biochem. Biophys. Res. Comm. **2002**, *296*, 1228-1237.

23. Shvadchak, V.; Sanglier, S.; Rocle, S.; Villa, P.; Haiech, J.; Hibert, M.; Van Dorsselaer, A.; Mely, Y.; de Rocquigny, H. Identification of high throughput screening of small compounds inhibiting the nucleic acid destabilization activity of the HIV-1 nucleocapsid protein. Biochimie **2009**, *91*, 916-923.

24. Goudreau, N.; Hucke, O.; Faucher, A.M.; Grand-Maitre, C.; Lepage, O.; Bonneau, P.R.; Mason, S.W.; Titolo, S. Discovery and structural characterization of a new inhibitor series of HIV-1 nucleocapsid function: NMR solution structure determination of a ternary complex involving a 2:1 inhibitor/NC stoichiometry. J. Mol. Biol. **2013**, *425*, 1982-1998.

25. Turner K.B.; Hagan N.A.; Fabris D. Inhibitory effects of archetypical nucleic acid ligands on the interactions of HIV-1 nucleocapsid protein with elements of Ψ-RNA. Nuc. Acids Res. **2006**, *34*, 1305-1316.

26. Warui D.M.; Baranger A.M. Identification of small molecule inhibitors of the HIV-1 nucleocapsid-stem-loop 3 RNA complex. J. Med. Chem. **2012**, *55*, 4132-4141.

27. Larabee J.L.; Hocker J.R.; Hanas J.S. Mechanisms of Aurothiomalate-Cys_2His_2 Zinc Finger Interactions. Chem. Res. Toxicol. **2005**, *18*, 1943-1954.

28. Franzman M.A.; Barrios A.M. Spectroscopic Evidence for the Formation of Goldfingers. Inorg. Chem. **2008**, *47*, 3928-3930.

29. Mendes F.; Groessi, M.; Nazarov, A.A.; Tysbin, Y.O.; Sava, G.; Santos, I.; Dyson, P.J.; Cassini, A. Metal-Based Inhibition of Poly(ADP-ribose) Polymerase- The Guardian Angel of DNA. J. Med. Chem. **2011**, *54*, 2196-2206.

Chapter 3

Modification of the $[Pt(dien)L]^{2+}$ coordination sphere to develop inhibitors of HIV1 NCp7

Samantha D. Tsotsoros, Erica J. Peterson and Nicholas P. Farrell[*]

Department of Chemistry, Virginia Commonwealth University, 1001 W. Main Street,

Richmond, VA 23284-2006 USA

3.1   Contribution

This chapter is solely the work of S.D.T. with the exception of the EMSA experiments, which were designed by E.J.P..

3.2   Introduction

The $[M(dien)(nucleobase]^{n+}$ coordination sphere allows for modification in several ways to enhance the π-stacking interaction with Trp, as well as the cellular properties, such as cellular accumulation and cytotoxicity. Here, we evaluate the effect of methylation of the dien ligand as well as various nucleobase-derivatives as the π-stacking ligand. Results

suggest that addition of methyl groups to the dien ligand does not significantly impact cellular accumulation or cytotoxity, but the addition of xanthosine (Xan) results in a very strong π-stacking interaction when compared to the 9-ethylguanine compound.

3.3 Results and Discussion

3.3.1 Chemistry

The structures of the compounds reported in this paper can be found in Figure 3.1. Two main modifications were made on the $[Pt(dien)L]^{2+}$ structure; methylation of the dien and change in π-stacking ligand. Methylation of the dien may provide increased lipophilicity which may have implications for cellular accumulation, while the change in L affects the strength of the π-stacking interaction.
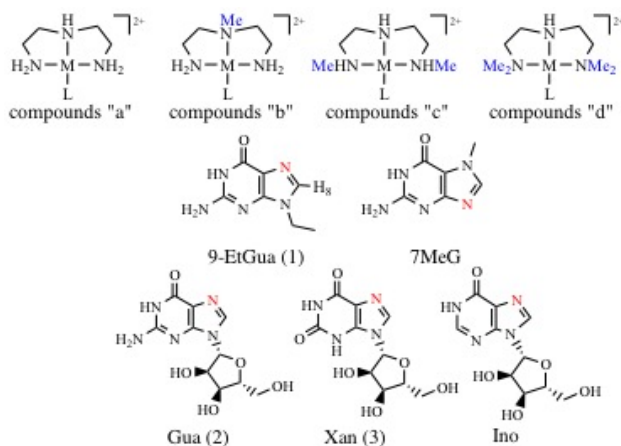
Figure 3.1: General structure for $[Pt(dien)L]^{2+}$ compounds, where the dien can be methylated (NMe, N,N'-dimethyl or N,N'-N,N'-tetramethyl) and L is a nucleobase.

The addition of methyl groups, besides adding lipophilic groups, also adds considerable steric hindrance about the platinum-nucleobase bond. This can be seen in the ^{1}H NMR of 1c and 1d. The H8 signal of the 9-EtGua splits into two singlets due to this restricted rotation. Temperature dependence studies of the H8 signal reveal a significant difference between the Me$_2$dien compound and the Me$_4$dien compound, Figure 3.2. The coalescence

temperature for the Me$_2$dien compound is 35°C, whereas the H8 signal for the Me$_4$dien complex does not coalesce up to 70°C. The calculated energies of the rotation barrier, E$_{barrier}$, was calculated based on the coalescence temperature following literature methods[1]. There is a >2 kcal/mol difference between E$_{barrier}$ for the two compounds, 15.90 for Me$_2$dien and >17.92 kcal/mol for Me$_4$dien. This energy difference highlights the significant steric hindrance created by the methyl groups. This splitting is also seen in the ^{195}Pt NMR, Figure 3.3
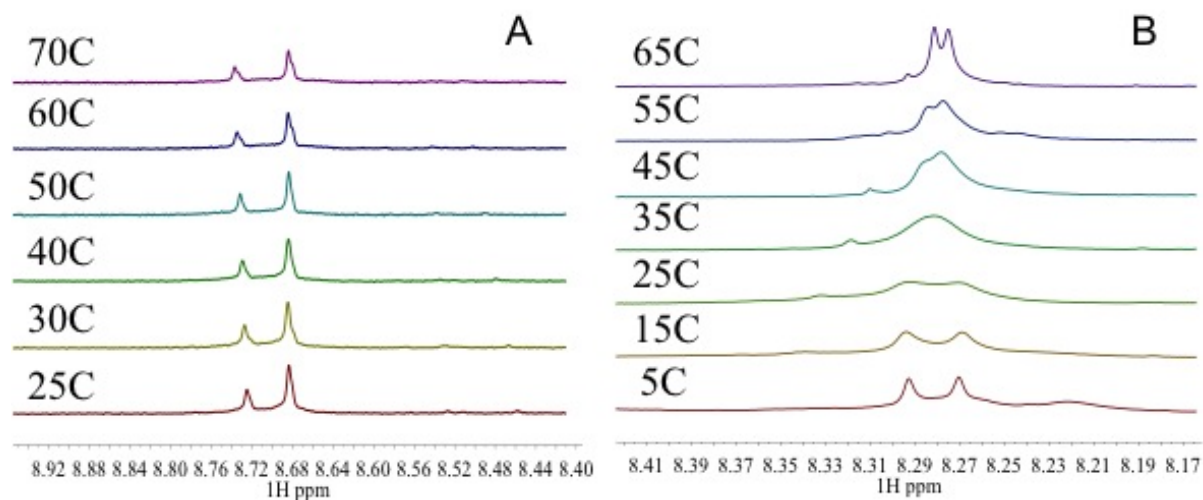
Figure 3.2: Temperature dependence of the ^{1}H NMR splitting of the H8 signal for A-[Pt(Me$_4$dien)(9-EtGua)]$^{2+}$ and B- [Pt(Me$_2$dien)(9-EtGua)]$^{2+}$.

As seen in Table 3.1, K$_a$ values are reported for the platinum-nucleobase complexes with N-AcTrp and the C-terminal ZF of HIV1 NCp7. The addition of the sugar moiety on guanosine (Gua) and Xan enhances the interaction with tryptophan slightly over the parent 9-EtGua compound. This may be due to addition H-bond contributions from the sugar. The most significant increase in association constant is between the Xan compounds (3a, 3b, 3c, 3d) and the C-terminal ZF of HIV1 NCp7; the additional double-bonded oxygen on the pyrimidine ring, a H-bond acceptor, may explain this trend. The C-terminal ZF contains several Lys residues in addition to an Arg, which are H-bond donors. Due to the lack of
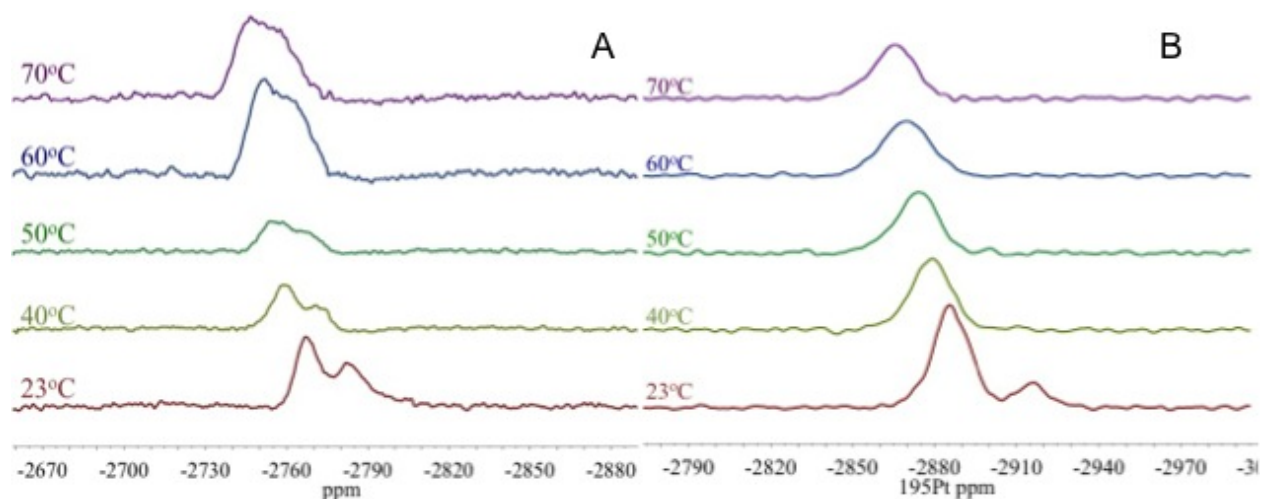
Figure 3.3: Temperature dependence of the ^{195}Pt NMR splitting of the signal for A-$[Pt(Me_4dien)(9\text{-}EtGua)]^{2+}$ and B- $[Pt(Me_2dien)(9\text{-}EtGua)]^{2+}$.

a large increase in Trp stacking, it is reasonable to assume these additional H-bonds may contribute to the strong interaction between the Xan compounds and the ZF.

Table 3.1: Association constants for PtN_4 complexes with N-AcTrp. Values in parentheses are K_a values for the C-terminal ZF of HIV1 NCp7.

	K_a (x10^3) M^{-1}			
L	$[Pt(dien)L]^{2+}$	$[Pt(NMedien)L]^{2+}$	$[Pt(Me_2dien)L]^{2+}$	$[Pt(Me_4dien)L]^{2+}$
7MeG	9.01 ± 0.09 (10.42 ± 0.29)	— —	— —	— —
Ino	5.63 ± 0.3 (3.20 ± 0.29)	— —	— —	— —
9-EtGua	6.88 ± 0.36 (13.10 ± 0.94)	13.52 ± 0.48 (14.70 ± 1.60)	7.40 ± 0.93 (12.02 ± 0.37)	11.78 ± 1.02 (18.30 ± 0.34)
Gua	13.10 ± 1.29 (15.80 ± 2.83)	12.78 ± 0.22 (12.11 ± 1.13)	6.84 ± 0.67 (11.37 ± 2.01)	15.19 ± 1.21 (9.16 ± 1.46)
Xan	16.13 ± 1.10 (46.64 ± 0.28)	11.56 ± 0.33 (60.22 ± 2.18)	11.74 ± 0.53 (35.80 ± 0.76)	$11.30 \pm 0.36)$ (48.67 ± 0.29)

3.3.2 Biology

It is important to understand the biological properties of the platinum-nucleobases reported here, therefore we have evaluated the cellular accumulation, cytotoxicity and inhibition of the complex formation between NCp7 and SL2. SL2 is one of the four stem loops that comprises Ψ RNA, a component of the HIV genome.

Our initial hypothesis was that the addition of methyl groups to the dien ligand would increase lipophilicity, in turn increasing the cellular accumulation. To evaluate this hypothesis, we tested CCRF-CEM and Jurkat cell lines. Both cell lines are CD4+ and HIV susceptible. As shown in Figure 3.4, the methylation of the dien did not result in a significant difference in the cellular accumulation for platinum complexes containing 9-EtGua (1a-d), Gua (2a-d) or Xan (a-d). Three compounds show greater accumulation compared to all others: 1a, 1b, and 2a. From 3 to 6 hours, a negligible increase in accumulation is seen for most compounds, with the exception of the three compounds that see the highest concentration of platinum per cell. The cell uptake trends are similar for the CCRF-CEM and Jurkat cells, which may be indicative of a similar uptake mechanism.

To rationalize the lack of trend upon dien methylation, the octanol-water coefficents (log $P_{oct/water}$) for compounds 1a-1d were calculated, Table 3.2. There does not appear to be a trend in the number of methyl groups and log $P_{oct/water}$ or cellular accumulation. This lack of correlation may be due to the charge on the compounds (2+).

Table 3.2: Association constants for PtN_4 complexes with N-AcTrp. Values in parentheses are K_a values for the C-terminal ZF of HIV1 NCp7.

Compound	LogP$_{oct/water}$
1a	-1.59 $\pm$ 0.28
1b	-0.36 $\pm$ 0.06
1c	0.22 $\pm$ 0.09
1d	-0.36 $\pm$ 0.04
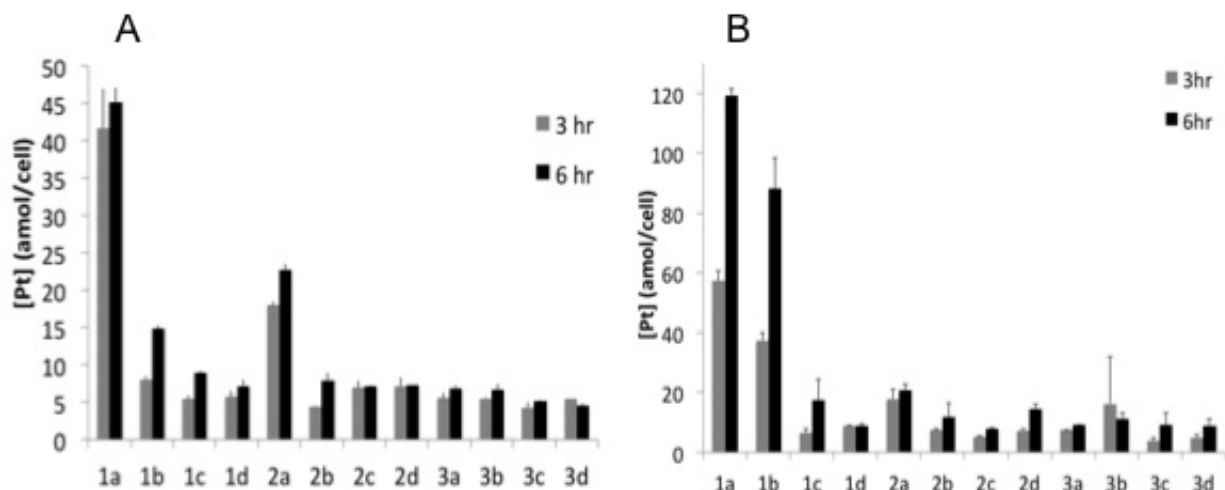
Figure 3.4: Cellular accumulation of platinum-nucleobase compounds in (A) Jurkat and (B) CCRF-CEM cells.

Table 3.3: IC$_{50}$ values for compounds 1a, 1b, 2a and 3a as determined by WST Assay.

| | IC$_{50}$ | |
Compound	CCRF-CEM	Jurkat
1a	>100	>100
1b	>100	>100
2a	>100	>100
3a	>100	>100

Based on the cellular accumulation profile, cytotoxicity studies were performed for compounds 1a, 1b and 2a as well as compound 3a (to test the cytotoxicity of Xan). The use of WST over MTT was necessary as CCRF-CEM and Jurkat cells are suspension cells and do not attach to the 96-well plate. None of the compounds exhibited significant cytotoxic properties as all of IC$_{50}$ values are over 100 μM, Table 3.3. This is a desirable property, as the compounds are designed to inhibit HIV without affecting normal cellular function.

Finally, the ability of the compounds to inhibit or dissociate the complex between NCp7 and SL2 was evaluated by EMSA gel shift assays. As part of the viral packaging process, NCp7 binds to viral Ψ RNA, which is comprised of four stem loops (SL). SL2 and

SL3 bind strongly to NCp7 and with similar affinity when compared to SL1 and SL4[2]. For this reason, we have selected the interaction between NCp7 and SL2 as a representative system to evaluate the compounds ability to inhibit the protein-RNA interaction. Figure 3.5 shows the EMSA gels for the compounds 1a, 1b, 2a and 3a. The control experiment, Figure 3.5A, shows the upward shift in the band associated with NCp7/SL2 complexation. NCp7 was preincubated with platinum compound for 30 minutes followed by addition of SL2 and incubation for an additional 30 minutes. Compound 1a shows the greatest inhibition, with nearly complete disappearance of the NCp7/SL2 band, while compound 1b shows very little inhibition. Compounds 2a and 3a show some inhibition of the complex. Compound 3a, Figure 3.5D, results in a band corresponding to a larger, slow-moving species at the top of the gel. A control experiment of SL2 and 3a was performed and the same aggregate species were observed, Figure 3.6. This suggests the inhibition of the NCp7/SL2 complex is a separate event from the formation of the large, slow-moving species.

The reverse reaction was performed where NCp7 was incubated with SL2 for 30 minutes, ensuring ample time for complexation, after which platinum was added and incubated for 30 minutes. Similar results were seen where compound 1a exhibited the greatest inhibition, though interestingly aggregates are seen at the top of the gel. This is not seen for the opposite reaction or compound 1b, Figure 3.7.

3.4 Conclusions

The work presented in this article highlights the various strategies we have employed to understand the interaction between platinum-nucleobase compounds and Trp as well as some of their basic biological properties. The stability of the PtN_4 coordination sphere allows for a targeted reaction with NCp7. In an effort to improve this specific reaction, we have found that the addition of Xan increases the association constant with the C-terminal ZF
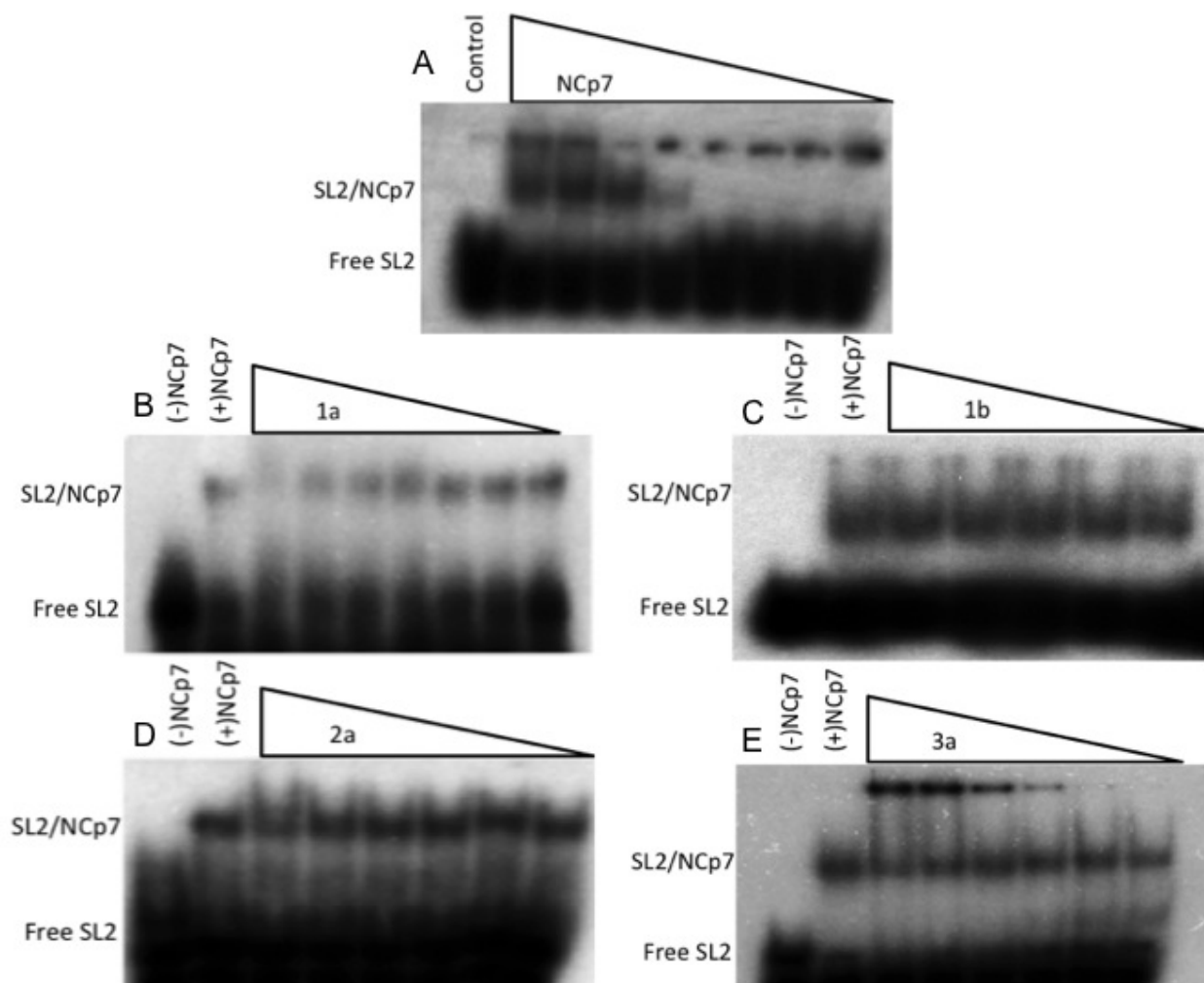
Figure 3.5: (A) Control experiment showing the formation of the SL2-NCp7 complex. Lane 1: Marker, Lane 2: SL2, Lanes 3-10: SL2 + NCp7 (500, 250, 125, 62.5, 31.25, 15.63, 7.81, 3.91 nM). (B-E) Addition of SL2 to NCp7/Drug solution. Lane 1: Marker, Lane 2: SL2, Lane 3: SL2 + NCp7, Lanes 3-10: NCp7/Drug + SL2 (1 mM, 500 μM, 250 μM, 125 μM, 62.5 μM, 31.25 μM, 15.63 μM).

greatly over the parent 9-EtGua compound. Addition of methyl groups to the dien did not result in a clear relationship to the lipophilicity of the compounds or cellular accumulation.

The lack of cytotoxicity exhibited by the compounds reported here is favorable. While there are no clear trends in cellular accumulation, the platinum-nucleobase compounds do
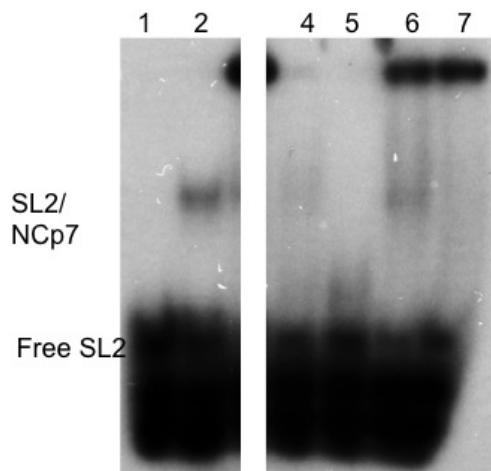
Figure 3.6: Control experiment incubating [Pt(dien)L]$^{2+}$ with SL2 or SL2/NCp7. Lane 1: SL2, Lane 2: NC + SL2, Lane 3: NC/1mM 1a +SL2, Lane 4: 1mM 1a +SL2, Lane 5: NC/1mM 3a +SL2, Lane 6: 1mM 3a +SL2.
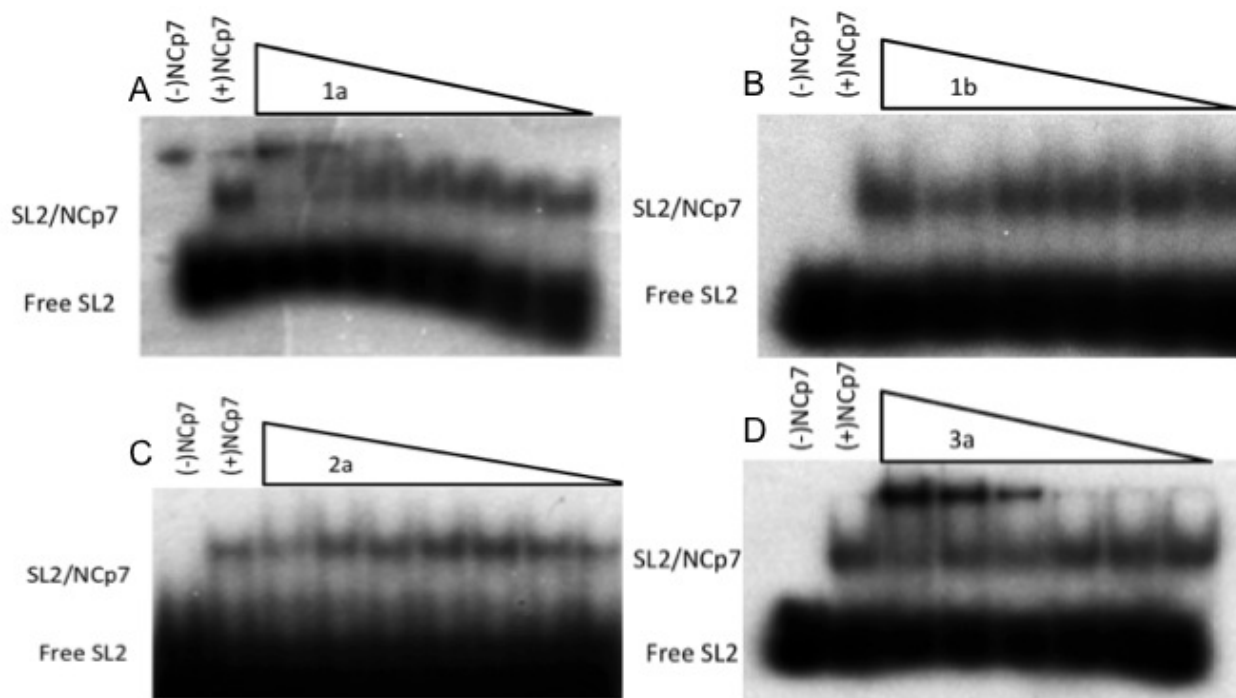
Figure 3.7: (A-D) Addition of SL2 to NCp7/Drug solution. Lane 1: Marker, Lane 2: SL2, Lane 3: SL2 + NCp7, Lanes 3-10: NCp7/Drug + SL2 (1 mM, 500 uM, 250 uM, 125 uM, 62.5 uM, 31.25 uM, 15.63 uM).

enter the cell and for the compounds that see the highest concentration of platinuim per cell, a clear increase between 3 and 6 hours of incubation was observed. Compound 1a was able to strongly inhibit the interaction between NCp7 and SL2, while the others only weakly interrupted this interaction. The IC_{50} values for compounds 1a and 2a are 250 μM and 1mM, respectively, when the platinum compound was pre-incubated with NCp7. For the reverse reaction, only compound 1a showed enough inhibition to determine an IC_{50} (1mM). These IC_{50} values are comparable to organic compounds reported in the literature[3]. It may be tempting to assume greater inhibition should have been seen for compound 3a over 1a due to the significantly higher association constant, but the addition of the sugar ring adds considerable bulk to the compound. While the exact mechanism of inhibition is not clear, it is reasonable to assume that the addition of the sugar on Xan and Gua would create steric constraints affecting the inhibition of NCp7/SL2 complexation. Overall, the biological properties displayed are favorable. The goal was to develop non-cytotoxic compounds that are able to inhibit the function of NCp7.

It is important to improve the compounds designed to target NCp7 as it is a challenging target. Previous work has used weak organic electrophiles to modify the Cys residues of the zinc finger but progress stalled due to a lack in selectivity and issues with toxicity[4−6]. We compare our substitution-inert PtN_4 compounds to these organic weak electrophiles and suggest that they possess intrinsic selectivity for NCp7 based on the molecular recognition of the stacking interaction between Trp and Gua/nucleobase[7].

3.5　Experimental

3.5.1　Synthesis

3.5.1.1　Materials and Reagents

The complexes [PtCl(dien)]Cl (dien = diethylenetriamine) and Me_2dien were prepared by literature methods[8,9] purity was confirmed by ^{1}H and ^{195}Pt NMR Spectroscopy, and Elemental Analysis (performed by QTI Laboratory, USA). Me_4dien was purchased from Matrix Scientific. All other reagents were purchased from Sigma Aldrich, USA and used without further purification. The NCp7 C-terminal peptide sequence (KGCWKCGKQEHQMKDC-TER) was purchased from GenScript Corporation.

3.5.1.2　Synthesis of PtN$_4$ complexes

[Pt(dien)(9-EtGua)](NO$_3$)$_2$ - [PtCl(dien)]Cl was dissolved in H_2O and 9-ethylguanine (1 mol eq.) and $AgNO_3$ (1.98 mol eq.) were added. The solution was heated at 50°C in the dark for 24 hours. The solution was cooled to room temperature and filtered through celite to remove the precipitated AgCl. The solution was rotovapped to dryness and acetone was added to precipitate the final product. The solid was dried in vacuo. Anal. Calcd for $C_{11}H_{22}N_{10}O_7$Pt: C 21.97; H, 3.69; N, 23.20. Found: C, 20.19; H, 3.39; N, 22.86. ^{1}H NMR (D_2O): 1.44 (3H, t), 3.00 (8H, m), 4.14 (2H, q), 8.19 (1H, s). ^{195}Pt NMR: -2850.

[Pt(dien)(Gua)]NO$_3$ Cl 0.8H$_2$O- [Pt(dien)(Gua)]NO$_3$ Cl was synthesized in a similar manner as [Pt(dien)(9-EtGua)](NO$_3$)$_2$. Briefly, [PtCl(dien)]Cl was dissolved in H_2O and guanosine (1 mol eq.) and $AgNO_3$ (0.98 mol eq.) were added. The solution was heated at 50°C in the dark for 24 hours. The solution was cooled to room temperature and filtered through celite to remove the precipitated AgCl. The solution was rotovapped to dryness

and acetone was added to precipitate the final product. The solid was dried in vacuo. Anal. Calcd for $C_{14}H_{27.6}N_9ClO_{8.8}Pt$: C 24.25; H, 4.01; N, 18.18. Found: C, 24.62; H, 3.99; N, 17.80. ^{1}H NMR (D_2O): 3.00 (8H, m), 3.78 (2H, m), 4.26 (1H, t), 4.39 (2H, t), 5.95 (1H, d), 8.42 (1H, s). ^{195}Pt NMR: -2857.

[Pt(dien)(Ino)](NO$_3$)$_2$ 0.06C$_3$H$_6$O - [Pt(dien)(Ino)](NO$_3$)$_2$ was synthesized in a similar manner as [Pt(dien)(9-EtGua)](NO$_3$)$_2$. Anal. Calcd for $C_{14.18}H_{25.36}N_9O_{11.06}Pt$: C 24.54; H, 3.68; N, 18.17. Found: C, 24.65; H, 3.47; N, 17.35. ^{1}H NMR (D_2O): 3.00 (8H, m), 3.90 (2H, m), 4.41 (1H, t), 4.73 (2H, t), 6.14 (1H, s), 8.32 (1H, s), 8.81 (1H, s). ^{195}Pt NMR: -2854.

[Pt(dien)(Xan)](NO$_3$)$_2$ 2H$_2$O - [Pt(dien)(Xan)](NO$_3$)$_2$ was synthesized in a similar manner as [Pt(dien)(9-EtGua)](NO$_3$)$_2$. Anal. Calcd for $C_{14}H_{29}N_9O_{14}Pt$: C 22.65; H, 3.94; N, 16.98. Found: C, 22.35; H, 3.24; N, 16.73. ^{1}H NMR (D_2O): 3.00 (8H, m), 3.93 (2H, m), 4.37 (2H, m), 4.56 (2H, t), 5.93 (1H, s), 8.43 (1H, s). ^{195}Pt NMR: -2849.

[Pt(dien)(7MeG)](NO$_3$)$_2$ - [Pt(dien)(7MeG)](NO$_3$)$_2$ was synthesized in a similar manner as [Pt(dien)(9-EtGua)](NO$_3$)$_2$. Anal. Calcd for $C_{14.18}H_{25.36}N_9O_{11.06}Pt$: C 24.54; H, 3.68; N, 18.17. Found: C, 24.65; H, 3.47; N, 17.35. ^{1}H NMR (D_2O): 3.00 (8H, m), 3.99 (3H, s), 8.12 (1H, s). ^{195}Pt NMR: -2890.

[PtCl(NMedien)]Cl 0.5H$_2$O - [Pt(NMedien)Cl]Cl was prepared in the same manner as [PtCl(dien)]Cl[8]. Anal. Calcd for $C_5H_{15}N_3Cl_2Pt$: C 15.31; H, 4.11; N, 10.71. Found: C, 15.49; H, 4.00; N, 10.19. ^{1}H NMR (D_2O): 3.03 (11H, m). ^{195}Pt NMR: -2598.

[Pt(NMedien)(9-EtGua)](NO$_3$)$_2$ - [Pt(NMedien)(9-EtGua)](NO$_3$)$_2$ was synthesized in a similar manner as [Pt(dien)(9-EtGua)](NO$_3$)$_2$. Anal. Calcd for $C_{12}H_{24}N_{10}O_7Pt$: C 23.42; H, 3.93; N, 22.76. Found: C, 23.16; H, 3.35; N, 22.20. ^{1}H NMR (D_2O): 1.44 (3H, t), 3.03 (11H, m), 4.14 (2H, q), 8.18 (1H, s). ^{195}Pt NMR: -2725.

[Pt(NMedien)(Gua)](NO$_3$)$_2$ 0.75H$_2$O - [Pt(NMedien)(Gua)](NO$_3$)$_2$ was synthesized in a similar manner as [Pt(dien)(9-EtGua)](NO$_3$)$_2$. Anal. Calcd for $C_{15}H_{29.5}N_{10}O_{11.75}Pt$: C 24.58; H, 4.06; N, 19.11. Found: C, 24.11; H, 3.48; N, 19.04. ^{1}H NMR (D_2O): 3.03 (11H,

m), 3.89 (2H, m), 4.26 (1H, t), 4.40 (2H, t), 4.72 (1H, t), 5.97 (1H, d), 8.42 (1H, s). ^{195}Pt NMR: -2729.

[Pt(NMedien)(Xan)](NO$_3$)$_2$ 2.5H$_2$O- [Pt(NMedien)(Xan)](NO$_3$)$_2$ was synthesized in a similar manner as [Pt(dien)(9-EtGua)](NO$_3$)$_2$. Anal. Calcd for C$_{15}$H$_{32.05}$N$_{9.05}$O$_{14.65}$Pt: C 23.53; H, 4.21 N, 16.47. Found: C, 23.44; H, 4.20; N, 15.99. ^{1}H NMR (D$_2$O): 3.03 (11H, m), 3.93 (2H, m), 4.37 (2H, m), 4.56 (2H, t), 5.93 (1H, s), 8.43 (1H, s).

[PtCl(Me$_2$dien)]Cl 0.5H$_2$O- [Pt(Me$_2$dien)Cl]Cl was prepared in the same manner as [PtCl(dien)]Cl[8]. Anal. Calcd for C$_6$H$_{17}$N$_3$Cl$_2$Pt: C 18.14; H, 4.31; N, 10.58. Found: C, 18.33; H, 3.84; N, 10.41. ^{1}H NMR (D$_2$O): 2.88 (14H, m). ^{195}Pt NMR: -2824.

[Pt(Me$_2$dien)(9-EtGua)](NO$_3$)$_2$ 2H$_2$O - [Pt(Me$_2$dien)(9-EtGua)](NO$_3$)$_2$ was synthesized in a similar manner as [Pt(dien)(9-EtGua)](NO$_3$)$_2$. Anal. Calcd for C$_{13}$H$_{30}$N$_{10}$O$_9$Pt: C 23.46; H, 4.54; N, 21.05. Found: C, 23.07; H, 4.21; N, 20.73. ^{1}H NMR (D$_2$O): 1.50 (3H, t), 2.88 (14H, m), 4.21 (2H, q), 8.70 (1H, broad s). ^{195}Pt NMR: -2876, -2907.

[Pt(Me$_2$dien)(Gua)](NO$_3$)$_{2.5}$ 2.5H$_2$O- [Pt(Me$_2$dien)(Gua)](NO$_3$)$_2$ was synthesized in a similar manner as [Pt(dien)(9-EtGua)](NO$_3$)$_2$. Anal. Calcd for C$_{16}$H$_{35.5}$N$_{10.5}$O$_{15}$Pt: C 23.74; H, 4.36; N, 18.17. Found: C, 23.27; H, 3.83; N, 17.71. ^{1}H NMR (D$_2$O): 2.88 (14H, m), 3.90 (2H, m), 4.28 (1H, t), 4.43 (2H, t), 6.00 (1H, d), 8.88 (1H, d). ^{195}Pt NMR: -2880, -2912.

[Pt(Me$_2$dien)(Xan)](NO$_3$)$_{2.25}$ 2.5H$_2$O- [Pt(Me$_2$dien)(Xan)](NO$_3$)$_2$ was synthesized in a similar manner as [Pt(dien)(9-EtGua)](NO$_3$)$_2$. Anal. Calcd for C$_{16}$H$_{34.25}$N$_{9.25}$O$_{15.25}$Pt: C 24.17; H, 4.31; N, 16.30. Found: C, 24.16; H, 3.77; N, 15.71. ^{1}H NMR (D$_2$O): 2.88 (14H, m), 3.98 (2H, m), 4.43 (2H, m), 4.65 (2H, t), 6.02 (1H, s), 8.66 (1H, broad s).

[PtCl(Me$_4$dien)]Cl - [Pt(Me$_4$dien)Cl]Cl was prepared in the same manner as [PtCl(dien)]Cl[8]. Briefly, [Pt(dmso)Cl$_2$] was suspended in acetone, Me$_4$dien (1 mol. eq.) was added and the solution was refluxed for 3 hrs. The solution was cooled to room temperature and the solvent was reduced to near dryness. Ether was added to precipitate the final product and the solid was dried in vacuo. ^{1}H NMR (D$_2$O): 2.90 (20H, m). ^{195}Pt NMR: -2704.

[Pt(Me$_4$dien)(9-EtGua)](NO$_3$)$_{2.4}$ 3H$_2$O- [Pt(Me$_4$dien)(9-EtGua)](NO$_3$)$_2$ was synthesized in a similar manner as [Pt(dien)(9-EtGua)](NO$_3$)$_2$. Anal. Calcd for C$_{15}$H$_{36}$N$_{10.4}$O$_{11.2}$Pt: C 24.47; H, 4.93; N, 19.78. Found: C, 24.12; H, 4.43; N, 19.12. ^{1}H NMR (D$_2$O): 1.51 (3H, t), 2.90 (20H, m), 4.22 (2H, q), 8.69 (1H, d). ^{195}Pt NMR: -2758, -2773.

[Pt(Me$_4$dien)(Gua)](NO$_3$)$_{2.4}$ 3H$_2$O- [Pt(Me$_4$dien)(Gua)](NO$_3$)$_2$ was synthesized in a similar manner as [Pt(dien)(9-EtGua)](NO$_3$)$_2$. Anal. Calcd for C$_{18}$H$_{40.4}$N$_{10.4}$O$_{15.2}$Pt: C 25.72; H, 4.80; N, 17.33. Found: C, 25.44; H, 4.36; N, 16.83. ^{1}H NMR (D$_2$O): 2.90 (20H, m), 3.92 (2H, m), 4.31 (1H, t), 4.46 (2H, t), 6.03 (1H, d), 8.90 (1H, d). ^{195}Pt NMR: -2763, -2778.

[Pt(Me$_4$dien)(Xan)](NO$_3$)$_{2.4}$ 3H$_2$O- [Pt(Me$_4$dien)(Xan)](NO$_3$)$_2$ was synthesized in a similar manner as [Pt(dien)(9-EtGua)](NO$_3$)$_2$. Anal. Calcd for C$_{16}$H$_{34.2}$N$_{9.25}$O$_{15.25}$Pt: C 25.69; H, 4.67; N, 15.65. Found: C, 25.19; H, 4.19; N, 15.11. ^{1}H NMR (D$_2$O): 2.90 (20H, m), 4.00 (2H, m), 4.45 (2H, m), 4.66 (2H, t), 6.03 (1H, s), 9.00 (1H, s).

3.5.2 Preparation of the Zinc Finger

The peptide was dissolved in deionized water at a concentration of 2mM. The pH was adjusted to 7.2 using NH$_4$OH and zinc acetate (1.3 molar eq.) was added to the solution. For fluorescence experiments, a 5 μM solution of ZF was prepared by diluting the concentrated stock solution.

3.5.3 Nuclear Magnetic Resonance Spectroscopy

All samples were prepared in D$_2$O at a concentration of $\sim$4mg/mL for ^{1}H NMR and $\sim$15mg/mL for ^{195}Pt NMR. For ^{1}H NMR, the solvent peak (D$_2$O) was referenced to 4.80ppm. ^{195}Pt NMR samples were measured using Na$_2$PtCl$_6$ as an external reference. For temperature dependence studies, $\sim$4mg/mL solutions of 1c and 1d were heated in 5°C increments and a spectrum was recorded. The spectra of 1c and 1d were recorded from 5-65°C and 24-70°C,

respectively. The $E_{barrier}$ of rotation was calculated using the equation: $E_{barrier}$ (in kcal/mol) = $4.575\text{x}10^{-3}$ * T_c * $(9.972 + \log(T_c/\Delta\nu)^1$. Where T_c is the coalescence temperature and $\Delta\nu$ is the spacing between the H8 signals.

3.5.4   Fluorescence Experiments

Fluorescence studies were recorded on a Varian Cary Eclipse fluorometer with a single-cell Peltier accessory. Samples were irradiated with 280 nm light and spectra were recorded from 300 to 450 nm with a scan rate of 600 nm/min at 25^oC. The experiments were carried out in 20 mM Tris buffer with 50 mM NaCl at pH 7.4. 5 μM N-acetyl tryptophan or zinc finger was titrated with $[M(dien)L]^{n+}$ at molar ratios of drug from 10 to 100 for all complexes. The absorbance for all compounds at 100 molar equivalents was <0.05; therefore, the inner filter effect was disregarded[10]. The emission maximum (362 nm) was measured after each titration. The K_a was determined from Eadie Hofstee plots from an average of 3 trials using the equation: $\Delta F = (K_a)^{-1}$ * $\Delta F/[\text{quencher}] + \Delta F_c$

3.5.5   Cellular Accumulation

Four million cells were incubated in 10 mL of RMPI media (10% FBS, 1%Pen-Strep) with 50 μM drug for 3 or 6 hours. The solutions were centrifuged at 1500 rpm at 4^oC for 5 minutes, the media was removed and the cell pellet was washed with 2x10mL cold PBS. To digest samples for ICP-MS analysis, 1 mL of conc. HNO_3 was added to the pellet and left to digest for 72 hours. Two mL of water were added, the solutions were filtered through a 0.45 μM GHP filter, and run on the ICP-MS to determine the concentration of platinum in each sample.

3.5.6 Gel Shift Assay

As a control experiment, ^{32}P end-labeled SL2 RNA (2 nM) was incubated with varying concentrations of NC in binding buffer (50 mM Tris-HCl, 40 mM MgCl$_2$, 200 mM NaCl, 0.1 mM ZnCl$_2$, 5% glycerol, and 1% BME) for 1 hr at 30°C. In all subsequent reactions, 250 nM NC was incubated with increasing concentrations of platinum complex for 30 min in binding buffer. Subsequently, 2 nM SL2 was added to the buffer and the mixture incubated for an additional 30 minutes. For the reverse reaction, NCp7 was incubated with SL2 for 30 minutes, followed by incubation with increasing concentrations of platinum complex for 30 minutes.

3.5.7 Cytotoxicity

CCRF-CEM or Jurkat cells were seeded at a concentration of 2.5×10^4 cells/100 μL. Drugs 1a, 1b, 2a, and 3a were added at varying concentrations (100, 50, 25, 12.5, 6.25, 3.125, 1.6125 μM) and the cells were incubated at 37°C for 72 hours. WST-1 (10 μL of commerical solution) was added and incubated for 4 hours. The absorbance at 405 nm was recorded and the IC$_{50}$ was determined.

3.6 References

1. Zimmer, K. D.; Shoemaker, R.; Ruminski, R. R. Synthesis and characterization of a fluxional Re(I) carbonyl complex fac-[Re(CO)$_3$(dpop')Cl] with the nominally tridentate ligand dipyrido(2,3-a:3',2'-j)phenazine (dpopâĂš). Inorg. Chim. Acta **2006**, *359*, 1478-1484.

2. Amarasinghe, G. K.; de Guzman, R. N.; Turner, R. B.; Chancellor, K. J.; Wu, Z. R.; Summers, M. F. NMR Structure of the HIV-1 Nucleocapsid Protein Bound to Stem-

Loop SL2 of the Psi-RNA Packaging Signal. Implications for Genome Recognition. J. Mol. Biol. **2000**, *301*, 491-511.

3. Warui, D. M.; Baranger, A. M. Identification of Small Molecule Inhibitors of the HIV-1 Nucleocapsid-Stem-Loop 3 RNA Complex. J. Med. Chem. **2012**, *55*, 4132-4141.

4. Rice, W. G.; Schaeffer, C. A.; Graham, L.; Bu, M.; McDougal, J. S.; Orloss, S. L.; Villinger, F.; Young, M.; Oroszlan, S.; Fesen, M. R.; Pommier, Y.; Mendeleyev, J.; Kun, E. The site of antiviral action of 3-nitrosobenzamide on the infectivity process of human immunodeficiency virus in human lymphocytes. Proc. Nat. Acad. Sci. USA **1993**, *90*, 9721-9724.

5. Huang, M.; Maynard, A.; Turpin, J. A.; Graham, L.; Janini, G. M.; Covell, D. G.; Rice, W. G. Anti-HIV agents that selectively target retroviral nucleocapsid protein zinc fingers without affecting cellular zinc finger proteins. J. Med. Chem. **1998**, *41*, 1371-1381.

6. Tummino, P. J.; Scholten, J. D.; Harvey, P. J.; Holler, T. P.; Maloney, L.; Gogliotti, R.; Domagala, J.; Hupe, D. The in vitro ejection of zinc from human immunodeficiency virus (HIV) type 1 nucleocapsid protein by disulfide benzamides with cellular anti-HIV activity. Proc. Nat. Acad. Sci. USA **1996**, *93*, 969-973.

7. de Paula, Q. A.; Tsotsoros, S. D.; Qu, Y.; Bayse, C. A.; Farrell, P. Platinum-nucleobase PtN$_4$ complexes as chemotypes for selective peptide reactions with biomolecules. Inorg. Chim. Act. **2012**, *393*, 222-229.

8. Annibale, G.; Brandolisio, M.; Pitteri, B. New routes for the synthesis of chloro(diethylenetriamine)platinum(II)chloride and chloro(2,2':6',2'-terpyridine)platinum(II)chloride dihydrate. Polyhedron **1995**, *14*, 451-453.

9. Paul-Roth, C.; Raymond, K. N. Amide Functional Group Contribution to the Stability of Gadolinium(III) Complexes: DTPA Derivatives. Inorg. Chem. **1995**, *34*, 1408-1412.

10. Larsson, T.; Wedborg, M.; Turner, D. Correction of inner-filter effect in fluorescence excitation-emission matrix spectrometry using Raman scatter. Anal. Chim. Acta **2007**, *583*, 357-363.

Chapter 4

Modulation of the stacking interaction of MN_4 (M=Pt, Pd, Au) complexes with tryptophan through N-heterocyclic ligands

Samantha D. Tsotsoros[a], Aaron B. Bate[a], Martina G. Dows[a], Sarah R. Spell[a], Craig A. Bayse[b], and Nicholas P. Farrell[a*]

[a]Department of Chemistry, Virginia Commonwealth University, 1001 W. Main Street, Richmond, VA 23284-2006 USA

[b]Department of Chemistry and Biochemistry, Old Dominion University, 4541 Hampton Boulevard, Norfolk, VA 23529-0126 USA

4.1   Contribution

S.D.T.'s contribution is comprised of synthesis of $[Pt(dien)(DMAP)](NO_3)_2$, $[Pd(dien)(DMAP)]Cl_2$, assistanted M.G.D. with synthesis of $[Pt(dien)(bztz)](NO_3)_2$, $[Pt(dien)(4-pic)](NO_3)_2$, fluorescence experiments for $[Pt(dien)(DMAP)](NO_3)_2$, $[Pd(dien)(DMAP)]Cl_2$ with N-AcTrp and ZF, ^{195}Pt NMR for $[Pt(dien)(DMAP)](NO_3)_2$, ^1H NMR for $[Pt(dien)(DMAP)]$-$(NO_3)_2$ and $[Pd(dien)(DMAP)]Cl_2$, reaction of $[Pd(dien)(DMAP)]^{2+}$ with N-AcTrp by ^1H

NMR and preparation of the figures and written manuscript. A.B.B.'s contribution was synthesis of the platinum pyridine, MeOpyr, quin, and tz complexes and the corresponding fluorescence experiments. S.R.S.'s contribution was synthesis of $[Au(dien)(DMAP)]^{3+}$ and corresponding fluorescence experiments.

4.2   Introduction

N-quaternization of nucleobases enhances the stacking interaction, in part by lowering the energy of the lowest unoccupied molecular orbital (LUMO) of the nucleobase, making it closer in energy to the highest occupied molecular orbital (HOMO) of the Trp[1,2]. N-quaternization may be achieved by protonation, alkylation or metallation and it is possible that the lowering of the energy of the LUMO may be due in part to the removal of the lone pair of electrons on the nitrogen of the nucleobase[1,2]. We have been systematically examining the coordination chemistry of NCp7 with platinum-metal compounds based on the $[M(dien)(nucleobase)]^{n+}$ (MN_4) motif (dien = diethylenetriamine). On average, free 9-ethylguanine (9EtG), 5'-guanosine monophosphate (GMP), and 5'-cytosine monophospate (CMP) have K_a values for association with tryptophan of 3 x 10^3 M^{-1} whereas platination increases the K_a for the three species to 6.8, 6.9, and 7.0 x 10^3 M^{-1}, respectively[2–5]. Extension to the Trp-containing C-terminal finger of NCp7 with $[Pt(dien)(9EtG)]^{2+}$ and $[Pt(dien)(GMP)]$ gave K_a values of 7.5 and 12.4 x 10^3 M^{-1}, respectively[6].

4.3   Experimental

4.3.1   Materials and Reagents

The complexes $[MCl(dien)]Cl$ (M = Pt, Pd, Au; dien = diethylenetriamine) were prepared by literature methods[5,8,9]; purity was confirmed by ^1H and ^{195}Pt NMR Spectroscopy, and Elemental Analysis (performed by QTI Laboratory, USA). All reagents were purchased
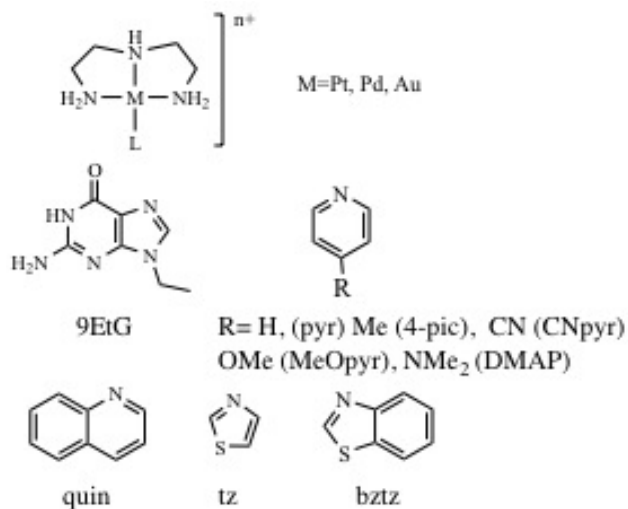
Figure 4.1: Structures of the metal (M = Pt, Pd, Au) N-heterocycle complexes studied.

from Sigma Aldrich, USA and used without further purification. The NCp7 C-terminal peptide sequence (KGCWKCGKQEHQMKDCTER) was purchased from GenScript Corporation.

4.3.1.1 Synthesis of N-heterocycle platinum complexes

[Pt(dien)(quin)](NO$_3$)$_2$: [PtCl(dien]Cl was stirred overnight in DMF with 1.98 equivalents of AgNO$_3$ in the dark. The solution was filtered through celite to remove the precipitated AgCl. Quinoline (3 eq.) was added to the filtrate and the solution was stirred overnight. The volume was reduced by rotary evaporation to near dryness, methanol and ether were added. The final product was obtained upon centrifugation and dried in vacuo (50% yield). Anal. Calcd for C$_{13}$H$_{20}$N$_6$O$_6$Pt: C, 28.32; H, 3.66; N, 15.24. Found: C, 27.76; H, 3.45; N, 14.88. ^{1}H NMR (D$_2$O): 3.00 (8H, m), 7.60 (1H, m), 7.90 (1H, m), 8.10 (2H, m), 8.50 (1H, m), 9.50 (2H, m). ^{195}Pt NMR: -2837.

[Pt(dien)(bztz)](NO$_3$)$_2$ 0.75H$_2$O: [Pt(dien)(bztz)](NO$_3$)$_2$ was synthesized in a similar manner as [Pt(dien)(quin)](NO$_3$)$_2$ using benzothiazole as the planar amine ligand and water as the solvent (29% yield). Anal. Cald for C$_{11}$H$_{19.5}$N$_6$O$_{6.75}$Pt: C, 23.14; H, 3.44; N, 14.72.

Found: C, 23.14; H, 3.29; N, 14.26. ^{1}H NMR (D$_2$O): 3.00 (8H, m), 7.70 (1H, m), 7.80 (1H, m), 8.10 (1H, m), 8.80 (1H, m), 9.70 (1H, s). ^{195}Pt NMR: -2861.

[Pt(dien)(pyr)](NO$_3$)$_2$: [Pt(dien)(pyr)](NO$_3$)$_2$ was synthesized in a similar manner as [Pt(dien)(bztz)](NO$_3$)$_2$ using pyridine as the planar amine ligand (62% yield). Anal. Cald for C$_{9.75}$H$_{19.5}$N$_6$O$_{6.75}$Pt: C, 20.99; H, 3.82; N, 16.32. Found: C, 21.28; H, 3.34; N, 15.86. ^{1}H NMR (D$_2$O): 3.00 (8H, m), 7.50 (2H, m), 8.00 (1H, m), 8.70 (2H, m). ^{195}Pt NMR: -2833.

[Pt(dien)(MeOpyr)](NO$_3$)$_2$ H$_2$O: [Pt(dien)(4-mopyr)](NO$_3$)$_2$ was synthesized in a similar manner as [Pt(dien)(bztz)](NO$_3$)$_2$ using 4-methoxypyridine as the planar amine ligand (24% yield). Anal. Cald for C$_{11}$H$_{22}$N$_6$O$_8$Pt: C, 21.86; H, 4.04; N, 15.30. Found: C, 21.31; H, 3.91; N, 15.41. ^{1}H NMR (D$_2$O): 3.00 (8H, m), 3.90 (3H, s), 7.10 (2H, d), 8.40 (2H, d). ^{195}Pt NMR: -2824.

[Pt(dien)(4-pic)](NO$_3$)$_2$ 0.75H$_2$O: [Pt(dien)(4-pic)](NO$_3$)$_2$ was synthesized in a similar manner as [Pt(dien)(bztz)](NO$_3$)$_2$ using picoline as the planar amine ligand (48% yield). Anal. Cald for C$_{10.75}$H$_{21.5}$N$_6$O$_{7.5}$Pt: C, 22.71; H, 4.10; N, 15.89. Found: C, 22.82; H, 3.69; N, 15.39. ^{1}H NMR (D$_2$O): 2.4 ppm (3H, s), 3.00 (8H, m), 7.40 (2H, d), 8.50 (2H, m). ^{195}Pt NMR: -2835.

[Pt(dien)(tz)](NO$_3$)$_2$: [Pt(dien)(tz)](NO$_3$)$_2$ was synthesized in a similar manner as [Pt(dien)(bztz)](NO$_3$)$_2$ using thiazole as the planar amine ligand (39% yield). Anal. Cald for C$_7$H$_{16}$N$_6$O$_8$SPt: C, 16.57; H, 3.18; N, 16.56. Found: C, 16.74; H, 2.67; N, 16.07. ^{1}H NMR (D$_2$O): 3.00 (8H, m), 7.75 (1H, d), 7.94 (1H, d), 9.20 (1H, s). ^{195}Pt NMR: -2820.

[Pt(dien)(CNpyr)](NO$_3$)$_2$: [Pt(dien)(CNpyr)](NO$_3$)$_2$ was synthesized in a similar manner as [Pt(dien)(bztz)](NO$_3$)$_2$ using 4-cyanopyridine as the planar amine ligand (23% yield). Anal. Cald for C$_7$H$_{16}$N$_6$O$_8$SPt: C, 22.25; H, 3.45; N, 18.16. Found: C, 21.93; H, 3.19; N, 18.11. ^{1}H NMR (D$_2$O): 3.00 (8H, m), 7.94 (1H, d), 9.00 (1H, d). ^{195}Pt NMR: -2839.

4.3.2 Techniques

4.3.2.1 Nuclear Magnetic Resonance Spectroscopy

All samples were prepared in D_2O at a concentration of ~ 4 mg/mL for ^{1}H NMR and ~ 15 mg/mL for ^{195}Pt NMR. For ^{1}H NMR, the solvent peak (D_2O) was referenced to 4.80 ppm. ^{195}Pt NMR samples were measured using Na_2PtCl_6 as an external reference.

4.3.2.2 Fluorescence Spectroscopy

Fluorescence studies were recorded on a Varian Cary Eclipse fluorometer with a single-cell Peltier accessory. Samples were irradiated with 280 nm light and spectra were recorded from 300 to 450 nm with a scan rate of 600 nm/min at 25°C. The experiments were carried out in 20 mM Tris buffer with 50 mM NaCl at pH 7.4. 5 μM N-acetyl tryptophan or zinc finger was titrated with $[M(dien)L]^{n+}$ at molar ratios of drug from 1 to 10 for DMAP complexes and 10 to 100 for all other complexes. The absorbance for the DMAP compounds at 362 nm at 10 molar equivalents and all other compounds at 100 molar equivalents was below 0.05; therefore, the inner filter effect was disregarded [17]. The emission maximum (362 nm) was measured after each titration. The K_a was determined from EadieâĂŞHofstee plots from an average of 3 trials using the equation: $\Delta F = (K_a) - 1 \ \Delta F \ / \ [quencher] + \Delta F_c$.

4.4 Results and Discussion

To examine the π-stacking potential of platinated N-heterocycle ligands an initial systematic survey was performed; Fig. 4.1 shows the structures of the synthesized complexes and pyridine was used as the comparison point when referring to the effects of electron donating or withdrawing groups.

Fig. 4.2 shows the % quenching of tryptophan fluorescence by the various

74

Table 4.1: Association constants for metal-N-heterocycle complexes with N-acetyltryptophan and the C-terminal zinc finger of HIVNCp7. Published values for the 9-ethylguanine complex were taken from a- Ref. [3] and b- Ref. [6] and for $[Au(dien)(DMAP)]^{3+}$ was taken from c- Ref. [15].

Compound	Ka $(\times 10^{-3})$ M^{-1}	
	NAcTrp	ZF
$[Pt(dien)(9EtG)]^{2+}$	6.88 ± 0.3^a	7.5^b
$[Pt(dien)(bztz)]^{2+}$	3.32 ± 0.36	3.20 ± 0.39
$[Pt(dien)(CNpyr)]^{2+}$	6.73 ± 0.26	7.72 ± 0.79
$[Pt(dien)(DMAP)]^{2+}$	25.0 ± 0.90	28.1 ± 1.76
$[Pd(dien)(DMAP)]^{2+}$	23.2 ± 0.31	—
$[Au(dien)(DMAP)]^{2+}$	25.5 ± 0.30^c	—

platinum compounds. The previously reported $[Pt(dien)(9EtG)]^{2+}$ displayed a fluorescence quenching of 94.34%. The pyr, MeOpyr, and 4-pic and thiazole complexes gave less than 10% fluorescence quenching.

Three complexes displaying high quenching - containing bztz, CNpyr and DMAP ligands - were evaluated to determine an association constant, Table 4.1. While the bztz and CNpyr compounds showed significant decrease in fluorescence intensity, the calculated K_as, 3.32 and 6.73 x 10^3 M^{-1} respectively, are similar to that of the 9EtG complex (6.88 x 10^3 M^{-1} [9]). In contrast, the presence of the DMAP ligand results in a compound with a significant increase in K_a (25.0 x 10^3 M^{-1}) over that of 9EtG.

There is no clear trend in this series with respect to the simple quenching except that all ligands represent potentially delocalized systems. This trend is reinforced by the observation that the addition of a delocalized π system in quinoline increased the fluorescence quenching over pyridine, albeit not to as significant an extent as that of DMAP and benzothiazole, and no K_a was measureable. The pKa for the platinated nitrogen may also give an indication of the strength of the stacking interaction between platinum complexes and Trp. The pKas under similar conditions for 9EtG, CNpyr, bztz and DMAP are 1.2[11], 1.9[12], 3.1[12], and 9.6[13], respectively. Clearly the strong donor DMAP has the most profound effect, even though the
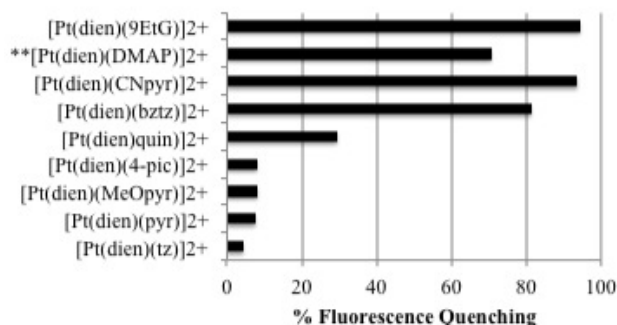
Figure 4.2: Percent fluorescence quenching of N-acetyltryptophan by platinum-N-hetero-cycle, $[Pt(dien)L]^{2+}$, complexes. ** The percent fluorescence quenching for $[Pt(dien)$-$(DMAP)]^{2+}$ refers to the quenching at 10 molar equivalents. The values for all other compounds refer to the percent fluorescence quenching at 100 molar equivalents.

platinated compound is actually slightly lower than free ligand, in contrast to the situation for free 9EtG. Basicity considerations and use of electron-donating substituents would seem important for identification of a wider group of improved N-heterocycle ligands.

The [M(dien)] structure allows for systematic study of electronic and steric effects (substitution on the dien ligand) and substitution effects where the isoelectronic M = Pt(II), Pd(II) and Au(III) compounds can be studied for effects of substitution lability of the central metal ion. We have contrasted the reaction products of C-terminal HIV NCp7 with $[MCl(dien)]^{n+}$ where M = Pt, Pd and Au [21]. It was therefore of interest to extend the DMAP findings to Pd(II) and Au(III) because of the strong stacking interaction the Pt-DMAP complex
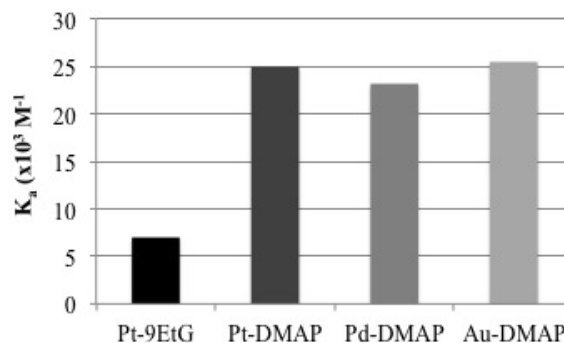
Figure 4.3: The association constants for $[M(dien)L]^{n+}$ complexes with N-acetyltryptophan as determined by fluorescence spectroscopy.

76

displays. In both cases, the calculated association constants confirmed the utility of the DMAP ligand, being 25.5 x 10^3 M^{-1} for [Au(dien)(DMAP)]$^{3+}$ [15], and 23.2 x 10^3 M^{-1} for [Pd(dien)(DMAP)]$^{2+}$, Fig. 4.3.

Again, both values are significantly higher than the corresponding 9-EtG complexes[3,15]. No reaction was seen between [Pd(dien)(DMAP)]$^{2+}$ with N-AcTrp at pH* 7.52 when followed by ^{1}H NMR over 2.5 h (data not shown). This implies improved complex stability over [Pd(dien)(9EtG)]$^{2+}$ which has been shown to react with N-AcTrp through displacement of the 9EtG ligand at increasing pH[4]. Interestingly, the changes in the chemical shifts for the DMAP protons are largest for Au(III) over that of the Pd(II) and Pt(II) complexes, Table 4.2. This may reflect the short central M\N bond observed in [AuCl(dien)]$^{2+}$ and the demonstrated acidity of the dien ligand when bound to Au(III)[15].

These results were then extended to the C-terminal ZF of NCp7, which contains a single tryptophan in its sequence, Fig. 4.4. Generally, the association constants for the nucleobase complexes increase for the ZF of NCp7 when compared to N-AcTrp[2]. This trend is not followed for all N-heterocycles. The K$_a$s for [Pt(dien)(bztz)]$^{2+}$ and [Pt(dien)(CNpyr)]$^{2+}$ are approximately the same for the ZF when compared to N-AcTrp and the K$_a$ for [Pt(dien)-(DMAP)]$^{2+}$ increases slightly. The interaction of the Au(III) and Pd(II) compounds with HIV NCp7 resulted in rapid displacement of the central Zn^{2+} ion and no association constant could be measured [Spell and Farrell, unpublished results].

Table 4.2: Major NMR ligand chemical shifts for [M(dien)(DMAP)]$^{n+}$ complexes. Values in parentheses are the difference in chemical shift (ppm) from free ligand followed by the ^{3}J$_{HH}$ coupling constants (Hz).

| Compound | ^{1}H($\Delta\delta^1$H) ppm, ^{3}J$_{HH}$Hz | | | δ^{195}Pt(ppm) |
	H2/H6	H3/H4	NâĂŞMe$_2$	
[Pt(dien)(DMAP)]$^{2+}$	6.64 (0.15), 5	8.02 (-0.20), 7.5	3.06 (0.06)	-2816
[Pd(dien)(DMAP)]$^{2+}$	6.66 (0.17), 7.5	7.92 (-0.31), 5	3.04 (0.04)	–
[Au(dien)(DMAP)]$^{2+}$	6.90 (0.41), 5	8.02 (-0.21), 5	3.22 (0.22)	–

The results here show that a limited number of N-heterocycle ligands, when metallated,

also effectively engage in π-stacking interactions with tryptophan and tryptophan-containing peptides. These findings further expand the structural variation of the MN_4 chemotype where we have suggested that use of a substitution-inert ligand such as an N-heterocycle group instead of the substitution-labile Cl, in for example [PtN_3X, X = leaving group), is an approach to selectivity for specific peptide-substitution reactions and templates for design of specific protein inhibitors[7]. The DMAP complexes all bind very strongly with Trp and the C-terminal ZF of NCp7, suggesting that they are suitable for further study with zinc finger proteins complementary to our studies with metallated natural nucleobases.
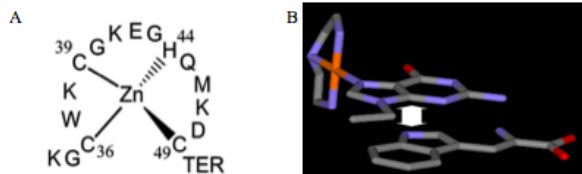
Figure 4.4: Figure 4: A- Structure of the HIV NCp7 zinc finger peptide and B- A model of the π-stacking interaction between [Pt(dien)(9EtG)]$^{2+}$ and N-acetyltryptophan.

With respect to zinc proteins in general, target selectivity is a major issue for specific inhibition using small molecules. In the case of zinc fingers, the results here extend the concept of "weak electrophiles" from organic chemistry to substitution-inert MN_4 platinum compounds in attempts to gain selectivity and distinguish between the cysteine nucleophilicity of the various coordination spheres Cys_2His_2, Cys_3His, and Cys_4[16−18]. The notable increase in association constant of [M(dien)(DMAP)]$^{n+}$ on the zinc finger through the "non-covalent" π-π stacking interaction allows further avenues for design of specifically targeted inhibitors and further confirms the viability of the medicinal chemistry dual approach of target recognition (non-covalent) followed by target fixation (covalent)[7].

4.5 References

1. Kawai, H.; Tarui, M.; Doi, M.; Ishida, T. Enhancement of aromatic amino acid-nucleic acid base stacking interaction by metal coordination to base: fluorescence study on a tryptophan-Pt(II)-guanine ternary complex. FEBS Letters **1995**, *370*, 193-196.

2. Anzelloti, A.I.; Bayse, C.A.; Farrell, N. P. Effects of nucleobase metalation on frontier molecular orbitals: potential implications for π-stacking interactions with tryptophan. Inorg. Chem. **2008**, *47*, 10425-10431.

3. Anzellotti, A.I.; Ma, E.S.; Farrell, N.P. Platination of nucleobases to enhance noncovalent recognition in protein-DNA/RNA complexes. Inorg. Chem. **2005**, *44*, 483-485.

4. Anzellotti, A.I.; Sabat, M.; Farrell, N. Covalent and noncovalent interactions for [Metal(dien)nucleobase]$^{2+}$ complexes with L-tryptophan derivatives: formation of palladium-tryptophan species by nucleobase substitution under biologically relevant conditions. Inorg. Chem. **2006**, *45*, 1638-1645.

5. Baddeley, W.H.; Basolo, F. Preparation and kinetic study of some sterically hindered palladium(II) complexes. J. Am. Chem. Soc. **1966**, *88*, 2944-2950.

6. Anzelotti, A.I.; Liu, Q.; Bloemink, M. J.; Scarsdale, J. N.; Farrell, N. Targeting retroviral Zn finger-DNA interactions: a small-molecule approach using the electrophilic nature of *trans*-platinum-nucleobase compounds. Chem. & Biol. **2006**, *13*, 539-548.

7. de Paula, Q.A.; Tsotsoros, S.D.; Qu, Y.; Bayse, C.A.; Farrell, P. Platinum-nucleobase PtN$_4$ complexes as chemotypes for selective peptide reactions with biomolecules. Inorg. Chim. Act. **2012**, *393*, 222-229.

8. A. Guiliano, M. Brandolisio, B. Pitteri, New routes for the synthesis of chloro (diethylenetriamine) platinum(II) chloride and chloro (2,2':6',2''-terpyridine) platinum(II)

chloride dihydrate. Polyhedron **1995**, *14*, 451-453.

9. Nardin, G.; Randaccio, L.; Annibale, G.; Natile, G.; Pitteri, B. Comparison of structure and reactivity of bis(2-aminoethyl)amine- and bis(2-aminoethyl)amido-chlorogold(III) complexes. J.C.S. Dalton **1980**, *2*, 220-223.

10. Larsson, T.; Wedborg, M.; Turner, D. Correction of inner-filter effect in fluorescence excitation-emission matrix spectrometry using Raman scatter. Anal. Chim. Acta **2007**, *583*, 357-363.

11. Eicher, T.; Hauptmann, S.; Speicher, A. *The Chemistry of Heterocycles: Structures, Reactions, Synthesis, and Applications 3rd*, Completely Revised; Wiley and Sons: Hoboken, NJ, 2013; Vol. 20.

12. Morell Cerda, M.; Amantia, D.; Costisella, B.; Houlton, A.; Lippert, B. Multiple metal binding to 6-oxopurine nucleobases as a source of deprotonation. The role of metal ions at N7 and N3. Dalton Trans. **2006**, 2894-3899.

13. In *Kirk-Othmer Encyclopedia of Chemical Technology, 4th Ed.*; Kirk-Othmer, Ed.; Wiley and Sons: Hoboken, NJ; Vol. 20.

14. de Paula, Q.A.; Mangrum, J.B.; Farrell, N.P. Zinc finger proteins as templates for metal ion exchange. Substitution effects on the C-terminal finger of HIV nucleocapsid NCp7 using M(chelate) species (M = Pt,Pd, Au). J. Inorg. Biochem. **2009**, *103*, 1347-1354.

15. Spell, S.R.; Farrell, N.P. Synthesis and properties of the first [Au(dien)(N-heterocycle)]$^{3+}$ compounds. Inorg. Chem. **2014**, *53*, 30-32.

16. Elder, R.C.; Watkins, J.W. Structure of trichloro(diethylenetriamine)gold(III), Au(dien)-Cl$_4$, determined by single-crystal x-ray diffraction, Raman and EXAFS spectroscopies:

an EXAFS caveat. Inorg. Chem. **1986**, *25*, 223-226.

17. Maynard, A.T.; Huang, M.; Rice, W.G.; Covell, D.G. Reactivity of the HIV-1 nucleo-capsid protein p7 zinc finger domains from the perspective of density-functional theory. Proc. Nat. Acad. Sci. USA **1998**, *95*, 11578-11583.

18. Maynard, A.T.; Covell, D.G. Reactivity of zinc finger cores: analysis of protein packing and electrostatic screening. J. Am. Chem. Soc. **2001**, *123*, 1047-1058.

Chapter 5

Investigation of the reaction of tDDP and cDDP with the C-terminal Zinc Finger of HIV1 NCp7

Samantha D. Tsotsoros and Nicholas P. Farrell

Department of Chemistry, Virginia Commonwealth University, 1001 W. Main Street,

Richmond, VA 23284-2006 USA

5.1   Contribution

This chapter is the work of solely S.D.T.

5.2   Introduction

Our work has focused on the development of platinum complexes designed to target NCp7. By changing ligands on compounds with structure $[Pt(L)(L')(nucleobase)Cl]^+$, the preference for S binding over N binding can be controlled[1]. In fact, the complex *trans*-$[PtCl(py)_2(9\text{-EtGua})]$ has been shown to have some antiviral activity *in vitro*[2]. Furthermore, the move to a more substitution-inert PtN_4 coordination sphere correlates to a shift towards

more selective compounds. The addition of $[Pt(dien)(9\text{-}EtGua)]^{2+}$ to the C-terminal ZF of HIV1 NCp7 results in a concentration-dependent decrease in the fluorescence of Trp37 from which a K_a of 6.88 x 10^3 M^{-1} can be calculated[3].

More recently, we have shown the N-terminal selective cleavage of the C-terminal ZF of NCp7 by a *trans*-dinuclear platinum complex, 1,1-t,t. Immediately upon mixing, a peak corresponding to the adduct of 1,1-t,t(-2Cl) and ZF (-KG) can be seen. Over time, there is an appearance of a sister peak which corresponds to zinc ejection. No peptide cleavage was seen for the *cis*-dinuclear complex, 1,1-c,c. This cleavage was the first reported peptide cleavage by a platinum complex at neutral pH[4]. It is therefore of interest to look at possible mechanisms for this peptide cleavage and to determine the mitigating factors. Here, we investigate the reactions between cDDP and tDDP with the C-terminal zinc finger of HIV1 NCp7 to understand if a dinuclear structure is necessary for peptide cleavage.
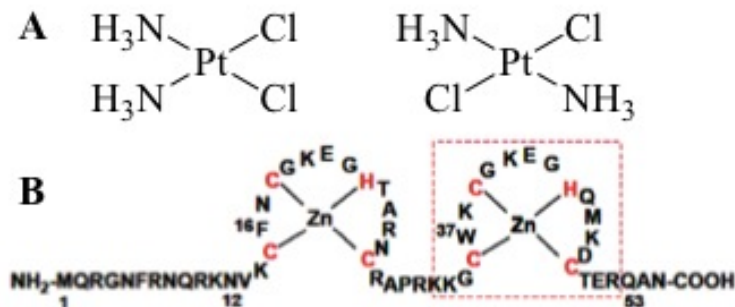
Figure 5.1: A- Structure of cisplatin (left) and transplatin (right), B- Structure of HIV1 NCp7. The C-terminal ZF used is highlighted by dashed red box.

5.3 Experimental

5.3.1 Materials and Reagents

The complexes cisplatin and transplatin were prepared by literature methods; purity was confirmed by ^{1}H and ^{195}Pt NMR Spectroscopy, and Elemental Analysis (performed by QTI

Laboratory, USA). All reagents were purchased from Sigma Aldrich, USA and used without further purification. The NCp7 C-terminal peptide sequence (KGCWKCGKQEHQMKDC-TER) was purchased from GenScript Corporation.

5.3.2 Preparation of the Zinc Finger

The peptide was dissolved in deionized water at a concentration of 2mM. The pH was adjusted to 7.2 using NH_4OH and zinc acetate (1.3 molar eq.) was added to the solution. For fluorescence experiments, a 5 μM solution of ZF was prepared by diluting the concentrated stock solution.

5.3.3 Techniques

5.3.3.1 Fluorescence Spectroscopy

Fluorescence studies were recorded on a Varian Cary Eclipse fluorometer with a single-cell Peltier accessory. Samples were irradiated with 280 nm light and spectra were recorded from 300 to 450 nm with a scan rate of 600 nm/min at 37°C. A solution of 1:1 tDDP or cDDP and zinc finger was incubated at 37°C for up to 72 hours. Spectra were recorded every 5 minutes from t=0 to 60 minutes, every 30 minutes from t= 60 mins to 4 hours and every 2 hours from 4 hours to 72 hours.

5.3.3.2 Mass Spectrometry

For mass spectrometry experiments, initial 1mM reaction mixtures were made in water at 24°C and pH 7.2 (adjusted using ammonium hydroxide). The reaction solutions were incubated at 37°C and were sprayed using a final concentration of 10 μM. Experiments were carried out on an Orbitrap Velos from Thermo Electron Corporation operated in positive mode. Samples (20 μL) were diluted with methanol (200 μL) and directly infused at a flow rate of 0.7 μL/min using a source voltage of 2.30 kV. The source temperature was maintained

at 230C throughout.

5.3.3.3 $\{^1\text{H}, \ ^{15}\text{N}\}$ HSQC

NMR experiments also followed published procedure and were conducted at 1 mM concentration (1:1) in 5% D_2O/95% H_2O (13). For HSQC ^{1}H,^{15}N NMR Spectroscopy the spectra were recorded at 37°C on a Bruker AVANCE III 600 MHz spectrometer (^{1}H, 600.1 MHz; ^{15}N, 60.8 MHz) fitted with a pulsed field gradient module and 5mm inverse quadruple resonance (QXI) probe. The ^{1}H NMR chemical shifts were internally referenced to trimethylsilyl propionate, the ^{15}N chemical shifts externally referenced to ^{15}NH$_4$NO$_3$. The two-dimensional $\{^1$H,^{15}N$\}$ HSQC spectra were recorded in phase sensitive mode using Echo/Antiecho-TPPI gradient selection. A total of 1024 points were acquired in the ^{1}H dimension and 96 complex points in the ^{15}N dimension with 128 transients. 1 mM platinum complex was allowed to react with 1 equiv. of ZF in 5% D_2O / 95% H_2O, and the reaction was followed by HSQC spectroscopy.

5.4   Results

The interaction of cDDP and tDDP with the C-terminal ZF of NCp7 was investigated by fluorescence, mass spectrometry, and $\{^1$H, ^{15}N$\}$ HSQC. Tryptophan fluorescence is often used to detect protein conformation. For a Trp containing protein, a decrease in fluorescence is indicative of Trp folded into a hydrophobic pocket (14). Here, the fluorescence of Trp37 in the C-terminal ZF of HIV1 NCp7 was monitored over time in the presence of 1 equivalent of either cDDP or tDDP. The results indicate a significantly slower reaction rate for cDDP. The reaction of tDDP with ZF results in 50% quenching of the Trp37 fluorescence over the course of 24 hours, while cDDP causes only a ~10% decrease. After 72 hours of reaction, cDDP induces a similar amount of quenching (33%) as the *trans* isomer, Figure 5.2. The quenching of the Trp fluorescence here may be indicative of Zn ejection and peptide folding
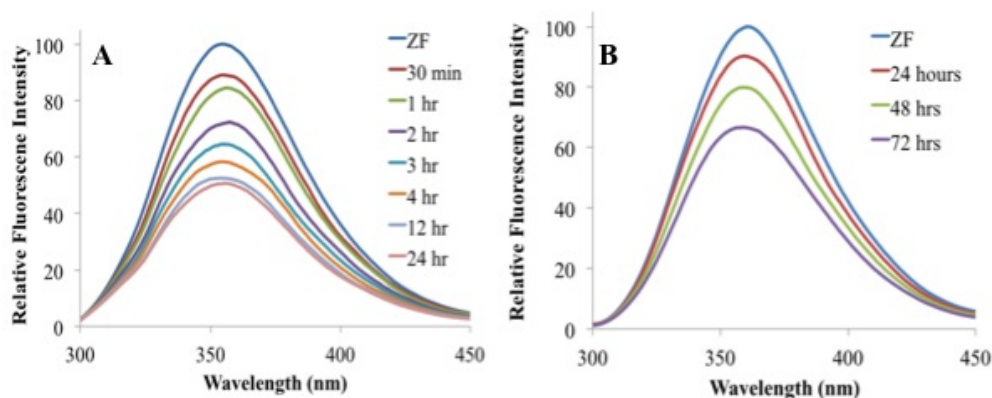
Figure 5.2: Fluorescence spectra of the 1:1 reaction of A) tDDP and B) cDDP with the C-terminal ZF of HIV1 NCp7.

as a result of the binding of platinum complex.

The reaction was also followed by ESI-MS. In the case of tDDP, both time points yield the same products, however, the intensity of the product peaks relative to free zinc finger increases over time with a concomitant decrease in the peaks seen for peptide (apo-C-terminal ZF). At both time points, the most dominant peak corresponds to intact zinc finger.

In the 30 minute spectrum, major product peaks for $Pt(NH_3)_2$/peptide (817.33 m/z, 3+ and 1225.49 m/z, 2+) and $2Pt(NH_3)_2$/peptide (1340.00 m/z, 2+) can be seen, Figure 5.3A. MS2 of these peaks reveals loss of NH_3 from the platinum moiety (Figure 5.4). Minor peaks corresponding to $Pt(NH_3)_2Cl$/peptide (1244.48 m/z, 2+) and Pt_2/ZF (893.67 m/z, 3+) are also present. MS2 of these peaks causes loss of Cl or NH_3 from the platinum, leaving the adduct with peptide intact and fragmentation of the protein for Pt_2/ZF. The isotopic distributions for all peaks match, as modeled by Isopro.

At 1 hour, smaller peaks corresponding to free peptide and larger product peaks relative to the intensity of the peaks corresponding to free ZF are seen, Figure 5.3B. The main products peaks are the same and MS2 yields the same daughter ions as seen at 30 minutes, Figure 5.5. Interestingly, there is a minor product peak for intact tDDP/peptide (1261.41 m/z, 2+), Figure 5.3. The isotopic distribution appears to match but the peak is in very
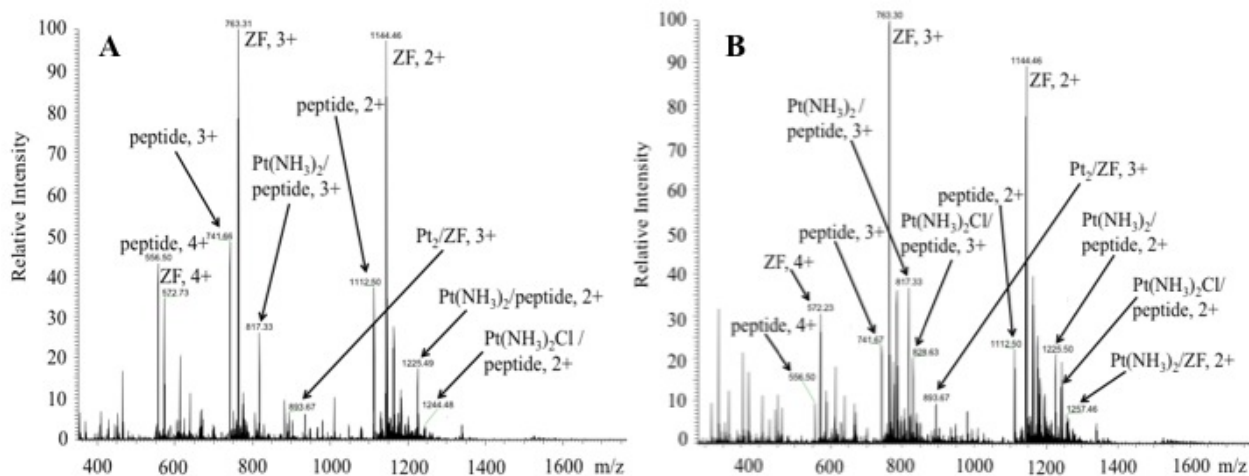
Figure 5.3: Mass spectra for the 1:1 reaction of tDDP with the C-terminal ZF of HIV1 NCp7 at A) 30 minutes and B) 60 minutes.
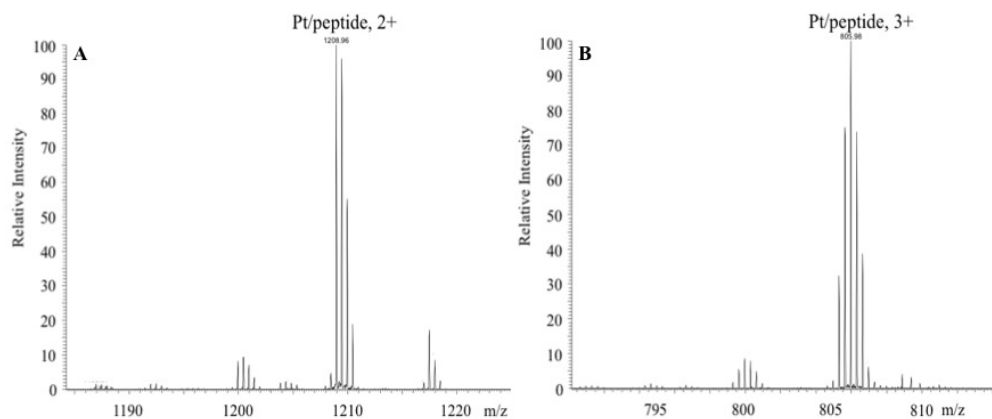
Figure 5.4: MS2 of the 1225.49 and 817.33 m/z peak corresponding to the 2+ and 3+ adducts of [Pt(NH$_3$)$_2$]/peptide. The major product peak is the 2+ species Pt/peptide at 1208.98 m/z (t= 30 minutes).

close proximity to another peak making identification slightly less clear. This peak is not seen in the 30 min spectrum. It is unlikely that the adduct is a noncovalent interaction between the platinum compound and peptide given the rapid rate of reaction for *trans*-platinum complexes and the most likely explanation is the formation of "5-coordinate zinc". Previously, we have seen a similar 5-coordinate Zn species when [M(dien)Cl]$^{n+}$ was reacted
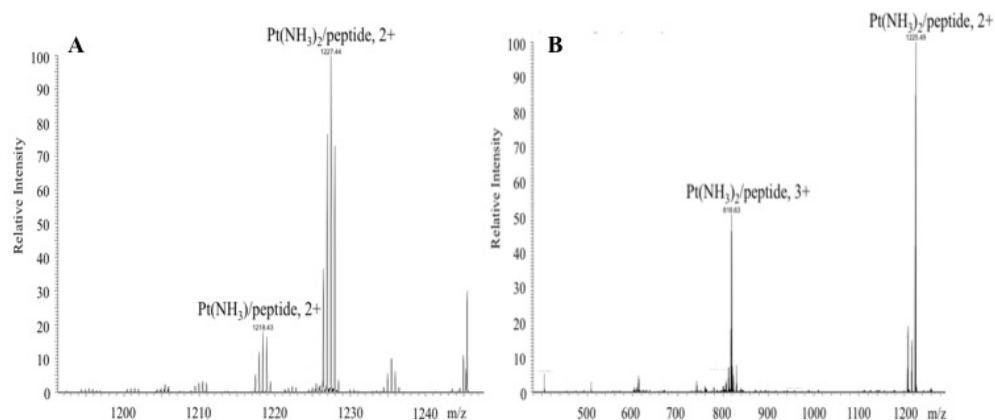
Figure 5.5: MS2 of the 1244.40 and 829.90 m/z peak corresponding to the 2+ and 3+ adducts of [Pt(NH$_3$)$_2$Cl]/peptide. The major product peaks are the 2+ and 3+ species of [Pt(NH$_3$)$_2$]/peptide at 1225.49 and 816.63 m/z and the 2+ species of [Pt(NH$_3$)]/peptide at 1218.43 m/z (t= 60 minutes).

with the C-terminal ZF of HIV NCp7 as well as with the Zn model chelate [Zn(bme-dach)$_2$] (15) (16).
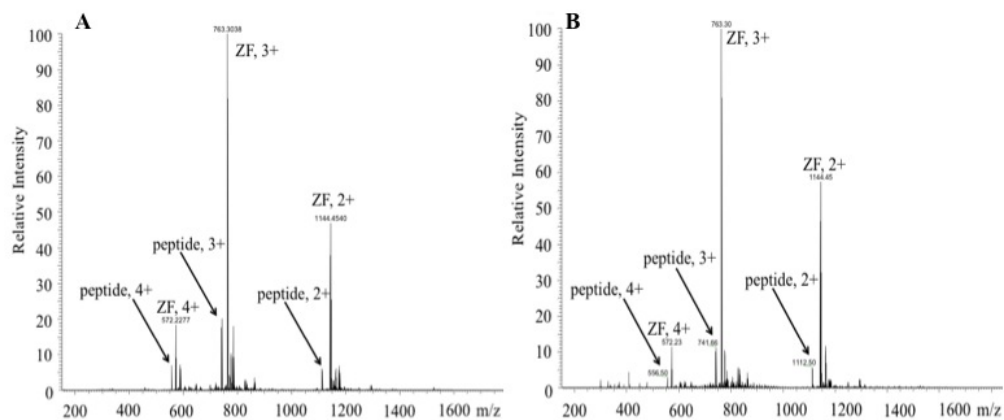
Figure 5.6: Mass spectra for the 1:1 reaction of cDDP with the C-terminal ZF of HIV1 NCp7 at A) 30 minutes and B) 60 minutes.

The reaction of cDDP and ZF confirms the slower rate of reaction for compounds in a *cis*-orientation rather than *trans*, where rapid *trans*-labilization of the Cl by a S-bound species allows for very fast reactions. The only species seen at 30 and 60 minutes are intact ZF, Figure 5.6. It is not until 4 hours that a platinum adduct is detectable, Figure 5.7. The

single platinum adduct observed is [Pt(NH$_3$)]/ZF].
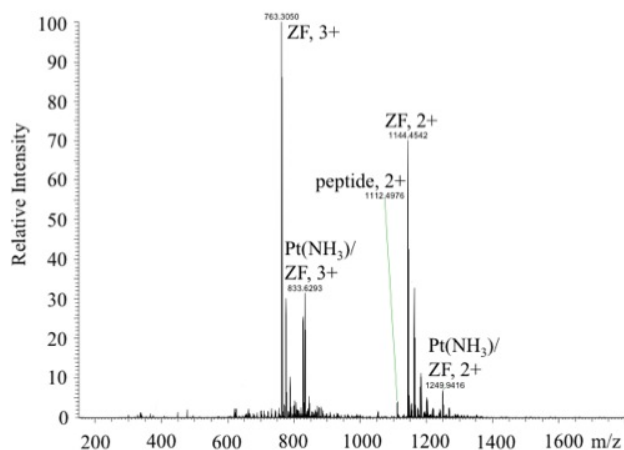
Figure 5.7: The 1:1 reaction of cDDP with C-terminal ZF of HIV1 NCp7 at 4

No peptide cleavage was observed for either cDDP or tDDP, illustrating the need for a dinuclear structure. Table 5.1 lists the expected and observed m/z ratios for the platinum-ZF adducts. The slow reaction rate for cDDP is consistent with studies conducted using cDDP to probe the reactivity of a C$_4$ ZF protein. Only upon binding of two platinum moieties was zinc release observed (17). Our work with *trans*-[PtCl(py)$_2$(9-EtGua)] revealed similar results as zinc loss was observed upon binding of two [Pt(py)$_2$] units (13).

Finally, {^{1}H, ^{15}N} HSQC of ^{15}N-labeled tDDP or cDDP with zinc finger can be seen in Figure 5. The parent peak for tDDP is seen at {3.61, -64.7}ppm with platinum coupling peaks at {3.57, -62.4} ppm and {3.65, -67.0}ppm. The hydrolysis of tDDP occurs at a must faster rate than cDDP as seen by the immediately present hydrolysis peak for the *trans*-isomer at {3.81, -63.2} ppm. A similar hydrolysis peak is seen for cDDP after approx. 1 hour.

The reaction of tDDP is complete within 27 minutes and after 24 hours, no changes are seen in the spectrum (Figure 6). Three new products peaks are found at {3.85, -59.1}, {3.77, -58.5}, and {3.57, -59.3} all of which are consistent with S-binding. Given that there are multiple Cys residues in the sequence of the C-terminal ZF, it is plausible that one or

Table 5.1: Major NMR ligand chemical shifts for $[M(\text{dien})(\text{DMAP})]^{n+}$ complexes. Values in parentheses are the difference in chemical shift (ppm) from free ligand followed by the $^3J_{HH}$ coupling constants (Hz).

Species	Charge State	Observed m/	Calculated m/z
$Pt(NH_3)_2$ + peptide	3+	817.33	818.33
$Pt(NH_3)_2$ + peptide	2+	1225.49 1225.50	1227.00
$Pt(NH_3)_2Cl$ + peptide	2+	1244.48 1242.44	1244.48
$Pt(NH_3)_2Cl$ + peptide	3+	829.90	829.99
$2Pt(NH_3)_2$ + peptide	2+	1340.00	1341.51
$Pt(NH_3)_2Cl_2$ + peptide	2+	1261.41	1261.97
$Pt(NH_3)_2Cl$ + ZF	2+	1276.40	1276.78
$Pt(NH_3)_2Cl$ + ZF	3+	849.90	851.52
$Pt(NH_3)_2$ + ZF	3+	838.60	839.64
Pt_2 + ZF	3+	893.67	893.27
$Pt(NH_3)_2$ + ZF	2+	1257.90 1257.46	1258.96
$Pt(NH_3)/ZF$	3+	833.63	833.97

more of these peaks may correspond to a bridged S-Pt-S species (18). The spectra for the reaction of cDDP with ZF again displays a much slower rate of reaction. Two ^{15}N upfield shifted peaks at {3.61, -41.6} and {3.79, -40.6} ppm are seen after 1 hour of reaction. The upfield shift on the nitrogen scale of the new peaks is consistent with the binding of S to the Pt center. The reaction was followed from 27 mins to 24 hours, with spectra taken every 30 minutes and spectra taken every few days up to one week. After one week, the peak corresponding to free ^{15}N-cDDP was still present, illustrating the slower reaction rate of the *cis* isomer.

5.5 Discussion

The reaction of tDDP and cDDP with the C-terminal ZF of HIV1 NCp7 was followed
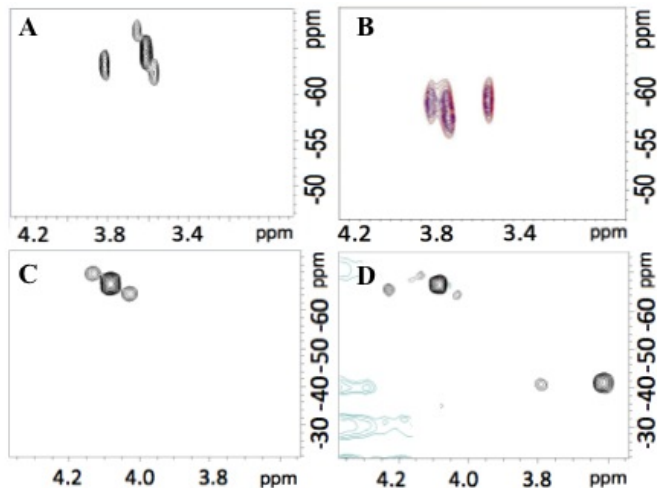
Figure 5.8: HSQC spectra of A) ^{15}N-tDDP, B) 1:1 reaction of ^{15}N-tDDP with C-terminal ZF of HIV1 NCp7 at blue- 27 minutes and red- 24 hours, C) ^{15}N-cDDP and D) 1:1 reaction of ^{15}N-cDDP with C-terminal ZF of HIV1 NCp7 at 24 hours.

using several different techniques. The results all show a significantly faster rate of reaction for the *trans* isomer when compared to the *cis*. This is consistent with known biological activity of *trans*-platinum complexes. The difference in reaction observed here is also consistent with studies on Sp1, a human transcription factor comprised of three C_2H_2 zinc fingers. A significantly faster rate of reaction was observed for tDDP when compared with cDDP and *trans*-planar amine platinum complexes (19). The rate reactivity of cDDP towards Sp1 increased upon incubation with the reducing agent, tris-(2-carboxyethyl)phosphine. This can be explained by the strong *trans* effect of the cDDP-bound reducing agents (20). Other studies have yielded similar results and the reaction of cDDP with other zinc finger proteins has been characterized (17, 21, 22).

Our results combined with those of others confirm the ability of bioinorganic chemistry to serve as a tool that can be used to study and tune the reactivity of metal complexes, specifically for metal-protein interactions. While it appears a dinuclear structure is necessary to induce peptide cleavage at neutral pH, the isomeric conformation of the platinum complexes leaves room for manipulation. This combined with the observed effects of various

ligands in *trans*-[PtCl(L)(L')(nucleobase)]$^+$ complexes opens the door to further development of platinum complexes designed to target ZF proteins.

5.6   References

1. Anzellotti, A.; Stefan, S.; Gibson, D.; Farrell, N. Donor atom preferences in substitution reactions of *trans*-platinum mononucleobase compounds: Implications for DNA-protein selectivity. Inorg. Chim. Acta **2006**, *339*, 3014-3019.

2. Sartori, D.A.; Miller, B.; Bierbach, U.; Farrell, N. Modulation of the chemical and biological properties of *trans* platinum complexes: monofunctional platinum complexes containing one nucleobase as potential antiviral chemotypes. J. Bio. Inorg. Chem. **2000**, *5*, 575-583.

3. Anzellotti, A.I.; Liu, Q.; Bloemink, M.J.; Scarsdale, J.N.; Farrell, N.P. Targeting retroviral Zn finger-DNA interactions: a small-molecule approach using the electrophilic nature of *trans*-platinum-nucleobase compounds. Chem. & Biol. **2006**, *13*, 539-548.

4. Mangrum, J.B.; Zgani, I.; Tsotsoros, S.D.; Qu, Y.; Farrell, N.P. Zinc finger peptide cleavage by a dinuclear platinum compound. Chem. Comm. **2013**, *49*, 6986-6988.

5. Meyer, E.A.; Castellano, R.K.; Diederich, F. Interactions with aromatic rings in chemical and biological recognition. Angew. Chem. Int. Ed. **2003**, *42*, 1210-1250.

6. Almaraz, E.; de Paula, Q.A.; Liu, Q.; Reibenspies, J.H.; Darensbourg, M.Y.; Farrell, N.P. Thiolate bridging and metal exchange in adducts of a zinc finger model and Pt(II) complexes: biomimetic studies of protein/Pt/DNA interactions. J. Am. Chem. Soc. **2008**, *130*, 6272-6280.

7. de Paula, Q.A.; Mangrum, J.B.; Farrell, N.P. Zinc finger proteins as templates for metal ion exchange. Substitution effects on the C-finger of HIV nucleocapsid NCp7

using M(chelate) species (M = Pt,Pd, Au). J. Inorg. Biochem. **2009**, *103*, 1347-1354.

8. Bose, R.N.; Wei, W.; Yang, W.; Evanics, F. Structural perturbation of a C_4 zinc-finger module by *cis*-diamminedichloroplatinum(II): insights into the inhibition of transcription processes by the antitumor drug. Inorg. Chim. Acta **2005**, *358*, 2884-2854.

9. Oehlsen, M.E.; Qu, Y.; Farrell, N. Reaction of polynuclear platinum antitumor compounds with reduced glutathione studied by multinuclear (^{1}H, ^{1}H-^{15}N gradient heteronuclear single-quantum coherence, and ^{195}Pt) NMR spectroscopy. Inorg. Chem. **2003**, *42*, 5498-5506.

10. Chen, S.; Xu, D.; Jiang, H.; Xi, Z.; Zhu, P.; Liu, Y. *Trans*-platinum thiazole complex interferes with Sp1-zinc finger protein. Angew. Chem. Int. Ed. **2012**, *51*, 12258-12262.

11. Chen, S.; Jiang, H.; Wei, K.; Liu, Y. Tris-(2-carboxyethyl) phospine significantly promotes the reactions of cisplatin with Sp1 zinc finger protein. Chem. Comm. **2013**, *49*, 1226-1228.

12. Morelli, M.A.; Ostuni, A.; Cristinziano, P.L.; Tesauro, D.; Bavoso, A. Interaction of cisplatin with a CCHC zinc finger motif. J. Pept. Sci. **2013**, *19*, 227-232.

13. Maurmann, L.; Bose, R.N. Unwinding of DNA polymerases by the antitumor drug, *cis*-diamminedichloroplatinum(II). Dalton Trans. **2010**, *39*, 7968-7979.

Chapter 6

Unpublished Work

Samantha D. Tsotsoros and Nicholas P. Farrell

Department of Chemistry, Virginia Commonwealth University, 1001 W. Main Street,

Richmond, VA 23284-2006 USA

6.1   Introduction

The work that comprises this chapter is part of the larger goal of this dissertation to develop compounds designed to target HIV1 NCp7. The compounds synthesized below were designed to target HIV1 NCp7 as structural modifications of the PtN_4 coordination sphere.

6.2   Experimental

6.2.1   Synthesis

K[PtCl$_3$NH$_3$] Cisplatin (6.96 mmol) was dissolved in 40 mL of water and 20 mL of HCl and the solution was heated to reflux for 7 hours. The volume was reduced and the solution cooled to 4°C overnight. Any precipitated cisplatin was filtered off and the volume was reduced to 1/2V and the solution was cooled to 4°C overnight. Cisplatin was filtered and

the solution was reduced to 2/3V and cooled to 4ºC. Any precipitated cisplatin was filtered off and the volume was doubled. The dilute solution was run down a DOWEX 50W8X-200 cation exchange column equilibrated with 2M KCl. The eluent was placed in the fridge over the weekend and red solid was collected. The crude solid was recrystallized by dissolving in water, filtering off any cisplatin and lyophilizing.

[PtCl$_2$(en)] (1) K$_2$PtCl$_4$ (0.892 mmol) was dissolved in 4.5 mL of water and 228 μL of ethylenediamine was added dropwise. The solution was stirred at room temperature for 1 hour. The yellow solid was collected and washed with ethanol and ether. 89% yield. ^{1}H NMR: 3.50 (4H, s). Anal. Calcd: C 7.37, H 2.47, N 8.59, Found: C 7.45, H 2.29, N 8.51.

[PtCl(en)(Gua)]NO$_3$ [PtCl$_2$(en)] (0.5107 g, 1.56 mmol) was suspended in 575 mL of DMF. A solution of AgNO$_3$ (0.258 g, 1.51 mmol) in 200 mL of DMF was added to the platinum solution dropwise over 5 hours. The solution was stirred at room temperature overnight in the dark. The AgCl precipitate was removed by filtration through celite and guanosine (0.4436 g, 1.56 mmol) was added to the filtrate. The filtrate was stirred at room temperature overnight and rotovapped to 50 mL. Acetone was added to precipitate the final product. The product was filtered and washed with acetone and the filtrate was reduced in volume and placed in the freezer. The first product was labeled Crop 1. Upon cooling, solid precipitated in the filtrate. The solution was filtered to isolate the precipitated product âĂŞ this solid was labeled Crop 2. Once again, the filtrate was placed in the freezer and again precipitation was seen. The solution was filtered and this product was labeled Crop 3. The filtrate was placed in the freezer, but no further precipitation was observed.

The initial ^{1}H NMR for Crop 1 showed mono-Gua product (H8 integrated at 1H) and free Gua (H8 integrated at 1.20H). In order to remove the free Gua, the solid was stirred in MeOH and filtered to remove any undissolved particles. After filtration, the volume was reduced

and acetone was used to precipitate the product. NMR of Crop 1-A showed mono-Gua product (H8 integrated at 1H), bis-Gua (H8 integrated at 0.35) and free Gua (H8 integrated at 0.22H). NMR for Crop 2 initially showed only the mono product with a small amount of free Gua. The solid was stirred in methanol to remove the free guanosine and the resulting solid was lableled Crop 2-A. The NMR for Crop2-A showed mono product, bis product and free guanosine. The NMR for Crop 3 showed mono product, a small amount of bis product and free guanosine. Separating of the mono and bis products is very difficult through solubility, and use of a column or possibly HPLC may be necessary to achieve complete separation.

[PtCl(en)(NH$_3$)]Cl

Method 1 (2)

K[PtCl$_3$(NH$_3$)] (110 mg, 0.31 mmol) was suspended in 15 mL of MeOH and heated. To ensure complete dissolution, 10 mL of water was added. Ethylenediamine (0.30 mmol) was added and the solution was heated at reflux for 3 hours. The solution was cooled to room temperature and rotovapped to 5 mL. A large excess of acetone was added and a very white product precipitated. The solid was filtered and washed with acetone and ether and placed in the desiccator to dry. Elemental analysis was indicative of the formation of [Pt(en)$_2$]. Anal. Calcd: 12.44, 4.18, 14.51, Found: 12.15, 4.03, 14.11.

Method 2 (1)

K[Pt(NHCl$_{33}$)] (111 mg, 0.315 mmol) was dissolved in 4 mL of water. Ethylenediamine (80 uL, 1.19 mmol) was added dropwise, very slowly. A salmon colored precipitate formed immediately. The reaction was stirred at room temperature for 1 hour. The solid was filtered and washed with ethanol and ether and placed in the desiccator to dry. 57 mg of solid was recovered. Product is precipitation of [PtCl$_3$(NH$_3$)][PtCl(en)(NH$_3$)]. Anal. Calcd: C 3.84; H 2.25; N, 8.95; Found: C 4.03; H 2.05; N, 8.82.

[PtCl$_2$(COD)] (2)(3) K$_2$PtCl$_4$ (1.62 mmol) was dissolved in 10 mL of water and filtered to remove impurities. Glacial acetic acid (16 mL) was added followed by cyclooctadiene (674 μL). The reaction was heated to 90°C with rapid stirring for 30 minutes. The solution was cooled to room temperature and the volume was reduced to <5 mL. The product precipitated and was filtered and washed with water, ethanol and ether. 78% yield. ^{1}H NMR: 1.53 (1H, s), 2.23 (5H, m), 2.67 (4H, m), 5.59 (4H, s).

[PtCl(terpy)]Cl (2)(3) [PtCl$_2$(COD)] (0.42 mmol) was suspended in 17 mL of H$_2$O and 2,2',6',2"-terpyridine (0.42 mmol) was added. The reaction was stirred at 40°C for 40 minutes. The solution was rotovapped to dryness and ether was added. Sonication was used to remove the red residue from the glass and the solid was filtered and washed with ether. ^{1}H NMR: 7.4-8.2 (11H m).

[Pt(terpy)(9EtG)](NO$_3$)$_2$ [PtCl(terpy)]Cl (0.1 mmol) was dissolved in 20 mL of water, 1.98 eq. of AgNO$_3$ was added and the reaction was stirred at room temperature overnight. The precipitated AgCl was removed by filtration through a celite pad and 9-ethylguanine (1 eq.) was added to the filtrate. The reaction was stirred at 50°C for 72 hours and cooled to room temperature. The solvent was reduced to 1/3V and acetone was added to precipitate the product. 40% yield. ^{1}H NMR: 1.58 (3H, t) 4.35 (2H, q), 7.2-8.5 (11H, m), 8.90 (1H, s).

[Pt(dien)(CMP)] [Pt(dien)Cl]Cl (0.42 mmol) was activated with 1.98 eq. of AgNO$_3$ overnight. The AgCl precipitate was filtered off and CMP (0.42 mmol) was added to the filtrate. The reaction was stirred at 50°C overnight. The solution was cooled to room temperature and lyophilized. 52.4% yield. ^{1}H NMR: 8.23 (1H, d), 6.21 (1H, d), 6.01 (1H, d), 4.35 (2H, m), 4.28 (2H, m), 3.99 (3H, m), 3.03 (8H, m).

N-N'-dimethylethylenetriamine

Synthesis of Ts$_3$dien (4) p-toluenesulfonylchloride (67.3067 g, 0.353 mol) was stirred in 176 mL of pyridine and heated to 40°C until all solid dissolved. Diethylenetriamine (12.6 mL, 0.102 mol) in 17.6 mL of pyridine was added slowly to maintain a reaction temperature of 50-60°C. The solution was stirred for 30 minutes and cooled to room temperature. 150 mL of water was added to the orange/brown solution and the solution was stirred overnight. The resulting solid was filtered and washed with ice-cold ethanol and dried at 60°C for 2 days. Recovered: 42.656 g, 65% yield.

Synthesis of Me$_2$Ts$_3$dien (5) Ts$_3$dien (42.6557 g, 0.754 mol) was dissolved in 271 mL of DMF and the solution was cooled on ice. NaH (11.02 g, 0.459 mol) was added and the solution was stirred until gas evolution subsided. Dimethyl sulfate (25.3 mL, 0.267 mol) was added dropwise. The solution was stirred for 1 hour at room temperature and 2 hours at 70°C. The solution was cooled to room temperature and NaOAc (9.0372 g, 0.117 mol) was added and the reaction mixture was stirred for 45 minutes. The solid was filtered and the filtrate rotovapped to dryness. The resulting solid was filtered and along with the first solid, washed with MeOH, H$_2$O, MeOH, and ether. Methylene chloride (180 mL) was added to dissolve the solid. Any remaining solid was filtered and the filtrate was reduced to 1/2V. A large excess of MeOH was added and the cream-colored precipitate was filtered and washed with MeOH and ether. Recovered: 43.040g, 95% yield.

Synthesis of Me$_2$dien (5) Acetic anhydride (107 mL) was cooled on ice and HBr (192 mL) was added dropwise. The solution was stirred on ice for 20 minutes and at room temperature for 12 hours. Ts$_3$me$_2$dien (43.0405 g, 0.2136 mol) was added to the acid solution and the reaction mixture was heated at reflux for 10 hours. The solution was cooled to room temperature, rotovapped to 1/2V, and extracted with 2x105 mL portions of ether. The aqueous

layer was rotovapped to 1/2V and ethanol was added to induce crystallization. The solution was cooled on ice and ether was added. The resulting solid was filtered and washed with 2:1 ethanol:ether and ether. The solid was mixed with NaOH (21.36 g, 0.534 mol) and was stirred until smoking subsided. The resulting slurry was extracted with methylene chloride and any remaining solid was filtered and washed with methylene chloride. The filtrate was rotovapped to remove the methylene chloride. Recovered: 5.0295 g, 53% yield.

[Pt(dien)(Xnt)](NO$_3$)$_2$ [PtCl(dien)]Cl (0.47 mmol) was dissolved in 10 mL of water, 1.98 eq. of AgNO$_3$ and 1 eq. of xanthine were added and the reaction was stirred overnight at 50°C. The solution was filtered through a celite pad to remove the precipitated AgCl and the filtrate was rotovapped to 1/3V. A large excess of acetone was added to precipitate the product and the solid was filtered and washed with acetone and ether. 70% yield. ^{1}H NMR: 2.15 (1H, s), 3.00 (8H, m), 8.68 (0.3H, s), 7.95 (0.2H, s), 8.10 (0.1H, s), 8.25 (0.2H, s). The appearance of multiple H8 peaks is indicative of platinum binding to multiple sites on the Xnt. Therefore, the reaction should be carried out at an appropriate pH so that only the H8 is deprotonated.

[Pt(me$_4$dien)(Cl)]PF$_6$ (2) Pt(dmso)$_2$Cl$_2$ (1g, 2.36mmol) was suspended in 200 mL of methanol and placed at 50°C with stirring. Me$_4$dien (440 μL, 2.36 mmol) in 40 mL of MeOH was added to the Pt solution and heated at reflux for 2.5 hours. The solution was cooled to room temperature and a small amount of white solid precipitated. The solvent was reduced to 1/3V and NH$_4$PF$_6$ (2.36 mmol) was added. The solution was placed in the freezer overnight. 337mg of large yellow crystalline solid was collected. ^{1}H NMR: 3.00 (20H, m) Anal. Calcd: C, 17.97; 3.96; N, 7.86 Found: C, 17.71; H, 3.79; N, 7.41.

[Pt(me$_4$dien)(GMP)]PF$_6$- [Pt(me$_4$dien)Cl]PF$_6$ (0.167 mmol) was dissolved in 8.6 mL of

water. AgNO$_3$ (1 eq) was added and the reaction was left in the dark at 37°C overnight. The AgCl precipitate was filtered off and 5'GMP (1 eq.) disodium salt was added. The reaction was placed at 50°C for 24 hours. The volume was reduced to dryness, 2 mL of ether was added and the solid was scraped from round-bottom flask. The solid was placed in the dessicator to dry overnight. 80.2% yield.

[Pt(me$_4$dien)(9EtG)]PF$_6$- [Pt(me$_4$dien)Cl]PF$_6$ (0.20 mmol) was dissolved in 14 mL of H$_2$O and heated to 37°C with intermittent sonication to dissolve. AgNO$_3$ (0.196 mmol) was added to solution and the reaction was placed in the dark at 37°C for two days. The AgCl precipitate was filtered using celite. 9-ethylguanine (0.20 mmol) was added to the filtrate and the reaction was placed at 50°C with stirring for five days. The solution was cooled to room temperature and filtered to remove any precipitate. The solution was rotovapped to dryness, leaving a white solid. 78.6% yield. ^{1}H NMR in D$_2$O: 8.7 ppm (0.76H, d), 8.3 ppm (0.34H, s), 4.2 ppm (2.15H, m), 2.9 ppm (8H, m), and 1.5 ppm (3H, m).

6.2.2   Techniques

Circular Dichroism

CD spectra were recorded on a Jasco J-600 Spectropolarimeter (Jasco, Corp., Tokyo, Japan). Each spectrum was recorded from 190 nm to 250 nm in a 0.1 cm cuvette path length at room temperature under N$_2$. Spectra were baseline corrected using the Jasco software and noise-reduced using Origin. Pt compounds were added to the peptides at a ratio of 1:1 and incubated at 37°C for 15 minutes, 1 hour, 3 hours, 5 hours or 24 hours accordingly. The pH of the solutions was adjusted to 7.2-7.4 with NH$_4$OH.

Fluorescence Spectroscopy

A. Association Constant Determination: Fluorescence spectra were recorded on a Varian Cary Eclipse Fluorescence Spectrometer with a single-cell Peltier accessory. Fluorescence spectra were recorded from 300 nm to 450 nm with a scan rate of 120 nm/min. Measurements were recorded at 20°C. The maximum intensity of the spectrum was measured and the association constants for each drug were calculated from the Eadie-Hofstee plots. The data presented is an average of 3 trials.

B. TSQ Assay: 2μM zinc finger was prepared in water with 50 μM TSQ (with or without 1 eq. of platinum complex) at a final volume of 3 mL. The sample was excited at 344 nm and emission was monitored at 365 nm. To prepare a standard curve, Zn was added from 0.5-3.0 μM.

Reaction of [Pt(dien(L)](NO$_3$)$_2$ with N-AcCys by ^{1}H NMR

[Pt(dien)(L)](NO$_3$)$_2$ and N-AcCys were dissolved in 500 μL of D$_2$O at a 1:1 ratio and the ^{1}H NMR was monitored on a 300 MHz Varian NMR Spectrometer once an hour for 15 hours and once a day for 7 days.

DNA Melting Point

DNA melting studies were recorded on a JASCO V-550 UV/Vis spectrometer. Studies were performed with drug to nucleotide ratios (ri) of 0.01, 0.03, 0.05, 0.075, and 0.1 in 10 mM NaClO$_4$ at pH 6.10. The concentration of Calf Thymus DNA was 100 μM for each experiment. The results were determined from an average of 2 trials.

Cellular Accumulation

CCRF-CEM and Jurkat cells were seeded at 2 million cells per plate. 20 μM cDDP and AH78 was added and the cells were incubated for 3 and 6 hours. The media was removed and the cells were washed twice with 10 mL of cold PBS. The pellets were stored in the

freezer. To digest samples for ICP-MS analysis, 1 mL of conc. HCl was added to the cell pellets and left to digest for 2 hours. Water (1 mL) was added to dilute the solution and the samples were run.

Cytotoxicity Assay

Cell viability of HCT116, A2780, MCF7, and MDA-MB-231 cells was studied by MTT assay. 5000 cells/well were plated on a 96-well plate and incubated in quadruplet with [Pt(dien)L]n+ for 72 hours at various drug concentrations (HCT116, A2780: 200, 100, 50, 25, 12.5, 6.25, and 3.125 μM or MCF7, MDA-MB-231: 50, 25, 12.5, 6.25, 3.125, 1.5625, 0.78125 μM). The drug solution was removed and 100 μL of 0.5 mg/mL MTT solution was added and incubated for 4 hours. The MTT solution was removed and 100 μL of DMSO was added to solubilize the formazan crystals. The absorbance at 570 nm was determined on a μQuant Microplate Spectrophotometer from Bio-Tek instruments.

Fourier Transform Ion Cyclotron Resonance Mass Spectrometry

Experiments were conducted on a modified Bruker Daltonics (Billerica, MA) SolariX FTICR-MS equipped with a 12T superconducting magnet. Analyses were carried out by direct infusion using tapered quartz nanospray emitters loaded with 5-10 μL of sample with a spray voltage between 800-1100 V relative to the capillary inlet supplied by an inserted stainless steel wire. Solutions were prepared as follows:

A. Control experiment was performed as discussed in Chapter 4.

B. 1:1 reaction of NCp7 with [Pt(dien)(Gua)]$^{2+}$

A solution of NC (7.5 μM in 1 μL H$_2$O) was added to a solution of [Pt(dien)(Gua)]$^{2+}$ (7.5 μM in 1 μL) and the volume was brought up to 10 μL with 7 μL 150 mM ammonium acetate and 1 μL isopropyl alcohol. The mixture was analyzed immediately in negative ion mode.

C. 5:1 reaction of NCp7 with [Pt(dien)(Gua)]$^{2+}$

A solution of NC (7.5 μM in 1 μL H$_2$O) was added to a solution of [Pt(dien)(Gua)]$^{2+}$ (37.5 μM in 1 μL) and the volume was brought up to 10 μL with 7 μL 150 mM ammonium acetate and 1 μL isopropyl alcohol. The mixture was analyzed immediately in negative ion mode.

D. A solution of NC (7.5 μM in 1 μL H$_2$O) and [Pt(dien)(Gua)]$^{2+}$ (7.5 μM in 1 μL) was incubated for 30 minutes at room temperature. SL2-RNA (7.5 μM in 1 μL), 6 μL 150 mM ammonium acetate, and 1 μL isopropyl alcohol were added and the mixture was analyzed immediately in negative ion mode.

E. A solution of NC (7.5 μM in 4 μL H$_2$O) was added to a solution of SL2 (7.5 μM in 2 μL H$_2$O) to form the 2:1 NC/RNA complex. The complex formed immediately; no significant incubation was necessary. A solution of [Pt(dien)(Gua)]$^{2+}$ (7.5 μM in 2 μL) was added and volume was brought up to 10 μL with 1 μL 150 mM ammonium acetate and 1 μL isopropyl alcohol. The mixture was analyzed in negative ion mode immediately.

6.3   Results and Discussion

6.3.1 ^{1}H NMR Spectroscopy

It is important to understand the reactions between platinum complexes and S-containing amino acids, such as Cys, due to the high concentrations of proteins like human serum albumin (HSA) and glutathione. These proteins are responsible for binding to platinum, essentially deactivating the drugs leading to removal from the system. Reactions with sulfur proteins have been found to be the main source of toxic side effects caused by cisplatin(6). The compounds [Pt(dien)(9EtG)]$^{2+}$, [Pt(dien)(1-MeCyt)]$^{2+}$ and [Pt(Me$_4$dien)(9EtG)]$^{2+}$ are designed to have very slow or non-existent reactions with S-containing species. The 1:1 overnight reaction of [Pt(dien)(9EtG)]$^{2+}$ (Figure 6.1); [Pt(dien)(1MeCyt)]$^{2+}$ (Figure 6.2); and [Pt(Me$_4$dien)(9EtG)]$^{2+}$, Figure 6.3 with N-AcCys was monitored by ^{1}H NMR. No major changes were seen in the spectrum indicating the inertness of the PtN$_4$ coordination sphere.

In the presence of more than one equivalent of a Cys-containing species at 37°C, displacement of the 9EtG has been seen to some extent (7).
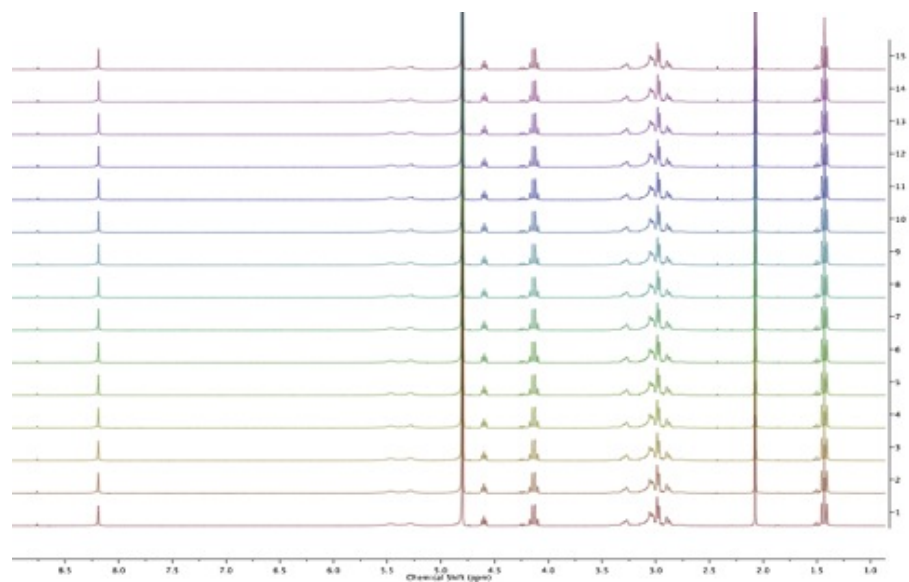
Figure 6.1: ^{1}H NMR of a 1:1 reaction (D$_2$O) of [Pt(dien)(9EtG)]$^{2+}$ with N-AcCys
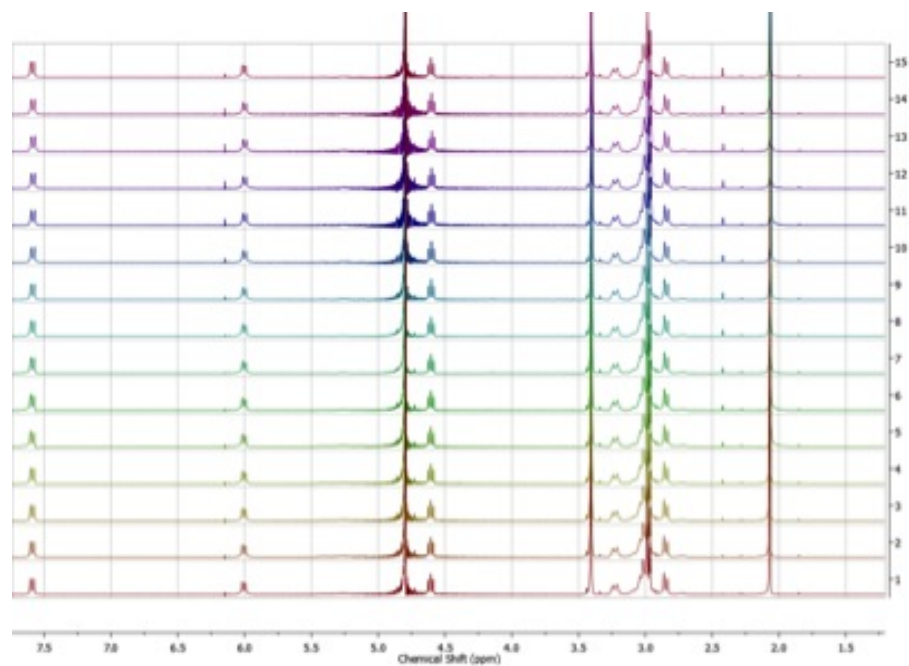
Figure 6.2: ^{1}H NMR of a 1:1 reaction (D$_2$O) of [Pt(dien)(1MeCyt)]$^{2+}$ with N-AcCys.
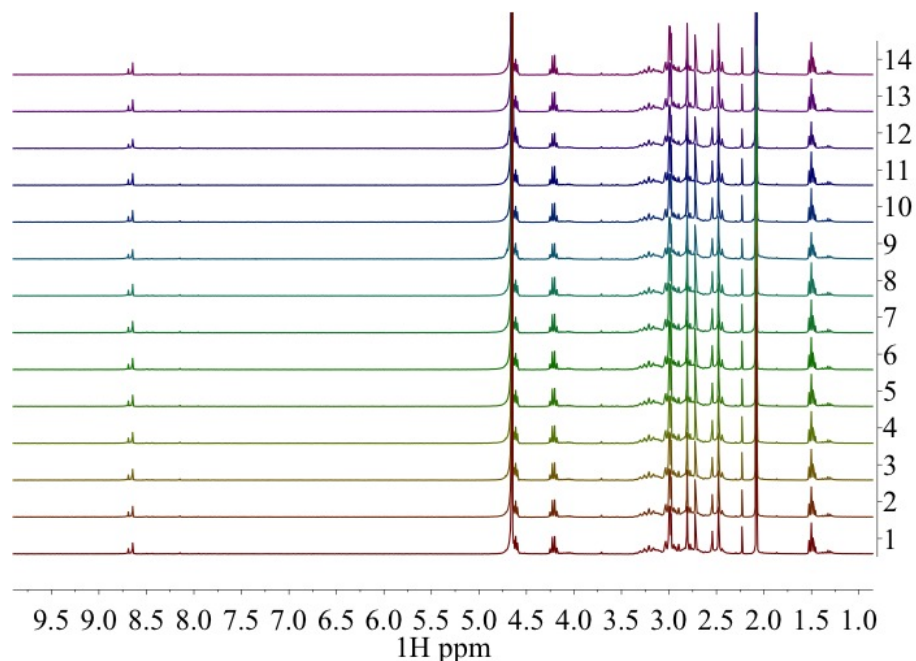
Figure 6.3: ^{1}H NMR of a 1:1 reaction (D_2O) of [Pt(Me$_4$dien)(9EtG)]$^{2+}$ with N-AcCys.

6.3.2 Temperature Dependence of the H8 Signal Splitting in [Pt(me$_4$dien)GMP]

As seen in Chapter 5, addition of a nucleobase to [Pt(Me$_4$dien)] results in a very sterically hindered complex. The ^{1}H NMR of [Pt(Me$_4$dien)GMP] shows the sample splitting of the H8 of Gua as [Pt(dien)(9EtG)]$^{2+}$ due to the hindered rotation of the nucleobase about the Pt-N bond. A temperature-dependant NMR experiment was performed from 24°C to 65°C. The increase in temperature caused a slight decrease in the spacing and broadening of the two H8 peaks, indicating that the methyl groups on the dien provide a significant amount of steric hinderance, Figure 6.4. If the temperature had continued to be raised, it is reasonable to assume that the two signals would have coalesced.

6.3.3 UV-Vis of PtN$_4$ compounds

The UV absorption for the compounds studied in Chapter 5 was obtained. The maximum
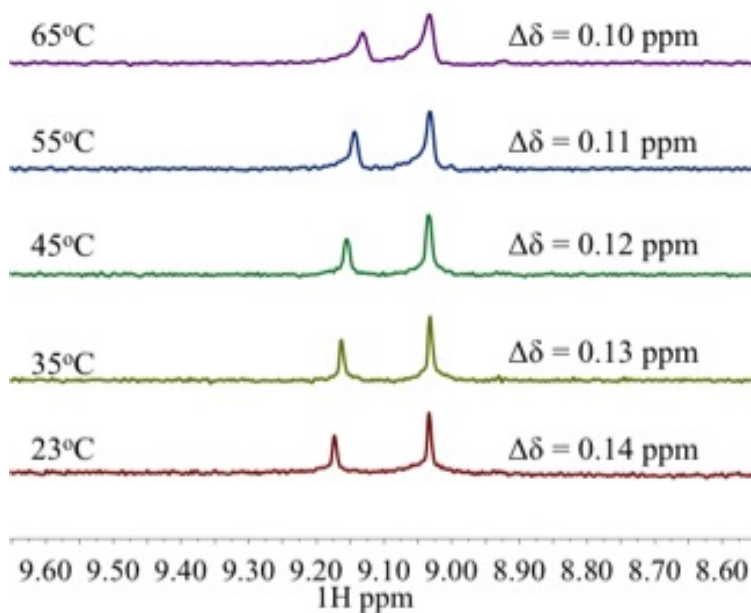
Figure 6.4: Temperature-dependent ^{1}H NMR spectrum of [Pt(me$_4$dien)(5'-GMP)].

absorbances and extinction coefficients can be found in Table 6.1.

6.3.4 Circular Dichroism studies with zinc finger peptides

Circular dichroism gives information about the secondary structure of proteins. Therefore, it is a useful tool in studying the reaction between compounds and peptide sequences. Here, we studied the interaction of an inert PtN$_4$ coordination sphere compared to the more reactive PClN$_3$ compounds. The basis for these studies is targeting the C-terminal ZF of HIV1 NCp7. It is important to understand how the zinc coordination sphere affects the reactivity of the zinc finger and therefore several sequences were used: the C-terminal ZF of NCp7, mutant peptides based on the C-terminal knuckle of NCp7 with the Met residue removed, and F3 of Sp1 (Figure 6.5 (C$_2$H$_2$).

6.3.4.1 Circular Dichroism of Apo-Peptide vs. Zinc Finger

Incubation of the free peptides with 1.3 equivalents of ZnOAc in water at pH 7.2-7.4 results in a decrease in the negative intensity of the peak at 197 nm with a red shift to 200 nm and

Table 6.1: UV-Vis of all compounds synthesized and reported in Chapter 5. Values in parenthesis are the extinction coefficient, ϵ in L mol^{-1} cm^{-1}.

Compound	λmax (nm)		
[Pt(dien)(7MeG)]$^{2+}$	280 (6087)	256 (5716)	208 (26135)
[Pt(dien)(Ino)]$^{2+}$	—	257 (9293)	208 (26684)
[Pt(dien)(9EtG)]$^{2+}$	281 (6152)	256 (8511)	206 (26246)
[Pt(NMedien)(9EtG)]$^{2+}$	275 (5627)	255 (7361)	207 (24836)
[Pt(me$_2$dien)(9EtG)]$^{2+}$	281 (6152)	256 (7641)	206 (26508)
[Pt(me$_4$dien)(9EtG)]$^{2+}$	282 (4203)	258 (6298)	208 (25787)
[Pt(dien)(Gua)]$^{2+}$	280 (6632)	260 (9026)	205 (21798)
[Pt(NMedien)(Gua)]$^{2+}$	277 (6818)	258 (8906)	207 (26513)
[Pt(me$_2$dien)(Gua)]$^{2+}$	279 (6039)	259 (8559)	208 (27132)
[Pt(me$_4$dien)(Gua)]$^{2+}$	283 (4704)	258 (7768)	209 (27021)
[Pt(dien)(Xan)]$^{2+}$	281 (7557)	255 (7333)	208 (26048)
[Pt(NMedien)(Xan)]$^{2+}$	280 (6087)	256 (5716)	208 (26135)
[Pt(me$_2$dien)(Xan)]$^{2+}$	279 (6327)	256 (6522)	208 (26906)
[Pt(me$_4$dien)(Xan)]$^{2+}$	280 (5554)	257 (5929)	208 (27566)
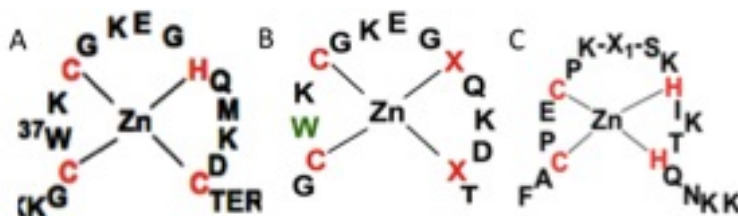
Figure 6.5: Structures of the zinc fingers studied. A- C-terminal ZF of HIV1 NCp7, B- Mutant peptides, X= Cys or His and C- SP1 F3.

an increase in positive ellipticity from 210-230 nm, indicative of the formation of zinc finger.

6.3.4.2 Circular Dichroism of the C-terminal ZF of HIV1 NCp7

The reaction of the C-terminal zinc finger of HIV1 NCp7 with [PtCl(dien)]$^+$, [Pt(dien)-(1MeCyt)]$^{2+}$ and [Pt(dien)(9EtG)]$^{2+}$ was monitored over 24 hours. As seen in Figure 6.6, 24

hours of incubation with $[PtCl(dien)]^+$ resulted in a decrease in the positive ellipticity at 220 nm and an increase in the negative band at 200 nm; both changes are indicative of zinc ejection. In contrast, both PtN_4 species showed no change to the CD spectra. This result highlights the inertness of $[Pt(dien)(nucleobase)]_{2+}$ complexes when reacted with S-containing species, especially compared to the more reactive parent compound, $[PtCl(dien)]^+$.

6.3.4.3   Circular Dichroism of the C-terminal ZF of C_3H Mutant Peptide

Upon incubation of the zinc finger with $[Pt(dien)Cl]^+$, structural perturbation was seen as indicated by the large increase in negative intensity and small shift towards 197 nm, Figure 6.7. The reaction of this drug with the mutant zinc finger was greater than that with the NCp7 C-terminal sequence. This may be attributed to the strain in the zinc finger caused by a smaller zinc coordination sphere. The N_4 analog, $[Pt(dien)(9EtG)]^{2+}$, did not induce
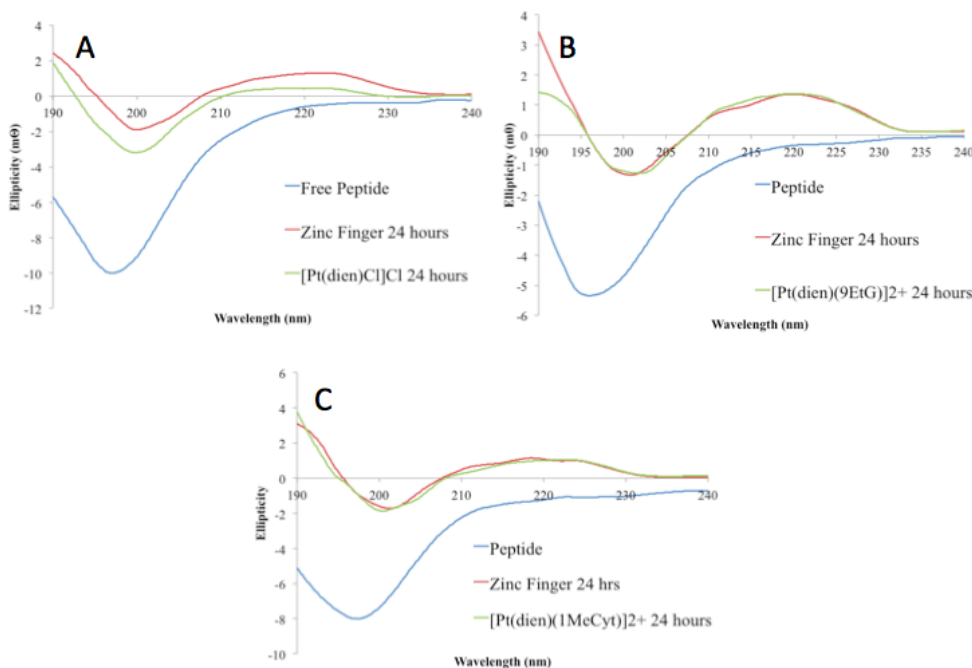
Figure 6.6: Circular dichroism of the C-terminal ZF of HIV1 NCp7 with A- $[PtCl(dien)]^+$, B- $[Pt(dien)(9EtG)]^{2+}$, and C- $[Pt(dien)(1MeCyt)]^{2+}$.

structural changes. This result is expected, as the N_4 analogs are inert species that should not covalently interact with the zinc peptides.

6.3.4.4 Circular Dichroism of the Full NCp7

The CD spectra of the full NCp7 protein showed changes over time, Figure 6.8. This may be due to the flexibility in the protein. Due to the changes seen for NCp7 alone, study of the reaction with compounds does not lead to any clear results. Therefore, another technique would be more suitable to study this reaction or the CD can be taken at very low temperatures to slow the motion of the protein.

6.3.4.5 Circular Dichroism of SP1 F3 C2H2 Zinc Finger

The incubation of this zinc finger at 37ºC with no drug showed structural changes, however to account for this a spectrum was run at each incubation time point to allow for direct comparison when the zinc finger was incubated with drug. Incubation of the Sp1 F3 C_2H_2 zinc finger with $[Pt(dien)Cl]^+$ over 24 hours did not result in any structural changes to the peptide. This result suggests a slower reaction rate for the drug with the C_2H_2 zinc finger than the C_3H NCp7 and mutant zinc fingers, Figure 6.9. This is expected due to the
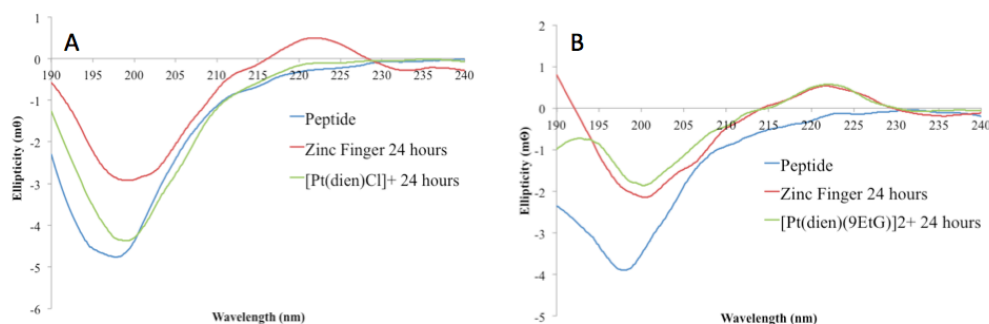
Figure 6.7: Circular dichroism of the C-terminal ZF of HIV1 NCp7 with A- $[PtCl(dien)]^+$, and B- $[Pt(dien)(9EtG)]^{2+}$.
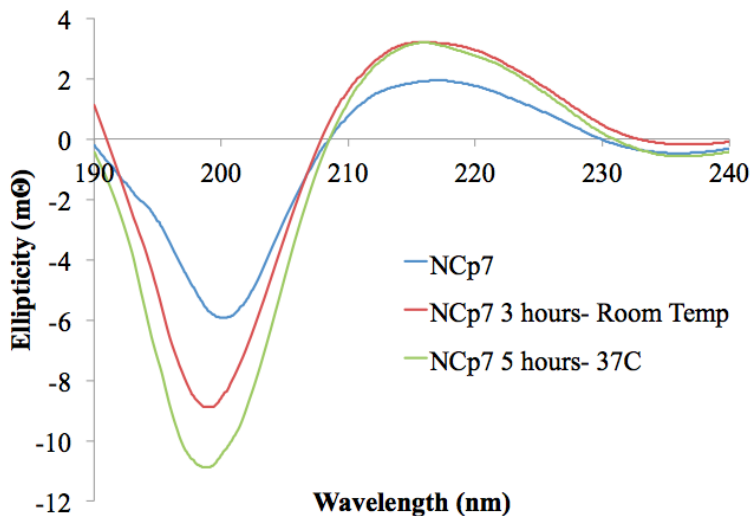
Figure 6.8: Circular dichroism spectra for the full NCp7 over a span of 24 hours.

decrease in the number of cysteine residues, which are reactive towards Pt. Incubation with $[Pt(dien)(9EtG)]^{2+}$ also did not induce any structural changes to the zinc finger.
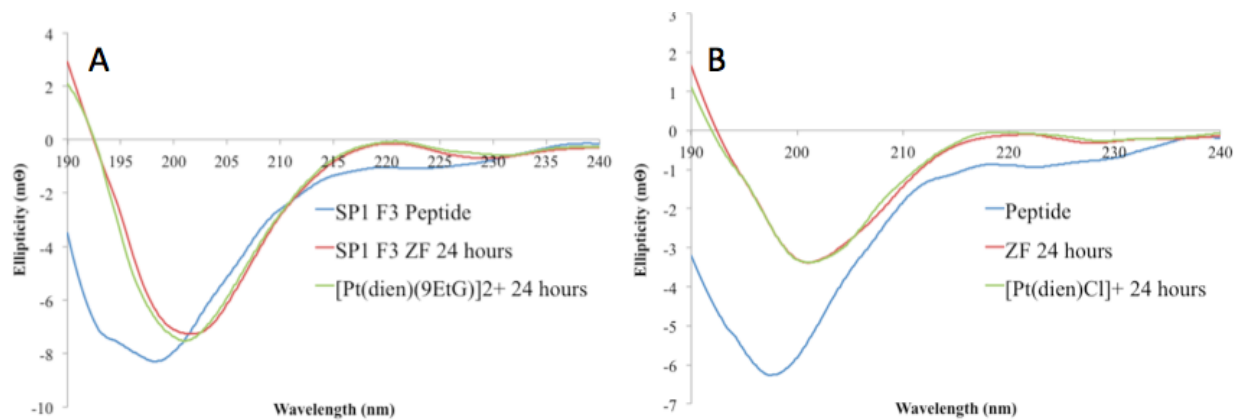
Figure 6.9: Circular dichroism of SP1 F3 with A- $[PtCl(dien)]^+$, and B- $[Pt(dien)(9EtG)]^{2+}$.

6.3.5 Fluorescence Spectroscopy

6.3.5.1 Determination of Association Constant

Fluorescence spectroscopy has been used to determine the association constant for platinum compounds with N-AcTrp and the C-terminal ZF of HIV1 NCp7 (8, 9, 10). Here, we determined the association constant for the C_3H and C_2H_2 mutant peptides to determine if the change in coordination sphere affects π-stacking interactions with $[Pt(dien)(9EtG)]^{2+}$. The association constants are all very close in value and can be considered the same within the error calculated. This indicates that the constricted coordination sphere (C_3H) mutant and change in the number of cysteines (C_2H_2) do not affect the strength of the π-stacking interaction, Table 6.2.

Table 6.2: The association constant calculated for $[Pt(dien)(9EtG)]^{2+}$ with different peptide sequences.

Compound	Ka (x10^{-3}) M^{-1}
NCp7 C-Terminal C_3H	13.10 ± 0.94
C_3H Mutant	12.17 ± 0.07
C_2H_2 Mutant	13.93 ± 1.71

6.3.5.2 TSQ Assay

N-(6-Methoxy-8-quinolyl)-p-toluenesulfonamide (TSQ) is used as a probe for the presence of zinc. Upon addition of zinc, a complex of TSQ_2Zn is formed and fluoresces at 365 nm, compared to 385 nm for TSQ without zinc. This fluorescence can be used to quantitate the release of zinc from zinc finger proteins. Here, the C-terminal ZF of HIV1 NCp7 and Sp1F3 were analyzed for release of zinc, Figure 6.10. The addition of TSQ to a solution of the C-terminal ZF of NCp7 resulted in immediate release and chelation of zinc from the ZF; therefore, this assay is unsuitable for use to monitor the reaction of platinum complexes with

the ZF. The incubation of Sp1 F3 with TSQ resulted in a significantly slower time-dependent release of Zn but the chelation of Zn by TSQ makes this assay unsuitable to study the rate of Zn release caused by a platinum compound.
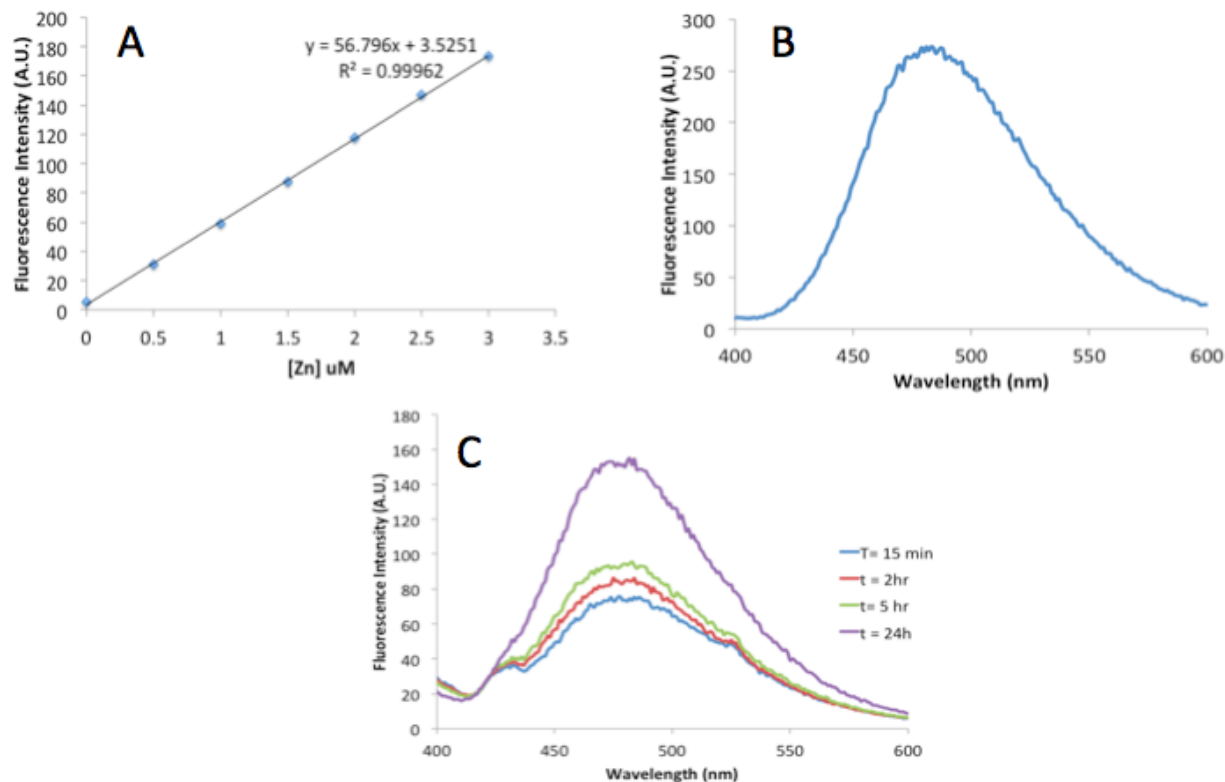
Figure 6.10: A- Standard curve for addition of Zn^{2+} to a $50\mu M$ TSQ solution, B- Fluorescence of the C-terminal ZF of HIV1 NCp7 immediately upon addition of TSQ, and C- Time-dependent release of Zn^{2+} from Sp1 F3 upon incubation with TSQ.

6.3.6 DNA Melting Point Studies

Cytotoxic platinum agents, such as cisplatin, exert their toxic effects through binding to DNA leading to apoptosis. The compounds developed in this dissertation should not exhibit such binding, as PtN_4 coordination spheres are relatively stable and should react slowly. The melting point of Calf Thymus DNA was determined by UV-Vis spectroscopy after 24

hour incubation with platinum complex. As seen in Table 6.3, addition of platinum drug to DNA had little to no effect on the melting point, indicating a lack of reactivity. This is complementary to the work already published (7).

Table 6.3: The melting point of calf thymus DNA after incubation with platinum-nucleobase compound as determined by UV-Vis spectroscopy.

	Dilution (R_i)					
Compound	0	0.01	0.03	0.05	0.075	0.1
$[PtCl(dien)]^+$	68.5	69.5	68	67.3	66.5	65
$[Pt(dien)(9EtG)]^{2+}$	68.5	67.85	68.2	68.45	69.75	68.05
$[Pt(dien)(GMP)]$	69	67.3	68.8	69.7	69.3	68.7
$[Pt(dien)(7MeG)]^{2+}$	68.5	68.7	70.2	71.75	71.2	72.5
$[Pt(dien)(Gua)]^{2+}$	68.5	68.3	68.9	69.2	68.2	68.4
$[Pt(me4dien)Cl]^{2+}$	68.5	67.5	66.7	68.4	65.5	66.2

6.3.7 Cytotoxicity Assays

Ideally, the platinum compounds developed within this dissertation are selective for HIV1 NCp7 and therefore should not affect normal cellular functions. As part of this specificity, the compounds should not be cytotoxic. The *in vitro* activity of certain $[Pt(dien)L]^{n+}$ complexes has not yet been studied. Therefore, MTT assays to determine cytotoxicity for the complexes $[Pt(dien)Cl]^+$, $[Pt(dien)(9EtG)]^{2+}$, $[Pt(dien)(GMP)]$, and $[Pt(dien)(1MeCyt)]^{2+}$ were performed in HTC116, human colon carcinoma; A2780, human ovarian carcinoma; MCF7, human breast carcinoma; and MDA-MB-231, human breast carcinoma. As shown in Table 6.4, the compounds can generally be considered non-cytotoxic with the exception of $[Pt(dien)(GMP)]$ in A2780 cells. The enhanced cytotoxicity of the GMP compound in A2780s is not entirely surprising as these cells are known to be very sensitive to platinum agents. Overall, the cytotoxicity results displayed below support the idea of specificity, in that the compounds are not toxic to non-HIV cells.

Table 6.4: *In vitro* cytotoxicity of $[PtCl(dien)]^+$ and platinum-nucleobase complexes in HCT116, A2780, MCF7 and MDA-MB-231 cell lines as determined by MTT assay.

Compound	IC$_{50}$ (μM)			
	HCT116	A2780	MCF7	MDA-MB-231
$[PtCl(dien)]^+$	>200	>200	—	—
$[Pt(dien)(9EtG)]^{2+}$	100	140.5	>50	>50
$[Pt(dien)(GMP)]$	73.9	2.5	>50	>50
$[Pt(dien)(1MeCyt)]^{2+}$	>200	126.5	—	—

6.3.8 Cellular Accumulation Studies

As evidenced in Chapter 5, cellular accumulation studies are another important tool to determine the activity profile of platinum drugs. As a control experiment, the cellular accumulation of cisplatin and AH78 was studied using CCRF-CEM and Jurkat cell lines. These cell lines are both CD4+ and therefore HIV-susceptible. Figure 16.11 shows the uptake profile for both compounds. As expected, AH78 enters the cells at a much faster rate than cisplatin. The cellular accumulation of both compounds varied between cell lines, but an increase in the amount of drug between 3 and 6 hours is indicative of active cell uptake. The mechanism of this uptake remains to be investigated.

6.3.9 FTICR-MS of NCp7 with SL2 in the presence of $[Pt(dien)(Gua)]^{2+}$

It is important to evaluate the platinum compounds studied in this dissertation for more than their basic properties, such as association with Trp. In order to evaluate the efficacy of these compounds, it is important to study their ability to interrupt the NCp7/RNA interaction. Interruption of this interaction may inhibit the virus from successful replicating. Figure 11 shows the interaction of NCp7 with $[Pt(dien)(Gua)]^{2+}$ in a 1:1 ratio. Small peaks corresponding to the 1:1 adduct can be seen and when the ratio of drug:NCp7 is increase
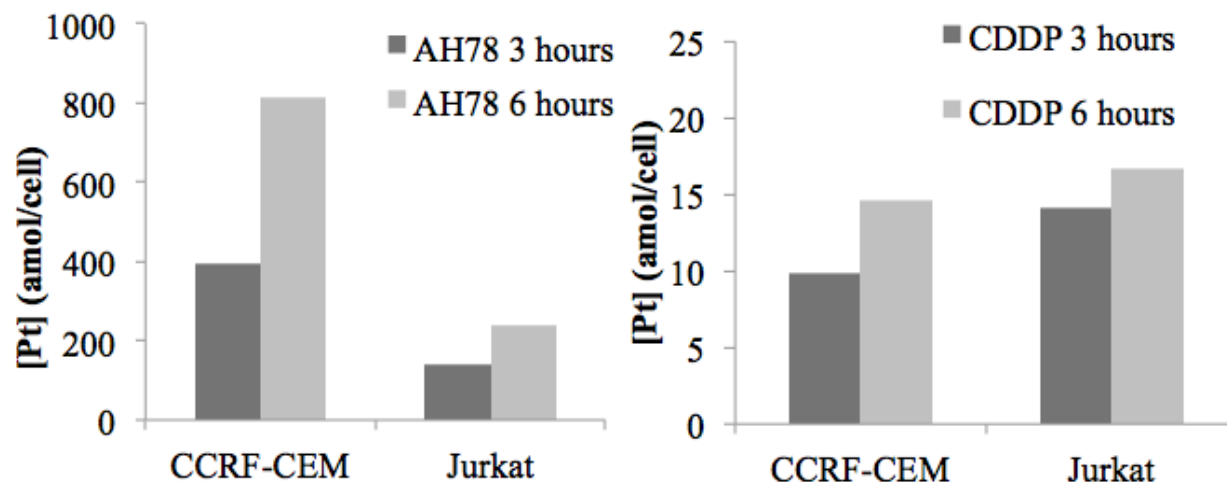
Figure 6.11: Cellular accumulation of AH78 (left) and cisplatin (right) in CCRF-CEM and Jurkat cell lines.

to 5:1, these peaks become higher in intensity. The incubation of drug with NCp7 followed by addition of SL2 RNA resulted in retardation of the formation of the NCp7/SL2 complex as evidenced by the peak for free SL2, Figure 12. Formation of the NCp7/SL2 complex followed by addition of the platinum drug was performed, but degradation of the SL2 solution convoluted the results and no conclusions can be made. It is reasonable to assume, based on the previous study and the study of $[Pt(dien)(9EtG)]^{2+}$ as discussed in Chapter 4, that the addition of $[Pt(dien)(Gua)]^{2+}$ to the intact NC/SL2 complex would result in some dissociation.

6.3.10   Conclusions

The studies presented in this chapter are complementary to the total work of this dissertation. The goal was to develop compounds designed to target HIV1 NCp7 and study the factors affecting this interaction. ^{1}H NMR and CD studies confirmed the inertness of the PtN_4 coordination sphere. No significant binding occurred between $[Pt(dien)(9EtG)]^{2+}$ or $[Pt(dien)(1MeCyt)]^{2+}$ with N-AcCys or zinc finger proteins. The cytotoxicity profiles ob-
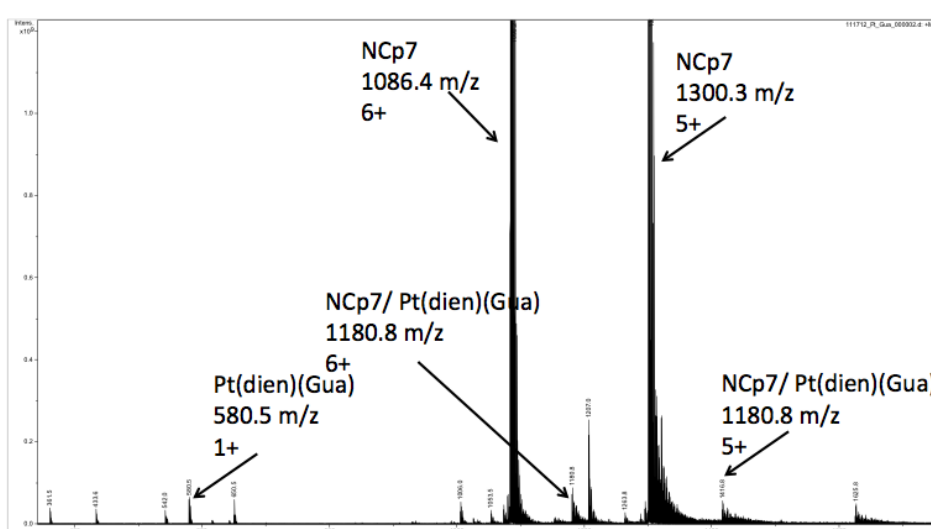
Figure 6.12: Mass spectrum of the 1:1 reaction of $[Pt(dien)(Gua)]^{2+}$ with NCp7.
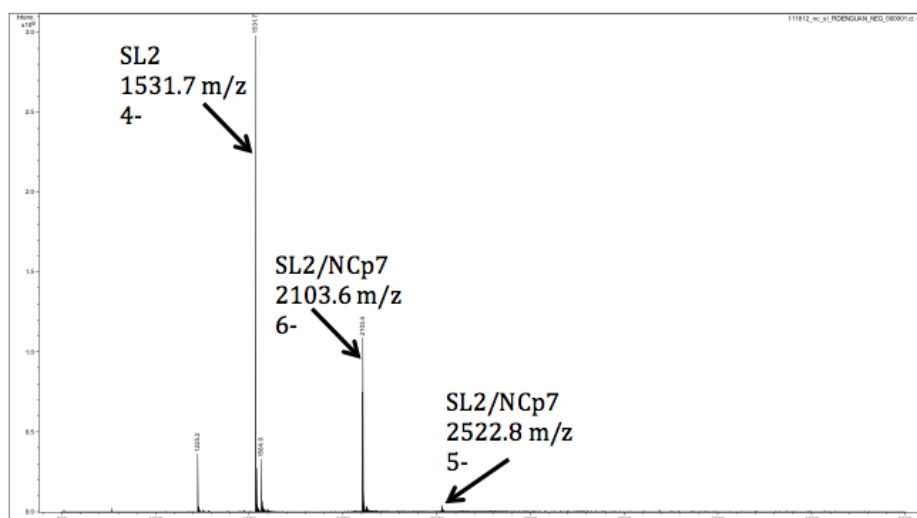
Figure 6.13: Mass Spectrum of the 1:1 reaction of $[Pt(dien)(Gua)]^{2+}$ with NCp7 followed by addition of SL2.

tained indicate a lack of cytotoxicity for compounds of the structure $[Pt(dien)L]^{n+}$. The lack of DNA binding is also indicative of specificity for these compounds. As a whole, the body of work presented here suggests that $[Pt(dien)L]^{n+}$ is a chemotype that specifically targets NCp7, which as discussed in earlier chapters, is a target of great interest for HIV treatment.

6.3.11   References

1. Chopade, S. M.; Phadnis, P. P.; Wadawale, A.; Hodage, A. S.; Jain, V. K. Synthesis and characterization of (ethylenediamine)/(diammine)platinum(II) coordinated to seleno ligands containing carboxylic acid functionality. Inorg. Chim. Acta **2012**, *385*, 185-189.

2. Annibale, G.; Brandolisio, M.; Pitteri, B. New routes for the synthesis of chloro (diethylenetriamine) platinum(II) chloride and chloro(2,2':6',2'-terpyridine)platinum(II) chloride dihydrate. Polyhedron **1995**, *14*, 451-453.

3. McDermott, J. X.; White, J. F.; Whitesides, G. M. Thermal decomposition of bis(phosphine)platinum(II) metallocycles. J. Am. Chem. Soc. **1976**, *98*, 6521-6528.

4. Atkins, T. J.; Richman, J. E.; Oettle, W. F. Macrocyclic Polyamines: 1,4,7,10,13,16-hexaazacyclooctodecane. Org. Synth. **1978**, *58*.

5. Paul-Roth, C.; Raymond, K. N. Amide Functional Group Contribution to the Stability of Gadolinium(III) Complexes: DTPA Derivatives. Inorg. Chem. **1995**, *34*, 1408-1412.

6. Montine, T. J.; Borcch, R. F. Role of endogenous sulfur-containing nucleophiles in an *in vitro* model of *cis*-diamminedichloroplatinum(II)-induced nephrotoxicity. Biochem. Pharmacol. **1990**, *39*, 1751-1757.

7. de Paula, Q. A.; Tsotsoros, S. D.; Qu, Y.; Bayse, C. A.; Farrell, P. PlatinumâĂŞnucleobase PtN4 complexes as chemotypes for selective peptide reactions with biomolecules. Inorg. Chim. Act. **2012**, *393*, 222-229.

8. Anzellotti, A. I.; Liu, Q.; Bloemink, M. J.; Scarsdale, J. N.; Farrell, N. P. Targeting retroviral Zn finger-DNA interactions: a small-molecule approach using the elec-

trophilic nature of *trans*-platinum-nucleobase compounds. Chem. & Biol. **2006**, *13*, 539-548.

9. Anzelloti, A. I.; Bayse, C. A.; Farrell, N. P. Effects of nucleobase metalation on frontier molecular orbitals: potential implications for π-stacking interactions with tryptophan. Inorg. Chem. **2008**, *47*, 10425-10431.

10. Tsotsoros, S. D.; Bate, A. B.; Dows, M. G.; Spell, S. R.; Bayse, C. A.; Farrell, N. P. Modulation of the stacking interaction of MN_4 (M=Pt, Pd, Au) complexes with tryptophan through N-heterocyclic ligands. J. Inorg. Biochem. **2014**, *132*, 2-5.

Chapter 7

Recovery of K_2PtCl_4 from Laboratory Waste

Samantha D. Tsotsoros, Daniel Lee, and Nicholas P. Farrell

Department of Chemistry, Virginia Commonwealth University, 1001 W. Main Street,

Richmond, VA 23284-2006 USA

7.1   Contribution

S.D.T.'s contribution is equal to Daniel Lee's. Both were responsible for the complete recovery process.

7.2   Purpose

Platinum is a precious and expensive metal, therefore it is desirable to recover and reuse platinum collected in experimental waste. The following procedure was adapted from (1) and (2).

7.3 General Schematic
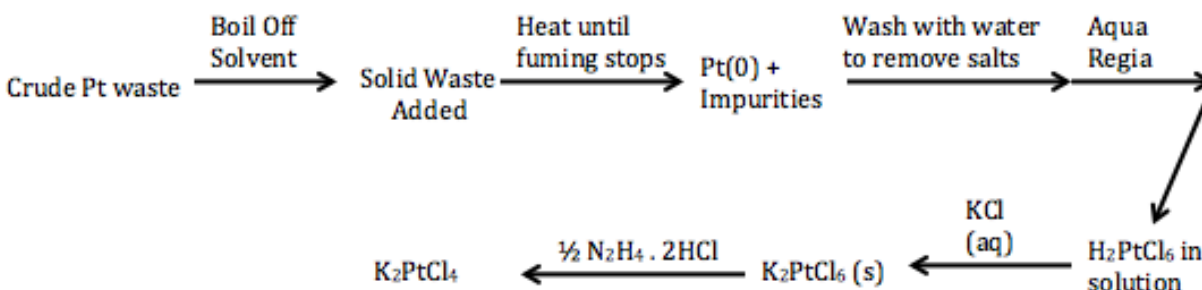
Figure 7.1: General schematic for the recovery of K_2PtCl_4 from laboratory waste.

7.4 Procedure

**Never leave any of these steps unattended for any extended period of time!

**Perform every step in the hood!

1. In a 3L beaker- liquid Pt waste had pH adjusted to 14 with NaOH and was heated on a hot plate to evaporate solvent. Increase temperature slowly if highly volatile solvents are present.

   - this step can take multiple weeks depending on the amount of solvent there is

2. The dried Pt waste was transferred to a porcelain dish and heated with a Meker burner until no smoke was seen.

3. The solid Pt waste was added to the same porcelain dish and heated with a Meker burner until no smoke was seen.

   - stir solid carefully to ensure even burning

- only add more solid to the dish when it is cool- if added when hot, the dish may crack

- when finished- no smoke present, solid will be black and charry looking

- if the solid does not appear to burn well, ask Dr. Qu to come take a look- may need at add $NaNO_3$

4. The ash was washed with hot water until the filtrate was clear.

   - initially the filtrate will be very yellow

   - this removes salts leftover —very important to rinse well

5. The solid was weighed and treated with aqua regia (30mL/g) and gently heated in batches. The solution was cooled to RT and filtered through filter paper. This was completed three times for each batch.

6. KCl (1g:1g ash) was added to the filtrate to precipitate K_2PtCl_6

   - the solvent was reduced by heating to 1/3V

   - the solution was cooled and placed in fridge to precipitate bright yellow solid

7. The K_2PtCl_6 was filtered and washed with cold water and ether and dried at 110^oF.
   The calculations for the next steps must be EXACT

8. The K_2PtCl_6 was suspended in water (40g/400mL) and hydrazine dihydrochloride (4g/40mL water) was added dropwise with stirring at 60-65°C. After 4 hours, the solution was heated to 80-90°C for 30 minutes

   - the solution turned from yellow to red over time

9. The solution was cooled to room temperature and filtered to remove any K_2PtCl_6 still present. The solid was washed with cold water.

10. The filtrate was concentrated by heating at 50-60°C, cooled to room temperature and placed in the fridge to precipitate solid.

11. The solid was filtered and the filtrate was concentrated and cooled in the fridge to collect a second crop. This was repeated until no solid was obtained.

12. Recrystallization of collected K_2PtCl_4.

   - Water was added to dissolve most of the collected solid. The solution was heated to reduce the volume and was filtered hot to remove any precipitated K_2PtCl_6. The filtrate was collected and the volume was reduced by heating. The concentrated solution was placed in the fridge and any precipitated solid was collected.
   - Recrystallization was performed as many times as necessary to remove all K_2PtCl_6.

13. Final yield of purified K_2PtCl_4: 90g.

7.5 References

1. Kauffman, G.B., Teter, L. A. and Rhoda, R. N. (2007) Recovery of Platinum from Laboratory Residues, in Inorganic Syntheses, Volume 7 (ed J. Kleinberg), John Wiley & Sons, Inc., Hoboken, NJ, USA. doi: 10.1002/9780470132388.ch61

2. Strukl, Joseph. Laboratory notebook.

Chapter 8

General Conclusions

Traditionally, platinum has been used as an anti-cancer agent in medicine. Three FDA approved compounds have not only created a multi-billion dollar industry but improved patient survival drastically. All three of these compounds have the ligands surrounding platinum in the *cis* orientation. Recently, use of *trans* platinum complexes has opened new avenues of interesting research.

Due to the rapid deactivation of *trans*-platinum compounds by sulfur-containing proteins, they do not exhibit cytotoxic properties *in vivo*. However, these rapid protein reactions create opportunities to study the interaction of DNA/RNA with proteins and to develop compounds designed to target proteins. Interestingly, one of the first cross-linking experiments used transplatin to determine the binding site of the HIV1 nucleocapsid protein, NCp7, to viral RNA.

NCp7 is an attractive drug target due to its intolerance to mutation and important role in nearly all stages of the viral life cycle. While previous work served as a "proof of concept" for the use of platinum compounds to target NCp7, the work preseneted within this dissertation served to improve upon the prototype compound, $[\text{Pt(dien)(9EtG)}]^{2+}$. Chapter 2 and Appendix A explored the chemistry of this prototype compound. Interestingly, the reaction with sulfur-containing tetrapeptides was enhanced by the presence of a tryptophan.

This further strengthens the idea of a two-step mechanism in which, recognition by the nucleobase/tryptophan is followed by covalent modification. The interaction between NCp7 and the viral RNA stemloop, SL2, was disrupted using the PtN_4 9EtG complex. The reverse reaction, where RNA was added to NCp7 followed by addition of platinum complex showed retardation of the protein-RNA complex. This is an important result as it confirms platinum-nucleobase compounds as the first inorganic class of drugs designed to inhibit the protein-RNA complexation.

Though the initial prototype 9EtG compound was successful in affecting the NCp7 interaction with viral RNA, it is important to try to improve the characteristics of the drug. Chapters 3 and 4 explored the various factors that affect how the platinum drug interacts with NCp7. By changing the aromatic ligand, the strength of the π-stacking interaction with tryptophan, either free or as part of a peptide sequence can be manipulated. The identification of two very strong stackers, xanthosine and 4-dimethylaminopyridine, hightlights the importance of tuning this property. The "carrier" dien ligand also provides room for manipulation in order to affect compound properties. The addition of liphophilic methyl groups was hypothesized to increase the cell uptake and possibly the octanol-water coefficient. While this trend did not hold true, the results are still of interest - drug development is a complicated task and requires many trials to obtain optimal results. Cytotoxicity results support the hypothesis of viral specificity for these complexes as they are not toxic to non-infected cells.

Another strategy for targeting NCp7 involves the use of covalently-binding platinum complexes. It has previously been determined that mono-functional platinum complexes covalently bind to the C-terminal ZF of NCp7 and eject Zn^{2+}. Zinc ejection is one main strategy used in the design of organic compounds targeting zinc finger proteins. Here, we have used *cis* and *trans* dinuclear platinum complexes to study the reactivity of the C-terminal ZF of HIV1 NCp7. Due to the fast reaction kinetics when compared to the *cis* isomer, the

trans dinuclear complex caused N-terminal specific cleavage of the ZF. The reaction of the C-terminal ZF of HIV1 NCp7 with the mononuclear cisplatin and transplatin did not result in peptide cleavage. Transplatin reacted in a significantly faster fashion.

Addtionally, the zinc coordination enviroment was changed to determine its role in zinc finger reactivity. When evaluted with a monofunctional platinum complex, it was found that the number of cysteines played an important role in the reactivity of the peptide. As previous studies have shown, the Cys_3His peptide had a greater structural change than the Cys_2His_2 peptide. The size of the coordination sphere also affected the degree of strucutural perturbance. The zinc finger of smaller, and possibly more strained, coordination sphere showed greater structural changes by circular dichroism than the finger with a slightly larger coordination sphere.

In total, the work presented here highlights the importance of systematic evaluation of the PtN_4 class of compounds. HIV is a global health concern and development of potent inhibitors is an important field of work. This goal combined with the tools of bioinorganic chemistry leads to a field of interesting and important possibilities.

Appendices

The following appendices are included in a format as close to the originally published version as possible. Contributions are outlined at the beginning of each appendix.

Appendix A

Platinum-nucleobase PtN$_4$ complexes as chemotypes for selective peptide reactions with biomolecules

Queite A. dePaula[a], Samantha D. Tsotsoros[a], Yun Qu[ab], Craig A. Bayse[b], and Nicholas P. Farrell[a*]

[a]Department of Chemistry, Virginia Commonwealth University, 1001 W. Main Street, Richmond, VA 23284-2006 USA

[b]Department of Chemistry and Biochemistry, Old Dominion University, 4541 Hampton Boulevard, Norfolk, VA 23529-0126 USA Inorg. Chim. Acta, 393 (2012) 222-229

A.1   Contribution

S.D.T.'s contributions were comprised of preparation of $[\text{Pt}(\text{dien})(9\text{EtG})]^{2+}$ following literature methods and DNA melting and ethidium bromide studies for the compound. Q.dP.'s contributions were mass spectrometry and NMR studies of the tetrapeptide and amino acid reactions with the platinum complex. Q.dP. was also responsible for the preparation of the

written manuscript. Figures were completed by S.D.T. and Q.dP.

A.2 Abstract

The reactions of a subsitution-inert complex $[Pt(dien)(9\text{-}EtGua)](NO_3)_2$, I, on DNA and model tetrapeptides were examined. The tetrapeptides Ac-GAXG (gly-ala-x-gly) and AC-GWXG (gly-trp-x-gly) (X= met or cys) were chosen to compare firstly the relative reactivity of the thioether versus thiol and secondly to compare the effect of possible stacking of the platinated nucleobase with tryptophan on subsitution reactions. Characterization of predicted products was made using [PtCl(dien)]Cl. Melting point and ethidium bromide inhibition assays confirmed lack of reactivity on DNA. ^{1}H NMR, ^{195}Pt NMR, and ESI-MS spectroscopy techniques showed that the cysteine-containing peptides reacted significantly faster than those of methionine. The reactivity differences were confirmed using simple N-AcMet and N-AcCys. The presence of tryptophan enhanced the rate of reaction slightly for the methionine-containing peptides. Theoretical calculations on the [Pt(dien)(9-EtGua)]-GWMG/GAMG interactions show that the GWMG species is roughly 5 kcal/mol more stable than formation of the GAMG species (-9.3 and -3.9 kcal/mol) due to the additional π-stacking interaction. The results show the utility of considering the PtN_4 chemotype for selective reactions with peptides and templates for drug design of specific protein inhibitors.

A.3 Introduction

Zinc finger proteins are involved in many fundamental biological processes including genetic information storage and transfer [1]. These structural proteins contain four Zn-bound residues from histidine (His, N-donor) and cysteine (Cys, S-donor). The nature of the coordination sphere (Cys_2His_2, Cys_3H, Cys_4) affects the chemical reactivity of the zinc site and especially the nucleophilicity of the metal-bound cysteine-ates [2,3]. Zinc finger proteins are rich templates for metal-ion replacement. Uses and applications of M replacement include

spectroscopic probes {Co(II), Cd(II)}; understanding of toxic and carcinogenic properties of inorganic ions {Ni(II), Pb(II), As(III)} and as possible targets for medicinal inorganic chemistry {Au(I), As(III), Sb(III), and Pt(II)} [4].

We have started examining the interactions of platinum-metal compounds with zinc fingers and the factors affecting chemical reactivity of this system. The nature of the coordination sphere and central metal ion modulates the reactivity of coordination compounds. The anti-cancer drug cisplatin (cis-[PtCl$_2$(NH$_3$)$_2$]) has previously been shown to react with a 30-amino acid synthetic zinc finger with eventual replacement of the zinc ion upon binding of two cisplatin moieties [5]. A mass spectral survey comparing [MCl(dien)]$^{n+}$ (M = Pt(II), Pd(II) and Au(III)) showed the formation of Pt(dien) and Pd(dien) adducts with the C-terminal (Cys$_3$His) finger of the HIV nucleocapsid NCp7 protein while for Au(III) all ligands were lost [6]. The analogous [MCl(terpy)]$^{n+}$ system showed only "metal-scrambling" with formation of [Zn(terpy)$_2$]$^{2+}$ and no evidence of M(Ligand)-ZF adducts [6]. Interestingly, these reactions of the platinum compounds can be reproduced using zinc chelate model systems [7].

A further set of *functionalized* platinum compounds under study is that based on platinum-nucleobase compounds of general formula [PtL$_3$(nucleobase)]$^{n+}$ compounds where L can be a combination of neutral and anionic ligands and nucleobase is guanine or cytosine-based [4]. Both *trans*-[PtCl(9-EtGua)(pyr)$_2$] and (SP-4-2) [PtCl((9-EtGua)(NH$_3$) (quin)]$^+$ eliminate Zn from the C-terminal zinc finger of NCp7 (ZF, see Fig. A.1) and indeed show incipient anti-viral activity - attributed to inactivation of the biological functions of the protein [8,9]. Model studies further showed the existence of intermediate Zn-Pt-9-EtGua species [10]. Targeting the zinc finger motifs of retroviral nucleocapsids is an attractive approach to designing drugs capable of interfering with specific steps in the viral life cycle of HIV-1 [11-13].

A critical feature in nucleopcapsid-DNA/RNA recognition is the stacking of aromatic

amino acids (phenylalanine, tryptophan) to purine and pyrimidine bases (guanine, cytosine) on DNA/RNA[14,15]. Platination and alkylation of purines and pyrimidines enhances π-π stacking with tryptophan over that of the free nucleobase [16,17]. The prototype PtN_4 compound $[Pt(dien)(9\text{-EtGua})]^{2+}$, I, has been shown to interact in a non-covalent manner with the C-terminal finger of HIVNCp7 containing the tryptophan residue, and this recognition motif may impart some selectivity to the reaction over other zinc fingers and biomolecules [8]. Further, in ESI MS-MS studies a small peak corresponding to a Pt(dien)-ZF adduct is observed, implying potential loss of the nucleobase ligand and covalent binding of the Pt(dien) moiety [6,8]. This finding implies that in the presence of a "non-covalent" interaction (i.e."target activation") a second, bond-forming interaction ("target fixation") can occur. Interestingly, the ^{1}H NMR study of ZF with the platinated oligonucleotide 5'-dTACGCC-3', (where the Pt(dien) moiety is bound to the N7 of the guanine nucleobase) shows a close approximation of the methionine S to the platinated nucleobase [18].

To examine these features further, and to ask whether prior "non-covalent" recognition can be manipulated to enhance reactivity, we have studied the interactions of $[Pt(dien)(9\text{-EtGua})]^{2+}$ with a series of small designed tetrapeptides. The analogous pairs of methionine and cysteine-containing peptides can assess the effect of a tryptophan (W) versus alanine (A) residue proximal to the putative binding site and also compare the reactivity of methionine versus cysteine-containing residues in otherwise similar sequences, as well as extending the chemistry of platinum-nucleobase compounds with protein models. These studies may contribute to understanding of the features required for development of new platinum-metal based electrophiles capable of selective interactions with proteins. Fig. A.1 shows the struc-
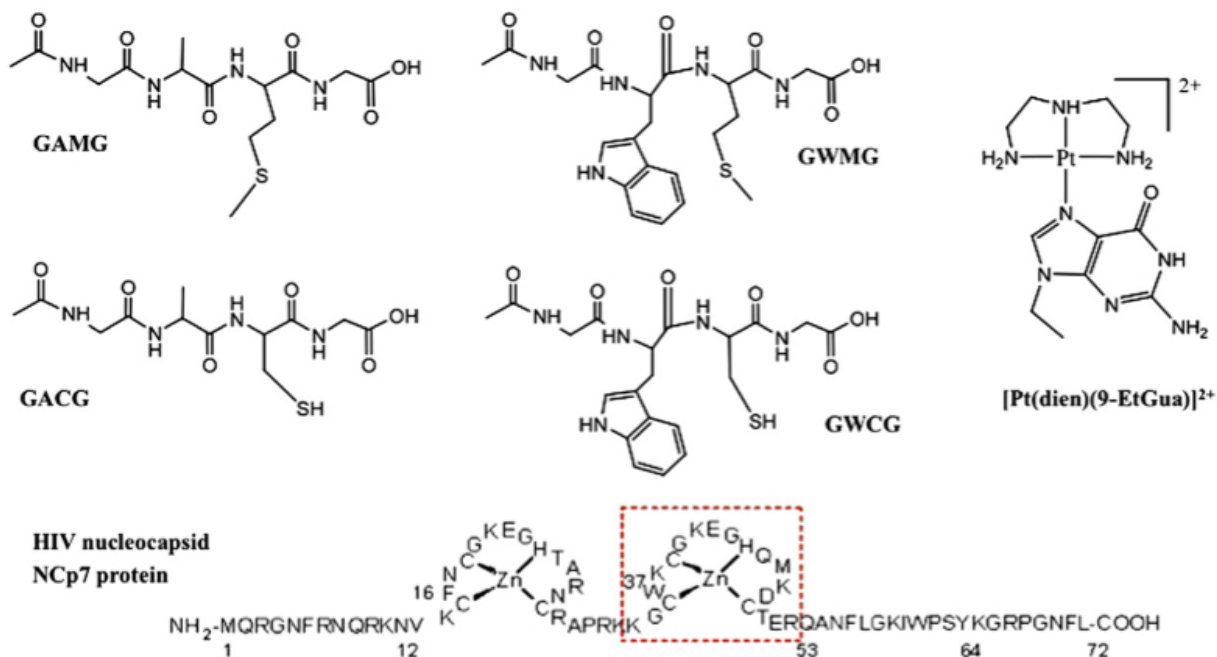
Figure A.1: Structures of [Pt(dien)(9-EtGua)]$^{2+}$, I, and the model tetrapeptides studied. The C-terminal residue of Nucleocapsid Protein NCp7 is shown in the red box.

tures of all compounds studied in this paper.

A.4 Experimental

A.4.1 Materials and Reagents

The complex [Pt(dien)(9-EtGua](NO$_3$)$_2$ (dien= diethylenetriamine) was prepared by literature methods [8]. Its purity was confirmed by ESI-MS, ^{1}H and ^{195}PtNMR spectroscopy, and elemental analysis (performed by QTI Laboratory, USA). The peptides N- acetyl-gly-ala-meth-gly (GAMG), N-acetyl-gly-trp-meth-gly (GWMG), N-acetyl-gly-ala-cys-gly (GACG), and N-acetyl-cys-trp- gly (GWCG) were purchased from GenScript Corporation. All reagents

and reactants were used without further purification.

A.4.2 ^{1}H and ^{195}Pt NMR spectroscopy

Experiments were conducted on a 300 MHz NMR Varian Spectrometer. The pH of the solutions were adjusted when necessary using DNO_3 and $NaOD$ solutions. The ^{195}Pt chemical shifts are reported relative to $PtCl_6{}^{2-}$ (external standard). Reagents were mixed in 1:1 stoichiometric ratio at 25°C (D_2O for ^{1}H NMR, D_2O/H_2O mixtures for ^{195}Pt NMR) and were mixed immediately before starting the spectral acquisition. For the ^{195}Pt NMR experiments, two separate fresh solutions were prepared containing (i) the Pt(dien)(9-EtGua)(NO$_3$)$_2$ compound (1.39x10^{-5} mol) in 0.5 mL of D_2O, and (ii) a stoichiometirc equivalent (1.39x10^{-5} mol) of the peptide dissolved in 1 ml of H_2O.

A.4.3 Electrospray ionization time of flight mass spectrometry (ESI-TOFMS)

Solutions were prepared as per NMR experiments. Experiments were conducted on a Waters/Micromass QTOF-2 instrument operated in positive ion mode. Solutions were directly infused in water at a flow rate of 3 μL/min using a source voltage of 2.75-2.95 kV and a cone voltage of 40 V. The source temperature was maintained at 110°C throughout. Collision gas was introduced into the hexapole to aid in ion cooling. All spectra were analyzed using the MassLynx 4.0 software provided from the manufacturer. In the spectra, all peaks are labeled with the monoisotopic masses for the proposed species; the observed masses covered the isotopic range expected. pH was adjusted using NH_4OH and HCl.

A.4.4 Fluorescence experiments with tetrapeptides

An X-300 spectrofluorometer was used to perform the fluorescence experiments. Several titrations were performed every 5 min using the GWMG or GWCG peptide (100 μM) in 3 mL of a buffer solution and addition of aliquots of [Pt(dien)(9-EtGua)](NO$_3$)$_2$ (30 μL, 1 mM

in buffer solution) in the range [peptide]/[Pt quencher] = 10-100. Tris-HCl (50 mM NaCl/10 mM Tris-HCl) buffer at pH 7.4 was used during all experiments, and the data were recorded at 22°C. The excitation wavelength was maintained at 315 nm while monitoring emission from 330 to 420 nm.

A.4.5 DNA Binding

Studies were performed as previously [19]. Briefly, DNA melting studies were recorded on a JASCO V-550 UV/Vis spectrometer with compound to nucleotide ratios (r_i) of 0.01, 0.03, 0.05, 0.075, and 0.1 in 10 mM NaClO$_4$ at pH 6. The concentration of calf thymus (CT) DNA was 100 μM for each experiment. The results were determined from an average of two trials. Ethidium bromide (EtBr) fluorescence studies were recorded on a Varian Cary Eclipse fluorometer with a single-cell Peltier accessory. Samples were irradiated with 525 nm light and emission was recorded at 600 nm with a scan rate of 600 nm/min at 25°C. The experiments were carried out in phosphate buffer at pH 7.4. CT DNA (100 μM) was incubated with compound for 1 h and titrated with EtBr at r_i values from 0.05 to 0.25. The results were determined from an average of three trials.

A.4.6 Theoretical Methods

Geometries were optimized at the DFT level using the SVWN exchange-correlation functional and the PQS software package [20]. The SVWN functional was selected as studies have shown that it provides a reasonable qualitative representation of π stacking interactions [21]. Platinum was represented by the Hay-Wadt relativistic effective core potential basis set commonly designated LANL2DZ [21]. All other atoms were represented by the Dunning split-double-f basis set with polarization functions on all heavy atoms and hydrogens attached to nitrogen or oxygen [23]. Reported structures are minima on the potential energy surface. Relative free energies of the systems were corrected for solvation in water using the COSMO

method [24].

A.5 Results

To examine the reactivity of a prototypical PtN4 chromophore with the selected tetrapeptides, the expected products were characterized using the more substitution-labile [PtCl(dien)]Cl as "control" and then their reactivity compared. Examination of the interaction of I with Calf Thymus (CT) DNA by melting point changes and interference with ethidium bromide (EtBr) intercalation showed essential no reactivity, in contrast to the well-studied chloride analog, Fig. A.2 [25].
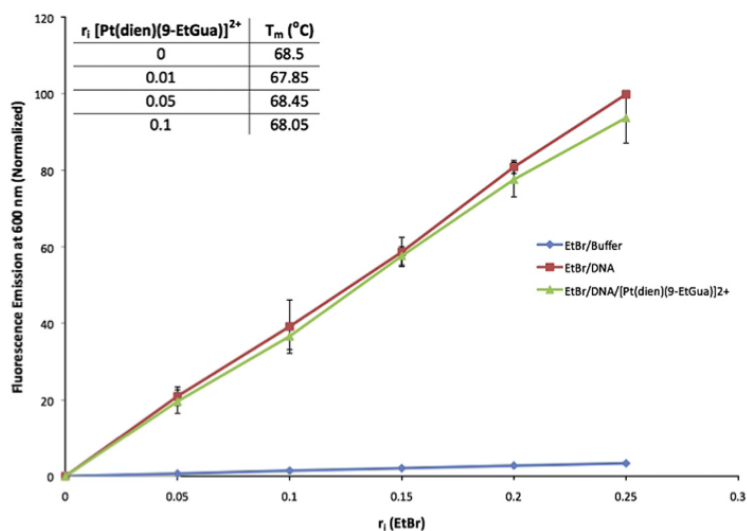
Figure A.2: Reactivity of I towards DNA as determined by competitive inhibition of ethidium bromide fluorescence.

A.5.1 Reactions of $[PtCl(dien)]^+$ and $[Pt(dien)(9\text{-}EtGua)]^{2+}$ with N-acetyl-methionine and methionine-containing tetrapeptides

The principal solution characterization of control reactions with [PtCl(dien)]Cl and N-Ac-methionine and methionine peptides is given in Table A.1. The reactions of [PtCl(dien)]Cl with N-AcMet gave a ^{195}Pt NMR spectrum with $\delta(\text{Pt})$ at -3374 ppm while the ^{1}H S-CH$_3$

chemical shifts at $\delta(2.547, \text{S-CH}_3)$ and $\delta(3.94, \text{S-}\alpha\text{CH}_2)$ are consistent with the literature [26]. The spectral properties of the products using GAMG and GWMG peptides are completely consistent with formation of [Pt(dien)(GAMG)] and [Pt(dien)(GWMG)] species, respectively, Fig. A.3 and Table A.1.
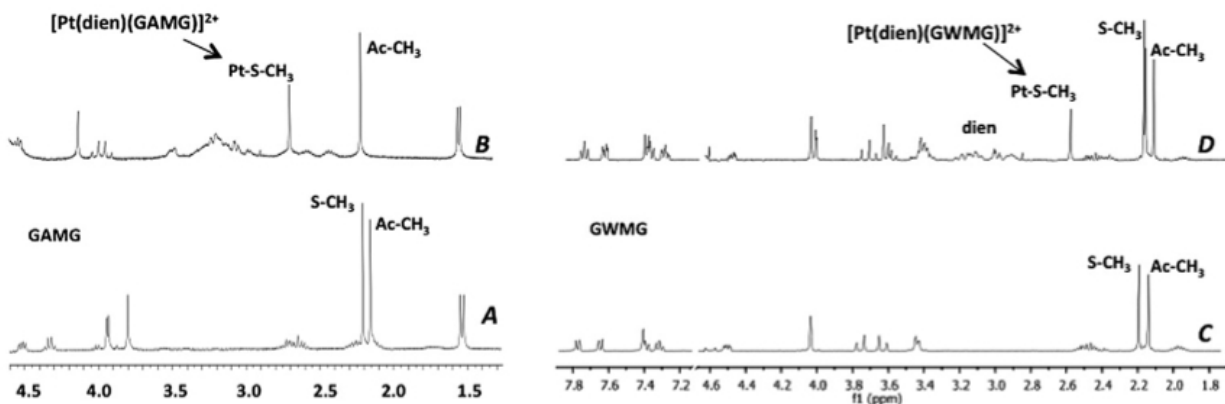
Figure A.3: ^{1}H NMR characterization of methionine chemical shifts in platinated GAMG and GWMG.

Table A.1: Characterization of [Pt(dien)]$^{2+}$ complexed to N-AcMethionine, N-AcCysteine and methionine tetrapeptides

	$\delta(^1\text{H NMR})$	$\delta(^{195}\text{Pt NMR})$	MS Calculated	MS Observed
][Pt(dien)(N-AcMet)]$^{2+}$	2.57 (S-CH$_3$)(S-αCH$_2$)	-3376	489.50	489.00
[Pt(dien)(N-AcCys)]$^{2+}$	3.30 (S-CH$_2$)	-3192	461.5	459.98
[Pt(dien)(GAMG)]$^{2+}$	2.70 (S-CH$_3$)	-3374	674.3	673.03
[Pt(dien)(GWMG)]$^{2+}$	2.60 (S-CH$_3$)	-3380	790.3	788.05

The reaction of [Pt(dien)(9-EtGua)]$^{2+}$, I, and N-AcMet in a 1:10 molar ratio, pH 7 and 37°C, did not show any formation of [PtN$_3$S] species until after 24 h reaction, when at that time a small amount of a white precipitate formed (presumably 9-EtGua which is only sparingly soluble in H$_2$O). After 3 days of reaction a peak at -3376 ppm may be observed in solution indicating the presence of the [PtN$_3$S] species (data not shown). To investigate the

formation of [PtN$_3$S] adducts with the tetrapeptides, 1:1 molar ratio reactions of I and the peptides GAMG and GWMG were followed by ^{195}Pt NMR at 20°C. The first ^{195}Pt NMR spectrum showed only one peak at -2851 ppm corresponding to the starting material. With GAMG an additional ^{195}Pt NMR spectrum for the colorless and clear solution was retaken after 3 days of incubation at 37°C and showed a very small peak at -3380 ppm. A slight increase in intensity is seen after a prolonged period of incubation (8 days, 37°C), Fig. A.4. Similar behavior was seen for GWMG, with somewhat increased reactivity and after prolonged reaction the solution turned yellow (see below). To attempt comparative integration between the two peptides the ratio of the Pt-peptide peak was integrated versus the Pt starting material normalized to 1. This approach showed an approximate two-fold increase in formation of [Pt(dien)-(GWMG)] over [Pt(dien)-(GAMG)] species. Given the nature of these reactions and possible alternative products these rate differences should be viewed as qualitative but nevertheless there does appear to be a preference for the tryptophan-containing peptide. In both cases small peaks corresponding to free 9-EtGua can be seen in the ^{1}H NMR spectra recorded at the latest time point.

A.5.2 Reactions with N-acetylcysteine and cysteine-containing tetrapeptides

A 1:1 M ratio reaction between the compound [Pt(dien)Cl]Cl and N-AcCysteine (at pH 7.1) was followed at 37°C by ^{195}Pt NMR Spectroscopy. Immediately, the solution turned yellow and a major new peak appeared at -3192 ppm, which is assigned to the PtN$_3$S species. With [Pt(dien)(9-EtGua)]$^{2+}$, after 12 h of reaction the ^{195}Pt NMR spectrum also showed the peak at -3192 ppm growing in intensity and a small amount of white solid precipitated. The $\delta(^{195}$Pt) shifts of [Pt(SR)(dien)] where SR = alkanethiolates have been reported in the -3150 to -3200 ppm range [27]. In the mass spectrum, as well as the peak corresponding to
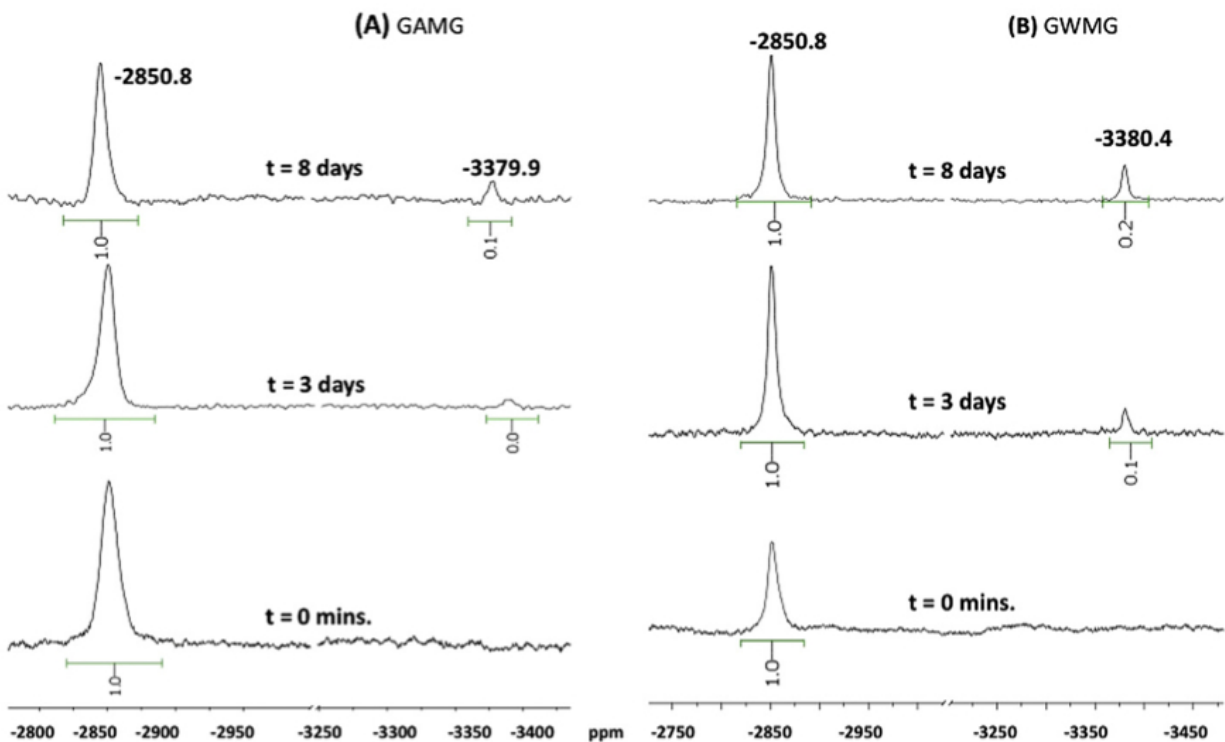
Figure A.4: Kinetic Profile of reactivity of $[Pt(dien)(9\text{-EtGua})]^{2+}$ toward GAMG and GWMG showing some enhancement of nucleobase substitution in presence of tryptophan. Comparative integration normalizing for starting material as 1.0 gave a relative ratio of 0.2-0.1 for for platination of GWMG over GAMG peptide (shown on spectra).

$[Pt(dien)(N\text{-AcCys})]^+$ a peak at 755.93 can be assigned to the dimer with bridging thiolate $\{[Pt(dien)]\text{-l-N-AcCys-}[Pt(dien)]\}$, (calculated value 759.7 (loss of $4H^+$). This is consistent with the pH-dependent interconversion between $[Pt(dien)GS)]^+$ and $[(Pt(dien)_2l\text{-GS}]^{3+}$ (GS = anion of glutathione) [28]. Both monodentate and bridged thiolates give similar $d(^{195}Pt)$ shifts [27].

For the non-tryptophan-containing peptide (GACG) the reaction after 24h gave clear evidence from ^1H, ^{195}Pt and MS spectra for formation of a significant yield of $[Pt(dien)(GACG)]$ species with concurrent loss of nucleobase, Fig. A.6. The ^{195}Pt NMR spectrum over a number of days showed an increase in the $[PtN_3S]$ species and the mass spectra also showed concomi-
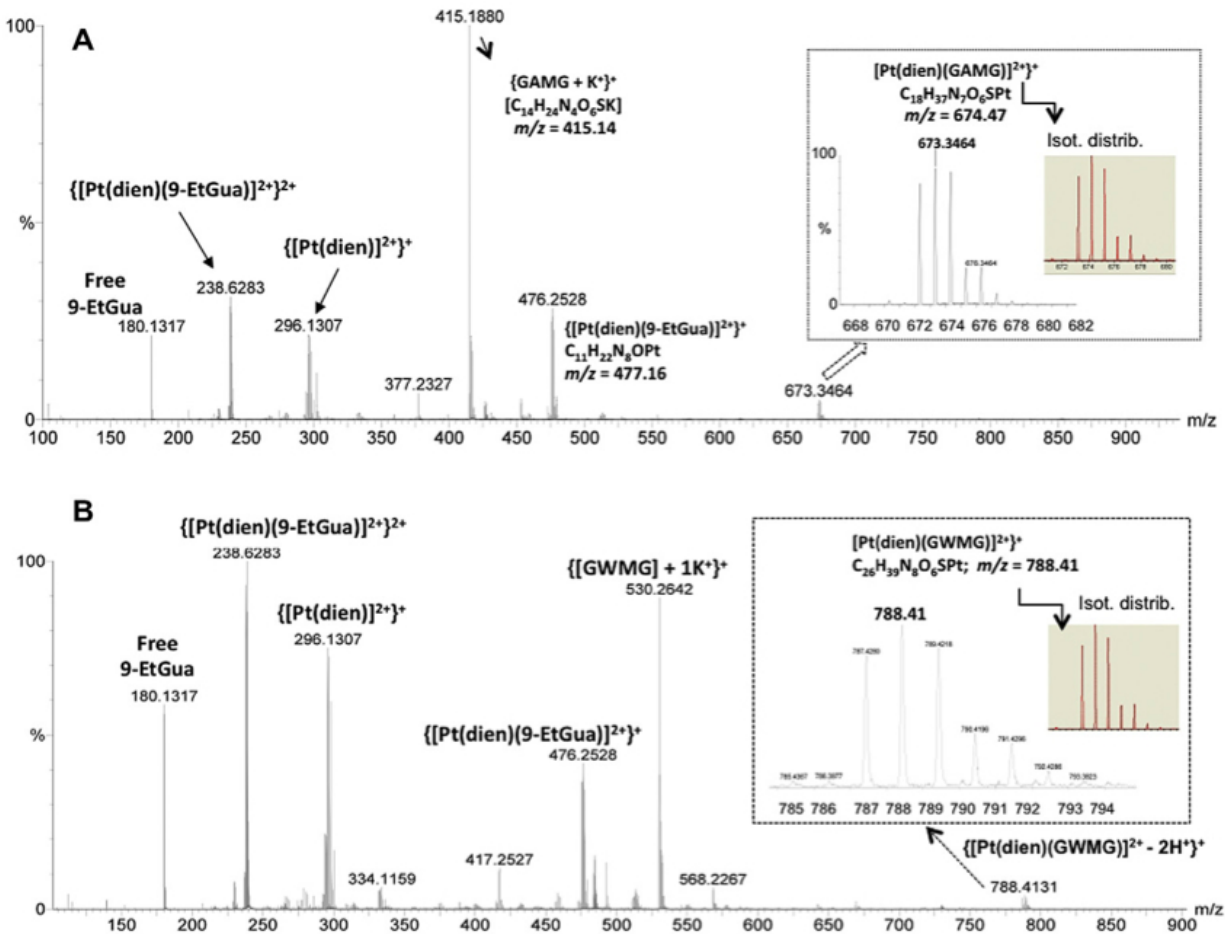
Figure A.5: Mass spectral characterization of the $[Pt(dien)(9\text{-}EtGua)]^{2+}$ reaction with GAMG and GWMG showing formation of the platinated peptide upon nucleobase substitution.

tant increases in product peak intensity. Unfortunately the analogous tryptophan-containing peptide gave an immediate cloudy yellow solution and spectral analysis was complicated. The presence of a peak at $\delta(^{195}Pt) = $ -3177 ppm confirmed formation of the corresponding $[PtN_3S]$ species within 12h. Again, after 24h mass spectra showed the evidence for product but as with GWMG a multitude of peaks may indicate peptide cleavage.

A.5.3 Theoretical Studies

The fluorescence quenching of tryptophan residues suggest the occurrence of π-π in-
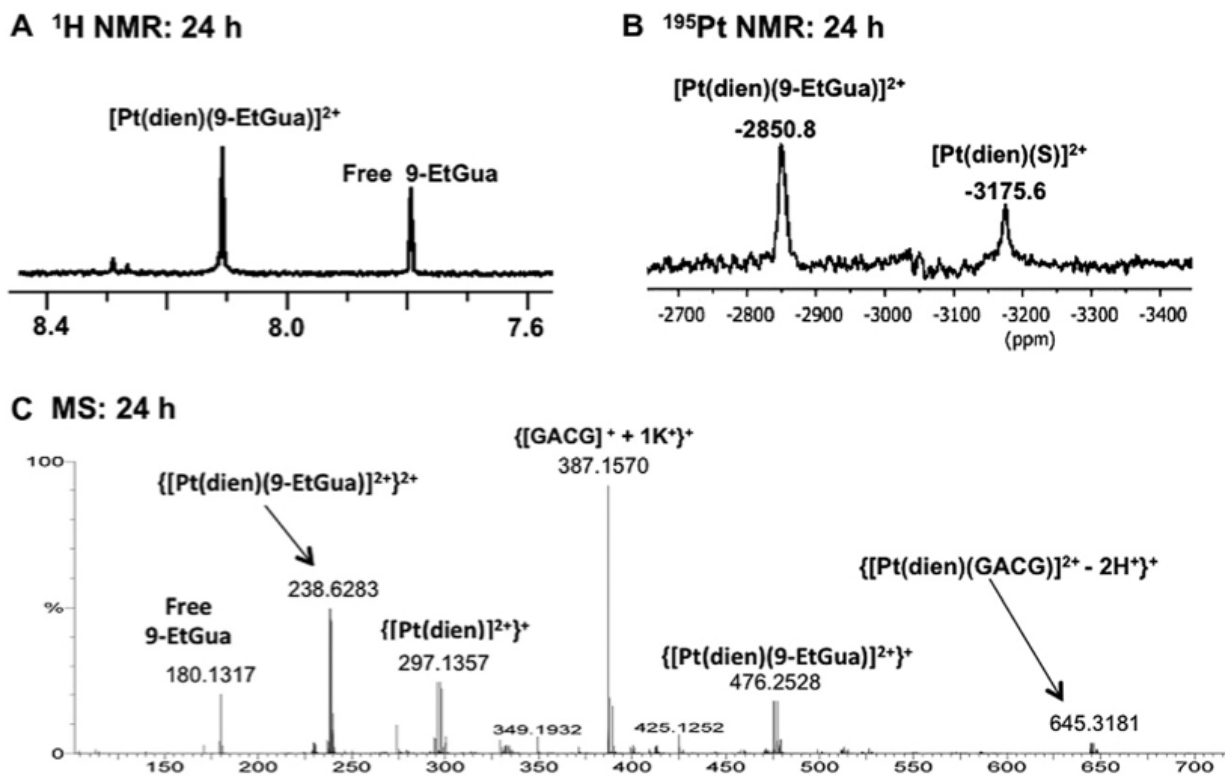
Figure A.6: ^{1}H NMR, [195]Pt NMR and mass spectral evidence for formation of platinated [Pt(dien)-GACG] by reaction with $[Pt(dien)(9\text{-}EtGua)]^{2+}$.

teractions between I and the GWXG peptides. To examine possible consequences on the reactivity the system was subjected to theoretical calculations. Structures representing the potential platinated Gua-GWMG/GAMG interaction were optimized with the SVWN functional. This modeling study assumed that platinated 9-MeGua forms a π-stacking interaction with the indole ring of GWMG in a similar conformation as that observed in the solution structure of NCp7 with a DNA 18-mer (i.e., with the carbonyl group at C6 forming a hydrogen bond forms with the W amide proton [15b]). The GWMG and GAMG peptides were truncated by replacing G by -NH$_2$ on the C-terminal end and -CHO on the N-terminal end. For the $[Pt(dien)(9\text{-}MeGua)]^{2+}$-GWMG complex, the stacking interaction optimizes to a conformation with the 6-membered ring of Gua centered over the W indole nitrogen and a

hydrogen bonding interaction between the central NH of the dien and the W backbone carbonyl group, Fig. A.7A. The inter-ring distance ranges from ~3.0 at the closest point near C2Gua to ~3.4 on the C8Gua end due to the positioning of one of the dien protons between the rings in close contact with C4Ind (2.09). In the analogous complex of non-metallated 9-MeGua with the GWMG model (Fig. A.7B), the rings are slightly further apart at the C2Gua end (~3.1) which may be attributed to weaker donor-acceptor and electrostatic contributions to the stacking interaction. For the $[Pt(dien)(9\text{-MeGua})]^{2+}$-GAMG model (Fig. 7C), the indole ring of the Pt-GWMG model complex was replaced by a hydrogen to convert W to A. The NH-OC6 and dien NH-OC backbone hydrogen bonding interactions were maintained in the optimized Pt-GAMG model for an overall similar configuration of the $[Pt(dien)(9\text{- MeGua})]^{2+}$ fragment and the peptide backbone. The relative energy of formation of the Pt-GWMG complex from platinated Gua and model peptide is -9.3 kcal/mol, roughly 5 kcal/mol more stable than formation of the GAMG species (-3.9 kcal/mol) due to the additional π stacking interaction. Although these calculations have not considered a full conformation search of the interaction of $[Pt(dien)(9\text{-MeGua})]^{2+}$ with the model peptides, they do suggest that, given a similar configuration of the Pt complex and the peptide backbone, the additional π interaction enhances the interaction by ~5kcal/mol. Noting that a dien proton is somewhat intercalated between the rings, formation of a cation-π interaction is an alternate or complementary explanation for the more favorable interaction with GWMG over GAMG. Stabilization of the "non-covalent" interaction may be reflected in the greater reactivity of the GWMG over GAMG with respect to nucleobase substitution. However, more reactive systems giving greater overall nucleobase substitution are required for confirmation - as stated the GXCG systems, although faster than GXMG, were not comparable
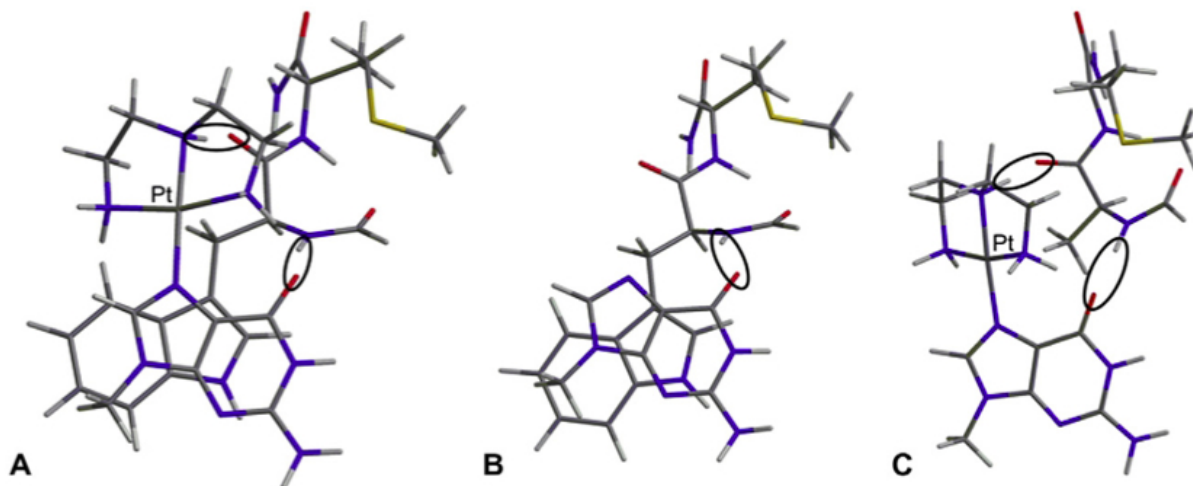
Figure A.7: DFT(SVWN)-optimized structures of the interaction of (A) [Pt(dien)(9-MeGua)]$^{2+}$ and (B) 9-MeGua with a truncated GWMG model peptide and [Pt(dien)(9-MeGua)]$^{2+}$ with a model of GAMG. Hydrogen bonding interactions conserved in the models are shown.

due to possible side-reactions.

A.6   Discussion

This work set out to examine the reactivity of substitution-inert platinum-nucleobases with amino acids and model peptides. The results are consistent with a slow displacement of the guanine nucleobase by cysteine. The reaction is clearly much faster and more favored than the analogous reactions with methionine. It is of interest that [Pt(dien)(Met)]$^{2+}$ has been shown to undergo surprising displacement of the sulfur amino acid by the 5'-guanosine-monophosphate (5'-GMP) nucleotide, and these results suggested possible pathways to final DNA adducts of anticancer drugs like cisplatin [26]. The slow displacement of the coordinated nucleobase shown here is consistent with the earlier observations on the "reverse" reaction. A second point of interest is that thiolate (as NACys) reactivity in these systems is significantly greater than thioether (as NAcMet). Using sterically hindered dien chelates, [PtCl(R$_4$(dien)]$^+$ (R = Me, Et) selective binding of the sulfhydryl group in glutathione was

seen compared to the methionine thioether of the dipeptide N-AcMetHis [29]. Steric bulk in the dien ligand has also been shown to allow discrimination between 5'-GMP and methionine [30]. Modulation of ligand leaving group is a further approach to selectivity and, unlike the sterically hindered complexes which still contain the substitution-labile chloride, allows distinction between DNA and protein binding. Thirdly, the results show that a reasonable explanation for the presence of the [Pt(dien)-ZF] adduct under ESI MS-MS conditions in the reaction of $[Pt(dien)(9\text{-}EtGua)]^{2+}$ with ZF is the nucleophilic displacement of the bound purine by a Zn-cysteinate [8]. Indeed the sequences used here are quite similar to the GCWK sequence surrounding the tryptophan residue in ZF, see Fig. A.1.

This study is one of the first systematic studies of reactivity using "inert" PtN_4 coordination spheres. While a significant amount of work has been performed on the interactions of thiols with Pt-Cl complexes, studies on PtN_4 systems, especially with a nucleobase, are scarce. There is some evidence that the Pt-N bond is susceptible to strong nucleophiles. The $[Pt(bipy)(en)]^{2+}$ cation reacts slowly with cysteine residues in thioredoxin [31], Matrix-assisted laser desorption-ionization time of flight mass spectrometry (MALDI-TOF MS) and UV spectroscopy indicated the formation of Pt(bpy)(Cys-Ala-Pro-Cys)-containing peptide fragments, indicating that the $Pt(bpy)^{2+}$ unit binds to the active site of thioredoxin. The thioredoxin-platinum complex has no catalytic activity for the reduction of glutathione disulfide in the presence of NADPH and thioredoxin reductase, so that the platinum complex functions as an inhibitor [31]. Conjugation of a cathepsin targeting ligand to the [Pt(dien)] moiety gave a $[Pt(dien)\text{-}NH_2R)]$ species which reacted slowly, over 72h, with cysteine giving two new peaks at $\delta(^{195}Pt)$ peaks at -3165 and -3203 ppm indicative of formation of the $[PtN_3S]$ species [32]. Kinetic studies using $[Pt(terpy)(guanosine)]^{2+}$ showed that L-cysteine and GSH are efficient nucleophiles with k2 values of 1.84 and 4.72 M^{-1} s^{-1}, respectively, for displacement of the guanosine [33].

Much of platinum complex drug development has been based on modulating reactivity of

Pt-Cl moieties for anti-cancer applications, with the implicit assumption of DNA as the final target by nucleobase displacement of the relatively substitution-labile chloride. The results shown here, combined with previous results on steric effects on "carrier" dien ligands [29,30] suggests that the PtN_4 chemophore is capable of systematic modulation for peptide and protein inhibition. The reactivity will depend on the nature of the PtN_4 coordination sphere - the $[Pt(dien)NH_2R)]$ species [32] appears to react slower than the $[Pt(dien)(nucleobase)]$ chemistry reported here - the chemical differences being a secondary amine N-donor versus a heterocyclic nitrogen. The non-covalent TriplatinNC does not undergo displacement of its "dangling" amine moieties even upon extended reaction with GSH [34].

With respect to zinc proteins in general, target selectivity is a major issue for inhibition using small molecules. In the specific case of zinc fingers, the concept of "weak electrophiles" from organic chemistry has been suggested as one way to gain selectivity and distinguish between the cysteine nucleophilicity of the various coordination spheres (Cys_2His_2, Cys_3His, Cys_4) [2,3]. We suggest that the coordination chemistry analogy of a weak electrophile, especially to target proteins, is substitution-inert or "semi-inert" coordination spheres such as $[Pt(dien)(9-EtGua)]^{2+}$ - a PtN_4 chromophore is capable of more extensive control than that of PtN_3Cl, containing the substitution-labile Pt-Cl bond. The extra stabilization of the "non-covalent" π-π stacking interaction as shown on the model peptides allows further avenues for design of specifically targeted inhibitors and further confirms the viability of the medicinal chemistry dual approach of target recognition (non-covalent) followed by target fixation (covalent).

Finally, the purpose of this paper was to examine the electrophilicity of I. It is notable that the mass spectral studies indicated some peptide cleavage for both GWXG peptides. This aspect was not examined in detail but the use of $[Pt(en)]^{2+}$ and $[Pd(en)]^{2+}$ can promote peptide cleavage next to a tryptophan residue, offering further opportunities for selective

protein inhibition [35].

A.7 Acknowledgment

A.8 References

1. A. Klug, Ann. Rev. Biochem. 79 (2010) 213.

2. A.T. Maynard, M. Huang, W.G. Rice, D.G. Covell, Proc. Natl. Acad Sci. USA 95 (1998) 11578.

3. A.T. Maynard, D.G. Covell, J. Am. Chem. Soc. 123 (2001) 1047.

4. S.M. Quintal, Q.A. dePaula, N.P. Farrell, Metallomics 3 (2011) 121.

5. R.N. Bose, W. Wei, W. Yang, F. Evanics, Inorg. Chim. Acta 358 (2005) 2844.

6. Q.A. dePaula, J.B. Mangrum, N.P. Farrell, J. Inorg. Biochem. 103 (2009) 1347.

7. E. Almaraz, Q.A. dePaula, Q. Liu, J.H. Reibenspies, M.Y. Darensbourg, N.P. Farrell, J. Am. Chem. Soc. 130 (2008) 6272.

8. A.I. Anzellotti, Q. Liu, M.J. Bloemink, J.N. Scarsdale, N. Farrell, Chem. Biol. 13 (2006) 539.

9. D.A. Sartori, B. Miller, U. Bierbach, N. Farrell, J. Biol. Inorg. Chem. 5 (2000) 575.

10. Q. Liu, M. Golden, M.Y. Darensbourg, N.P. Farrell, Chem. Comm. (2005) 4360.

11. E. deClercq, J. Med. Chem. 53 (2010) 521.

12. R.A. Musah, Curr. Topics Med. Chem. 4 (2004) 1605.

13. Y. Mely, H. deRocquigny, V. Shvadchak, S. Avilov, C.Z. Dong, U. Dietrich, J.-L. Darlix, Mini Rev. Med. Chem. 8 (2008) 24.

14. R.N. De Guzman, R. Wu, C.C. Stalling, L. Pappalardo, P.N. Borer, M.F. Summers, Science 279 (1998) 384.

15. (a) N. Morellet, H. Demene, V. Teilleux, T. Huynh-Dinh, H. De Rocquigny, M.-C. Fournie-Zaluski, B.P. Roques, J. Mol. Biol. 283 (1998) 419; (b) S. Bourbigot, N. Ramalanjaona, C. Boudier, G.F. Salgado, B.P. Roques, Y. MeÌĄly, S. Bouaziz, N. Morellet, J. Mol. Biol. 383 (2008) 1112.

16. A.I. Anzellotti, C.A. Bayse, N.P. Farrell, Inorg. Chem. 47 (2008) 10425.

17. A.I. Anzellotti, M. Sabat, N. Farrell, Inorg. Chem. 45 (2006) 1638.

18. S.M. Quintal, Q.A. dePaula, N.P. Farrell, Biochemistry 51 (2012) 1752.

19. A.L. Harris, J.J. Ryan JJ, N. Farrell, Mol. Pharmacol. 69 (2005) 666.

20. PQS version 3.3, Parallel Quantum Solutions, Fayetteville, AR, USA, 2007.

21. M. Swart, C.F. van der Wijst, C.F. Guerra, F.M. Bickelhaupt, J. Mol. Model. 13 (2007) 1245.

22. T.H. Dunning, J. Chem. Phys. 53 (1970) 2823.

23. (a) A. Klamt, G. Schuurmann, J. Chem. Soc., Perkin Trans. 2 (1993) 799; (b) J. Andzelm, C. Kolmel, A. Klamt, J. Chem. Phys. 103 (1995) 9312; (c) A. Klamt, V. Jonas, J. Chem. Phys. 105 (1996) 9972; (d) K. Baldridge, A. Klamt, J. Chem. Phys. 106 (1997) 6622.

24. V. Brabec, J. Reedijk, M. Leng, Biochemistry 31 (1992) 12397.

25. K.J. Barnham, M.I. Djuran, P. del Socorro Murdoch, P.J. Sadler, Chem. Comm. (1994) 721.

26. (a) A.K. Fazlurrahman, J.G. Verkade, Inorg. Chem. 31 (1992) 2064; (b) E.L.M. Lempers, J. Reedijk, Inorg. Chem. 29 (1990) 212.

27. M.I. Djuran, E.L.M. Lempers, J. Reedijk, Inorg. Chem. 30 (1991) 2648.

28. M.I. Djuran, D.P. Dimitrijevic, S.U. Milinkovic, Z.D. Bugarcic, Trans. Met. Chem. 27 (2002) 155.

29. R.D. Sandlin, M.P. Starling, K.M. Williams, J. Inorg. Biochem. 104 (2010) 214.

30. M. Kato, H. Yamamoto, T.-A. Okamura, N. Maoka, R. Masui, S. Kuramitsu, N. Ueyama, Dalton Trans. (2005) 1023.

31. S. van Zutphen, M. Krauss, C. Driessen, G.A. van der Marel, H.S. Overkleeft, J. Reedijk, J. Inorg. Biochem. (2005) 1384.

32. D. Bugarcic, F.W. Heinemann, R. van Eldik, Dalton Trans. (2004) 279.

33. B.T. Benedetti, E.J. Peterson, P. Kabolizadeh, R. Kipping, J.J. Ryan, N.P. Farrell, Mol. Pharm. 8 (2011) 940.

34. N.V. Kaminskaia, N.M. Kostic, Inorg. Chem. 40 (2001) 2368.

Appendix B

Zinc finger peptide cleavage by a dinuclear platinum compound

John B. Mangrum[a], Ibrahim Zgani[b], Samantha D. Tsotsoros[b], Yun Qu[b], and Nicholas P. Farrell[b*]

[a] The RNA Institute, University at Albany, State University of New York, 1400 Washington Avenue, Albany, NY 12222

[b] Department of Chemistry, Virginia Commonwealth University, 1001 W. Main Street, Richmond, VA 23284-2006 USA

B.1   Contribution

S.D.T.'s contributions were comprised of $\{^1\text{H}, ^{15}\text{N}\}$ HSQC NMR spectroscopy studies for 1,1-t,t and 1,1-c,c with ZF and preparation of the corresponding figures. I.Z's contribution was mass spectrometry experiments and J.B.M.'s contributions were mass spectrometry

studies and preparation of the written manuscript.

B.2 Abstract

Electrospray ionisation mass spectrometry (ESI-MS) and {^{1}H, ^{15}N HSQC} NMR spectroscopy has elucidated the binding of a dinuclear platinum compound to a zinc finger peptide with induced backbone cleavage. Cleavage is selective on the N-terminal side of the cysteine residue following incubation at neutral pH, and is further dependent on structure of dinuclear compound.

B.3 Introduction

Zinc finger proteins are involved in DNA recognition, transcription, apoptosis, repair and RNA packaging.[1] The electron-rich nature of the zinc coordination sphere renders the peptides susceptible to oxidation and nucleophilic attack by alkylating and metallating agents.[2,3] In this communication we report on the selective peptide cleavage of the C-terminal nucleocapsid zinc finger of HIVNCp7 (ZF) by dinuclear platinum complexes [PtCl(NH$_3$)$_2$2m-NH$_2$(CH$_2$)$_6$NH$_2$]$^{2+}$, Fig. B.1. The cleavage is specific for the N-terminal side NH$_3$-Lys-Gly-Cys-Trp-(KGCW) sequence and is also dependent on the geometry of the dinuclear compound.

The results have implications for zinc finger targeting.

Zinc finger proteins are excellent templates for metal ion substitution.[3] For platinum compounds, the
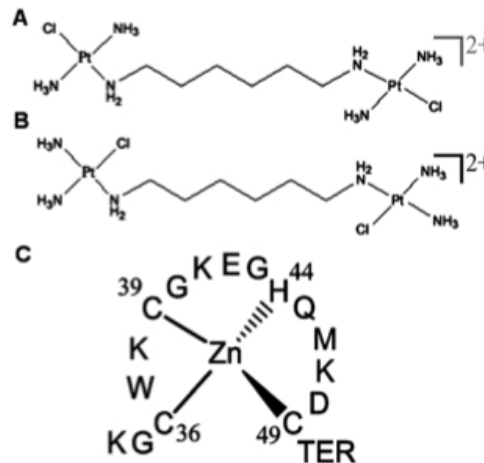

Figure B.1: Structures of (A) I (1,1-t,t) and (B) II (1,1-c,c) dinuclear platinum anti-cancer drugs and (C) the C-terminal finger (ZF) of HIVNCp7. Numbering as per full protein.

149

nature of the reaction depends on compound struc-

ture. For $[PtCl(dien)]^+$ formation of {ZF-Pt(dien)} by formal substitution of the Pt-Cl bond by cysteinate is observed, and the conclusion is supported by studies on model zinc chelates.[4,5]

Mass spectrometry and model studies also suggest the possibility of a Cl^- transfer from Pt to produce a 5-coordinate Zn.[4,5] The reaction of a 31-amino acid $ZnCys_4$ zinc-finger model with the anti-cancer drug cisplatin (cis-$[PtCl_2(NH_3)_2]$, cDDP) proceeds in a stepwise fashion with complete deligation of Zn(II) only seen upon coordination of two equivalents of the Pt complex.[6] Studies on the S/N-donor preferences of $[PtCl(Nucleobase)(L)(L')]^+$ (L = L' = pyridine (pyr) or L = NH_3, L' = pyr, quinoline (quin) etc.) suggest the potential for specific protein rather than nucleic acid reactions.[3,7] ESI-MS and CD spectra of *trans*-$[PtCl(9-EtGua)(pyr)_2]^+$ with ZF confirmed complex formation and subsequent loss of Zn, again in presence of two $[Pt(pyr)_2]$ units.[8] Similar behavior is also seen for [SP-4-2]- $[PtCl(9-EtGua)(NH_3)(quin)]^+$ and indeed this specific compound shows incipient and moderately selective antiviral activity, in contrast to the cytotoxic parent dichloride compound.[9]

B.4   Results and Discussion

To further analyze the parameters for zinc displacement and the apparent necessity for two Pt units, we have examined the interaction of the C-terminal zinc finger (ZF) of the HIV NCp7 nucleocapsid protein with the isomeric pair of dinuclear platinum complexes I and II, Fig. B.1.[10]

Using ESI-MS, the earliest product peak observed, immediately after mixing in water at 37^oC and pH 7.0, is at 978.6 m/z (3+), corresponding to a 1:1 adduct of I:ZF, Fig. B.3 (ESI). This could represent a non-covalent I:ZF association or displacement of Cl^- with transfer to Zn. Collision induced dissociation (CID) of this peak at 978.6 (A), showed the presence of intact ZF
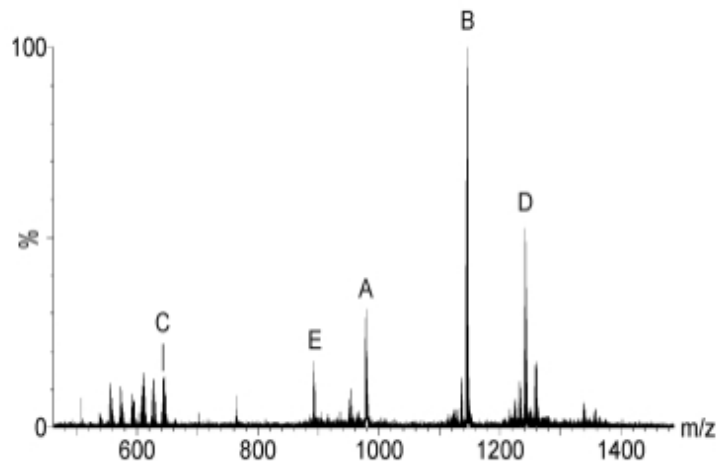
Figure B.2: ESI-MS/MS of the 978.6 peak (A) from 1,1-t,t (I) and intact ZF (1:1) immediately upon mixing.

1145.2 m/z (B) and platinum compound 645.5 m/z (C), indicating the presence of a non-covalent component, Fig. B.2. The spectrum also contains a peak at 1258.7 m/z (D), representing the 2+ ions of the {ZF + Pt(NH$_3$)$_2$}. A notable feature is the presence of a peak at 894.1 m/z (3+) (E, species III) corresponding to an adduct of I-2Cl$^-$ i.e. [Pt(NH$_3$)$_2$2m-H$_2$N(CH$_2$)$_6$NH$_2$] with a peptide formed by cleavage of the N-terminal KG amino acids ZF-KG, (Zn-CWKCGKEGHQMKDCTER). Isotopic distribution confirms the presence of a zinc ion in this species. A companion peak at 871.9 m/z (not shown) is assigned to the same species with loss of Zn. There is also significant fragmentation observed at lower m/z values of the 1,1/t,t compound itself representing loss
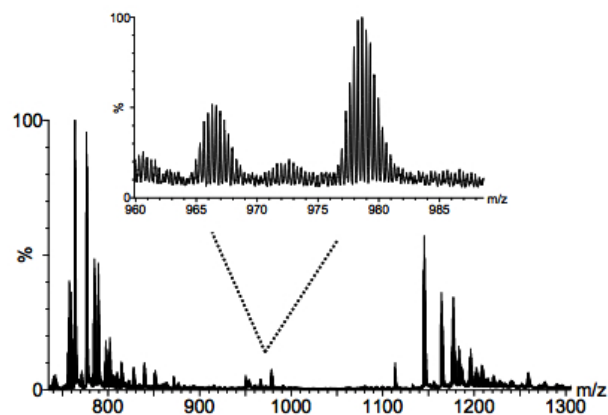
Figure B.3: ESI-MS of the 1:1 complex of I (1,1-t,t) with intact zinc finger. The non-covalent association of ZF and Pt compound is shown in the inset at 978 m/z.

151
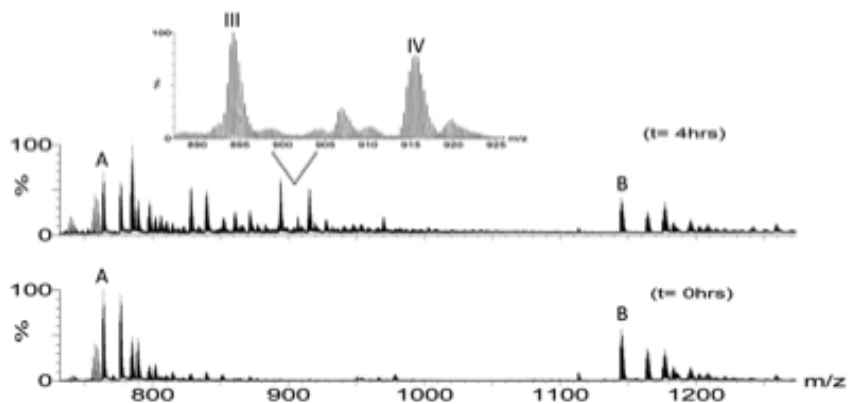
Figure B.4: Top- incubation of 1,1-t,t with ZF after 4 hours, bottom- spectrum at 0 hours. Peaks denoted (A and B) represent in this case intact ZF, 3+ and 2+, respectively. Peak III is peptide with loss of -KG.

of chloro and am(m)ine ligands, as observed previously.[11]

Fig. B.4 shows spectra at different time points for the I:ZF reaction, with decrease in intensity of free ZF peaks. Most interesting is the increase in intensity for species III at 894.1 m/z (3+) again corresponding to loss of the N-terminal KG amino acids (ZF-KG) in a platinated peptide. Thus, cleavage occurs even in the absence of added CID energy and III is a major product of the reaction. Species IV centered at 916.13 m/z may be assigned to the 3+ state of $[ZF + Pt(NH_3)_{22}]$ with two $\{Pt(NH_3)_2\}$ moieties bound to the peptide.Sequential ESI-MS/MS of the 894.1 m/z ion reveals mostly peptide cleavages producing y-type ions from y1 (Arg, R) through y13 (Gly, G) fragments from the C-terminal arginine. No platinated peptides are observed in these fragments. Importantly, there are no respective b-type ions from the -CWKC- region, and while free Arg and ArgGlu residues are readily observed no corresponding Lys or LysGly ions appear. Thus, the identifiable cleavages for I occur upstream from the zinc-coordinating cysteine on the N-terminal side of the peptide, NH3-X-Y-Cys-Trp-.

The ^{1}H NMR spectrum of ZF has been fully assigned[12] and the reaction with I results in immediate broadening of most peaks with concomitant decreases in intensity - attributed

principally to loss of ordered structure. The use of {^{1}H, ^{15}N} HSQC NMR spectroscopy has helped delineate the mechanism of DNA binding of mononuclear and polynuclear Pt complexes.[13] We have also used this technique to examine the reaction of I and II with the S-donors glutathione (GSH) and methionine (Met).[14−16] The {^{1}H, ^{15}N}HSQC NMR of fully ^{15}N-labeled I, Fig. B.5A, in presence of an equimolar amount of ZF shows the time-dependent appearance of three new peaks in the Pt-NH$_3$ region at {3.88/-62.2} (i); {3.73/-57.0} (ii), and {3.53/-59.2} (iii) ppm, shifted from the parent values of I at {3.87/-63.4} ppm.[14,15] Peak (ii) increases in intensity over time with concomitant disappearance of peak (iii). The number of peaks suggest the presence of more than one species but, importantly, the values are consistent with displacement of the Pt-Cl bond by an S donor ligand. Peak (i) may represent a S ligand *trans* to N in a [PtN$_3$S] coordination sphere.[14] The distinct ^{15}N downfield shifts for (ii) and (iii) are strongly indicative of [PtN$_2$S$_2$] coordination spheres. For example, in the reaction of tDDP with glutathione (GSH) the products *trans*-[Pt(NH$_3$)$_2$(GS)$_2$] and the related GS-bridged species [{*trans*-Pt(NH$_3$)$_2$(GS)$_2$m-GS]$^+$ occur at {3.52/-62.7} and {3.83/-59.1} ppm respectively.[14] Concomitantly, the peak at {5.022/-46.0} ppm corresponding to the linked -NH$_2$ simply decreases in intensity and eventually disappears. In summary the NMR results are consistent with Cys S displacement of the Pt-Cl bond with concomitant *trans*-labilization of the linker and match very well the mass spectroscopy results.

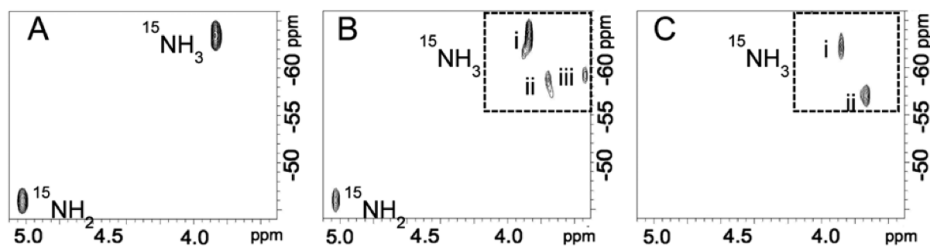Interestingly, the reaction of the 1,1/c,c isomer, II, with ZF yields a different set of

Figure B.5: {^{1}H, ^{15}N} HSQC NMR of ^{15}N-I, A, and I incubated with ZF for 3 hours, B, and 20 hours, C.

products. The major peak observed after four hours of incubation at 37°C, is at 922 m/z, assigned to the 3+ ion of the species {{ZF-Zn}-[{Pt(NH$_3$)}$_2$m-H$_2$N(CH$_2$)$_6$NH$_2$]}$^{3+}$, where II has lost the chloro ligands and two associated NH$_3$ groups while simultaneously displacing the zinc ion, Fig. B.6 (ESI). The species is formed by Pt-Cl substitution followed by *trans* labilization of the NH$_3$ group in II. No evidence is seen for peptide cleavage even at time points up to 24 h. The relative intensity of free ZF is also higher than for 1,1/t,t, in agreement with the slower substitution kinetics of the 1,1/c,c isomer.[17]

The natural hydrolysis of amide bonds in peptides and proteins is a slow process under native conditions.[18] Pd and Pt salts such as [M(H$_2$O)$_4$]$^{2+}$ and [M(en)(H$_2$O)$_2$]$^{2+}$ display peptidase activity in methionine-containing peptides - the thioether residue acts as an "anchor" through M-S bond formation, directing the adjacent peptide bond cleavage.[19] This initial "anchoring" is followed by either of two possible mechanisms: the metal ion binds a carbonyl oxygen making the peptide bond susceptible to water attack or attack of the amide bond by a metal complex with an aqua ligand.[20] Cisplatin also mediates peptide hydrolysis downstream from a methionine residue, with formation of multidentate peptide chelates inducing conformational stress and peptide backbone cleavage which occurs at the second amide bond in the N-terminal direction from the site of the coordinating side chain.[21] The strategy in all these cases requires the presence of labile sites (even on Pd) for rapid M-S and possibly M-N(histidine) bond formation and conditions are mildly to strongly acidic.

The complex system presented here may be explained by the above discussion and the known chemistry of dinuclear platinum complexes with sulfur thioether and thiol donors.[14][16] The pKa and aquation rates of the dinuclear compounds have been measured and equilibrium favors the chloro forms.[22,23] Glutathione binding through the cysteine residue rapidly (hours) labilizes the diamine linker of I.[14] In contrast, the diamine linker remains intact in the 1,1/c,c isomer and novel GS-bridged (m-thiolato) macrochelates are formed, as a result of the labile chloride being trans to the more substitution-inert NH$_3$ ligand.[16] Similar differences between
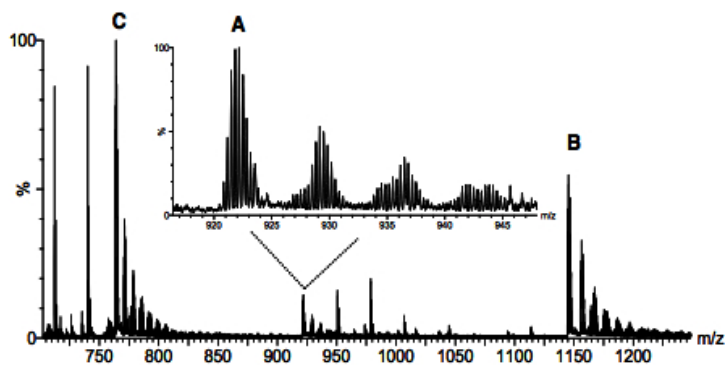
Figure B.6: Incubation of 1,1-c,c, II, with ZF after 4 hours. Peak denoted A represents loss of Zn and subsequent loss of NH_3 and Cl on the platinum compound. B is intact free ZF.

the two geometries are observed with methionine.[16] Based on these collected observations a stepwise mechanism of peptide cleavage may be proposed where Pt-Cl bond substitution in I by zinc-bound cysteinate results in *trans*-labilization of the Pt-NH_2(diamine) bond which will produce an available coordination site; further peptide back- bone bonding especially to a second Pt-Cys(S) bond (consistent with observation of [PtN$_2$S$_2$] species observed by NMR and {Pt(NH$_3$)$_2$}-ZF species in MS) is then possible with concomitant cleavage of the peptide bond and eventual zinc ejection:
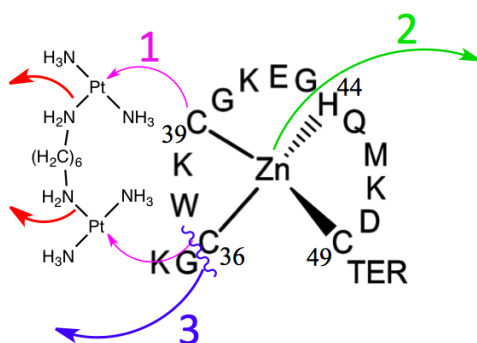
This scheme also explains the fragmentation (y1 to y13) pattern observed from mass spectrometry and the isomeric dependence of the reaction - in the 1,1/c,c I the ligand *trans* to S is the substitution-inert NH_3. Further, the Pt-m-SR(thiolato)-Zn coordination motif has been confirmed in model systems, suggesting analogies for the nature of the [PtN$_2$S$_2$]

155

species.[5] It is notable that reaction occurs at biologically relevant pH and the possibility exists of direct substitution by the highly nucleophilic zinc-cysteinates, as substitution on S can occur in absence of Pt complex hydrolysis.[14] To our knowledge, this is the first demonstration of metal-assisted peptide cleavage on zinc fingers and is a novel strategy for inactivation of this important biological target.[3] These initial intriguing results merit further study of this system.

B.5   Experimental

Platinum compounds and zinc finger starting materials were prepared as previously.[14,15]

B.5.1   Mass Spectrometry

For mass spectrometry experiments, initial 1mM reaction mixtures were made in water at 37°C and pH 7.0 adjusted using ammonium hydroxide, then H_2O/MeOH (6/94) aliquots of approx. 10 μM used for spraying. Experimental procedure in general followed published protocol.[8] The reaction solution was not adjusted for pH during the reaction.

B.5.2   NMR Spectrometry

NMR experiments also followed published procedure and were conducted at 1 mM concentration (1:1) in 5% D_2O/95% H_2O.[8]
For HSQC $\{^1H,^{15}N\}$ NMR Spectroscopy the spectra were recorded at 37°C on a Bruker AVANCE III 600 MHz spectrometer (^1H, 600.1 MHz; ^{15}N, 60.8 MHz) fitted with a pulsed field gradient module and 5mm inverse quadruple resonance (QXI) probe. The ^1H NMR chemical shifts were internally referenced to TSP, the ^{15}N chemical shifts externally referenced to $^{15}NH_4NO_3$. The two-dimensional [$^1H,^{15}N$] HSQC spectra were recorded in phase sensitive mode using Echo/Antiecho-TPPI gradient selection. A total of 1024 points were

acquired in the ^{1}H dimension and 96 complex points in the ^{15}N dimension with 128 transients. 1 mM platinum complex was allowed to react with 1 equiv. of ZF in 5% D_2O/95% H_2O.[8], and the reaction was followed by HSQC spectroscopy. 20 two-dimensional spectra were obtained at hourly intervals, which can determine the half-life of the reaction by the integration of $^{15}NH_3$ peaks.

B.6   References

1. A. Klug, *Annu. Rev. Biochem.*, 2010, 79, 213.

2. W. Maret and Y. Li, *Chem. Rev.*, 2009, 109, 4682.

3. S. M. Quintal, Q. A. de Paula and N. P. Farrell, *Metallomics*, 2011, 3, 121.

4. Q. A. dePaula, J. B. Mangrum and N. P. Farrell, *J. Inorg. Biochem.*, 2009, 103, 1347.

5. E. Almaraz, Q. A. dePaula, Q. Liu, J. H. Reibenspies, M. Y. Darensbourg and N. P. Farrell, *J. Am. Chem. Soc.*, 2008, 130, 6272.

6. R. N. Bose, W. Wei, W. Yang and F. Evanics, *Inorg. Chim. Acta*, 2005, 358, 2844.

7. A. I. Anzellotti, S. Stefan, D. Gibson and N. Farrell, *Inorg. Chim. Acta*, 2006, 359, 3014.

8. A. I. Anzellotti, Q. Liu, M. J. Bloemink, J. N. Scarsdale and N. Farrell, *Chem. Biol.*, 2006, 13, 539.

9. D. A. Sartori, B. Miller, U. Bierbach and N. Farrell, *J. Biol. Inorg. Chem.*, 2000, 5, 575. Experimental procedure in general followed published protocol.4,8 See ESI for further details.

10. G. Schaaf, Y. Qu, N. Farrell and V. H. Wysocki, *J. Am. Soc. Mass Spectrom.*, 1998, 33, 436.

11. S. M. Quintal, A. Viegas, S. Erhardt, E. J. Cabrita and N. P. Farrell, *Biochemistry*, 2012, 51, 1752.

12. S. J. Berners-Price, L. Ronconi and P. J. Sadler, *Prog. Nucl. Magn. Reson. Spectrosc.*, 2006, 49, 65.

13. M. E. Oehlsen, Y. Qu and N. Farrell, *Inorg. Chem.*, 2003, 42, 5498.

14. M. E. Oehlsen, A. Hegmans, Y. Qu and N. Farrell, *J. Biol. Inorg. Chem.*, 2005, 10, 433.

15. M. E. Oehlsen, A. Hegmans, Y. Qu and N. Farrell, *Inorg. Chem.*, 2005, 44, 3004.

16. N. Farrell, T. G. Appleton, Y. Qu, J. D. Roberts, A. P. S. Fontes, K. A. Skov, P. Wu and Y. Zou, *Biochemistry*, 1995, 34, 15480.

17. N. M. Milovíc and N. M. Kostíc, *Met. Ions Biol. Syst.*, 2001, 38, 145.

18. N. M. Milovíc, L. M. Dutca and N. M. Kostíc, *Inorg. Chem.*, 2003,42, 4036.

19. N. M. Milovíc, L. M. Dutca and N. M. Kostíc, *Chem. Eur. J.*, 2003, 9, 5097.

20. O. Hohage and W. S. Sheldrick, *J. Inorg. Biochem.*, 2006, 100, 1506. 22.

21. M. S. Davies, J. Cox, S. J. Berners-Price, W. Barklage, Y. Qu and N. Farrell, *Inorg. Chem.*, 2000, 39, 1710. 23.

22. J. Zhang, D. S. Thomas, M. S. Davies, S. J. Berners-Price and N. Farrell, *J. Biol. Inorg. Chem.*, 2005, 10, 652.

Appendix C

Zinc, metallated DNA-protein crosslinks as zinc finger conformation and reactivity probes

Sarah R. Spell[*], **Samantha D. Tsotsoros**[*] **and Nicholas P. Farrell**

Department of Chemistry, Virginia Commonwealth University, 1001 W. Main Street,

Richmond, VA 23284-2006 USA

[*]Sarah R. Spell and Samantha D. Tsotsoros contributed equally

C.1   Contribution

S.D.T.'s contribution is comprised of the following sections: Introduction, Targeting of Zinc Fingers by Cobalt Complexes, and Pt Complexes as DNA/Protein Crosslinkers. S.R.S.'s contributions include the sections: Interaction of platinum molecules with zinc fingers, platinated DNA affects zinc finger conformation and small molecule models for plati-

nated DNA-zinc finger interactions.

C.2 Synonyms

Anticancer metallodrugs; Antiviral metallodrugs; Cobalt Schiff base; Metallated DNA; Polynuclear Pt complexes; Pt-DNA adducts; Ternary crosslinks; Transcription factor hijacking; Zinc finger targeting

C.3 Definition

This entry describes the interactions of zinc finger peptides with metallated DNA and small molecule platinum-metal probes. The interactions have biological consequences from sequence-specific inhibition of zinc finger function to hijacking of transcription factors by binding to platinated DNA. Small molecule interactions have chemical consequences because the formal analogy between alkylation and metallation suggests the possibility of electrophilic attack of the cysteine and histidine residues with eventual zinc ion ejection and loss of tertiary structure and consequently biological function. These approaches create new opportunities to investigate the chemical properties of zinc fingers and may possibly produce new leads for disease intervention where zinc finger function is implicated.

C.4 Introduction

In biology, zinc serves either a structural or catalytic purpose. When zinc acts in a catalytic manner, it is bound to a water molecule that is converted to a hydroxyl ligand. Structural zinc is characterized by coordination to four amino acids, generally histidine and cysteine. These types of zinc sites include zinc fingers (ZF), which compose 2-3% of the human genome (Klug 2010). The most common role of zinc fingers in biology is in the binding of DNA to transcription factors and they are also involved in RNA packaging, transcriptional activation, regulation of apoptosis, and protein folding and assembly.
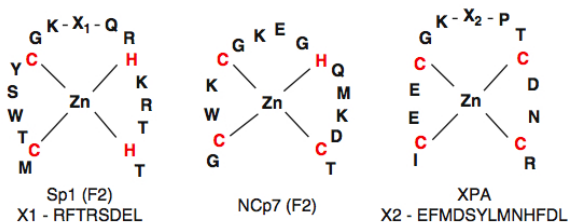
Figure C.1: The three main coordination environments of zinc fingers: C_2H_2, C_3H, and C_4

Zinc fingers are defined by the number and type of amino acids coordinated to the central zinc atom (Fig. C.1). Analysis of Cys_2His_2 zinc finger proteins has allowed for elucidation of DNA recognition mechanisms and their role in transcriptional regulation. The Cys_3His motif is involved in RNA and DNA recognition, cell-cycle control, and cellular signaling pathways. The third common zinc Cys_4 finger motif is found in human DNA repair enzymes and many nuclear localized systems.

Coordination to zinc enhances the nucleophilicity of the Zn-Cys bond, allowing for attack by small electrophiles. The chemical reactivity is dependent on the nature of the zinc coordination sphere (Cys_2His_2; Cys_3His, Cys_4) (Quintal et al. 2011). The interaction of zinc finger proteins with DNA and RNA can be inhibited upon chemical modification of the zinc binding ligands.

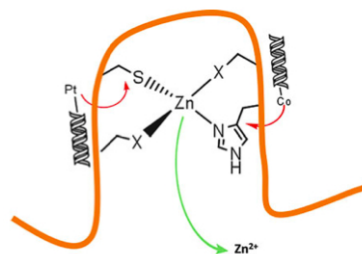Figure C.2: General schematic of electrophilic attack on a zinc finger. Platinum agents attack at cysteine residues, while cobalt agents attack at histidine residues. X= (Cys)(His) or Cys_2

There is a formal analogy between alkylation and metallation, where in the latter case chemical modification refers to electrophilic attack of the cysteine and histidine residues by Pt and Co agents, respectively (Fig. C.2).

161

In both cases, however, eventual loss of zinc is seen and the proteins lose tertiary structure and therefore loss of biological function. Tethering of the electrophilic agent to a sequence-specific DNA may allow for targeting and differentiation between different zinc fingers and enhancement of selectivity. In this review, the approaches to the use of small molecule metal-based electrophiles and formation of DNA-protein crosslinks as probes for zinc finger conformation and reactivity will be discussed. These approaches create new opportunities to investigate the chemical properties of zinc fingers and may possibly produce new leads for disease intervention where zinc finger function is implicated.

C.5   Targeting of Zinc Fingers by Cobalt Schiff Base Complexes

Cobalt(III) Schiff-base (Co-sb) complexes may disrupt the structure of a zinc finger peptide by axial ligation of the Co(III) ion to the nitrogen of the imidazole ring of a histidine residue. The reaction of Co(III)-sb with histidine is a dissociative ligand exchange process, with loss of the labile axial NH_3 ligands by H_2O facilitating histidine binding. The reaction of Co(III)-sb at the zinc finger site irreversibly inhibits protein activity as a result of zinc ejection due to the binding of cobalt to histidine (Harney, 2009). Zinc ejection causes loss of tertiary structure and therefore loss of function.

Initial studies showed that cobalt complexes inhibit binding of the human transcription factor Sp1, to its consensus sequence. DNA-coupled conjugates of the cobalt complexes selectively inhibited Sp1 in the presence of several other transcription factors. The Snail family of Cys_2His_2 zinc finger transcription factors, Slug, Snail, and Sip1, are emerging as anticancer drug targets as they are implicated in tumor metastasis through the regulation of epithelial-to-mesenchymal (EMT) transitions. Slug, Snail, and Sip1 bind to the Ebox consensus sequence CAGGTG in the promoter region of target genes with high specificity to

mediate transcriptional repression. To improve specificity for the Snail family of transcription factors, an oligonucleotide containing the DNA consensus sequence was conjugated to the Co(III) complex yielding Co(III)-Ebox (Fig. C.3) (Harney et al. 2009).
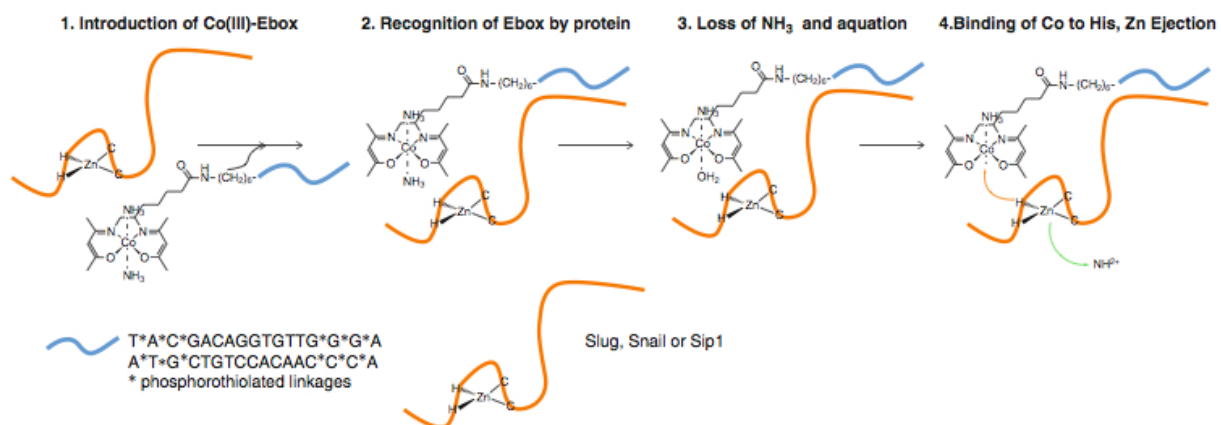

Figure C.3: Scheme for zinc finger-specific inactivation using Co(III)-sb-DNA conjugates. Co(III)-Ebox is recognized by the Snail family of transcription factors. Loss of axial ligands and subsequent binding of histidine results in eventual ejection of Zn^{2+} and transcription factor inactivation.

No significant changes in the structure of DNA occurred upon conjugation. Through addition of the Ebox DNA sequence to the Co(III) metal complex, peptide-binding specificity was improved 150-fold over Co(III)-sb. Co(III)-Ebox was found to effectively inhibit the Slug, Snail, and Sip1 zinc finger transcription factors from binding to their DNA targets with eventual loss of Zn^{2+} (Harney et al. 2009). Studies demonstrate that neither the oligo nor the Co(III) Schiff base complex alone is sufficient for transcription factor inactivation at concentrations where the conjugated complex mediates inhibition.

Subsequently, a Co(III) Schiff base DNA conjugate has been designed to target the Gli Cys_2His_2 transcription factors in the Hedgehog (Hh) pathway, which has been implicated in the formation and development of certain cancers such as medulloblastomas and basal cell carcinomas (Hurtado et al. 2012). In order to test the specificity and efficacy of Co(III)-

DNA complex, the authors tested the Ci consensus sequence alone, Co(III)-sb, Co(III)-Ci, and Co(III)-Mut (one base pair mutation). The complete structure of Co(III)-Ci was found to be the most effective at inhibiting Gli family ZF transcription factors. The mutation of one base pair in Co(III)-CiMut inhibited its specific and potent activity. The activity of Co(III)-Ci was specific, as no other zinc finger transcription factor tested was inhibited by the addition of the complex (Hurtado et al. 2012). These results show that subtle changes in the oligomer attached to Co(III) can modulate the specificity and activity of these Co(III)-DNA conjugates both *in vitro* and *in vivo*.
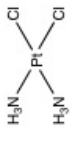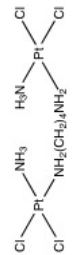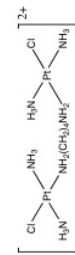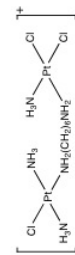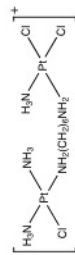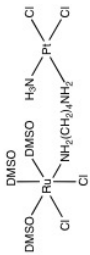
The studies performed using Co(III)-DNA complexes demonstrate the development of a versatile class of specific and potent complexes that may be used to study zinc finger proteins and may prove valuable as an experimental tool and as anticancer therapeutics.

C.6   Pt Complexes as DNA/Protein Crosslinkers

The structure and nature of DNA adducts of platinum complexes may be manipulated to facilitate ternary DNA-Pt-protein crosslinks. Table C.1 summarizes the compounds studied. One of the first examples is the use of *trans*-diamminedichloroplatinum(II) (tDDP). In order to map the section of HIV1 RNA that was recognized by the nucleocapsid (NC) protein, tDDP was used as a crosslinking agent. After digestion of a crosslinked solution of HIV1 RNA and NC protein, the crosslink was shown to form between positions 315-324 of the RNA. This suggests the possible recognition site for the NC protein on HIV1 RNA (Darlix et al. 1990).

Various mononuclear and dinuclear platinum complexes have been analyzed for their crosslinking abilities to zinc finger containing proteins such as the DNA repair proteins, UvrA and UvrB, and Sp1. The repair of the DNA adducts of the anticancer agent *cis*-diamminedichloroplatinum(II) (cisplatin, cDDP) was examined with the bacterial UvrABC

Table C.1: Various metal complexes form crosslinks with zinc finger proteins and DNA.

Compound	Structure	DNA Studied	Zn Finger Studied	Crosslink	Reference
cDDP		Plasmid pSP65	UvrAB	DNA monoadduct crosslink formation of UvrB	Lambert, 1995
tDDP		^{32}P HIV-1 RNA (311-415)	HIV1 NC	Crosslink formation between RNA (between positions 315-324) and HIV1 NC	Darlix, 1990
Pt-BCH		Plasmid pSP65	UvrA, UvrB	DNA monoadduct crosslink formation of UvrB	Lambert, 1995
(Pt-Pt)-2,2-c,c		49 bp duplex	UvrA, UvrB, Sp1	Crosslink formation between platinated DNA and UvrA and UvrB	Van Houten, 1993
(Pt-Pt)-1,1-t,t		49 bp duplex	UvrA, UvrB, Sp1	Crosslink formation between platinated DNA and UvrA and UvrB	Van Houten, 1993, Kloster, 2004
(Pt-Pt)-1,2-t,c		Plasmids pSP73KB and pUC19	Sp1	Crosslink formation between platinated DNA and Sp1	Kloster, 2004
(Pt-Pt)-1,2-c,c		Plasmids pSP73KB and pUC19	Sp1	Crosslink formation between platinated DNA and Sp1	Kloster, 2004
Pt-Ru		49 bp duplex	UvrA, UvrB	Crosslink formation between platinated DNA and UvrA and UvrB	Van Houten, 1993
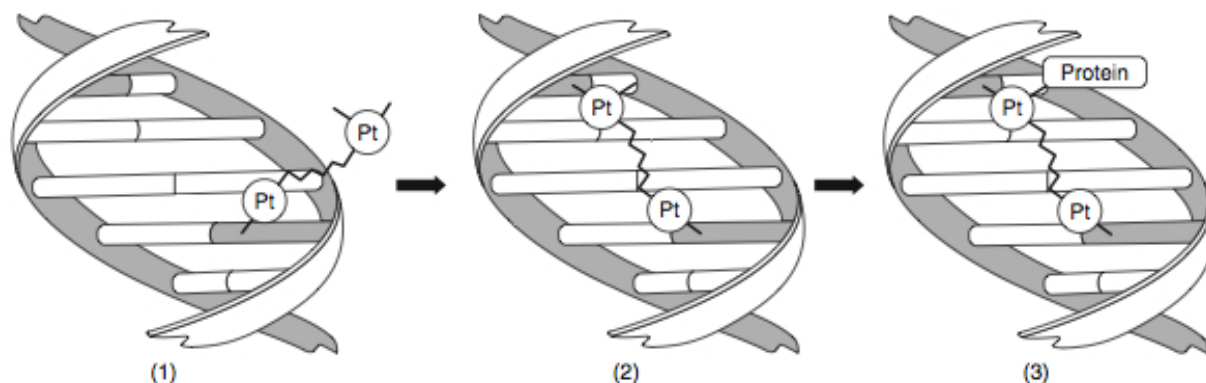
Figure C.4: The binding of dinuclear platinum complexes to DNA. (1) Initial monofunctional binding, (2) long-range bifunctional interstrand crosslink formation with second platinum unit and (3) binding of protein at the third active site.

complex (Lambert et al. 1995). A sterically hindered analog, exo-[N-2-methylamino-2,2,1-bicyclohepane] dichloroplatinum(II) (Pt-BCH) was compared for its protein crosslinking abilities. UvrAB proteins recognized the mono- and diadducts of Pt-BCH with a higher affinity than those of cisplatin. Analysis of the crosslinks showed the involvement of UvrB in the ternary nucleoprotein complexes. In general, UvrB has a greater affinity for the adducts formed by Pt-BCH over those formed by cisplatin (Lambert et al. 1995).

Dinuclear platinum complexes bind to DNA in a manner that is unique from cisplatin and other mononuclear complexes, the main adducts being long-range (Pt,Pt) interstrand crosslinks (Kloster et al. 2004). Dinuclear complexes may be formally bi, tri, or tetrafunctional (depending on number of substitution-labile chlorides present - see Table C.1). Even in the presence of a cDDP-like cis-[PtCl$_2$(amine)$_2$] coordi- nation sphere the (Pt,Pt)-interstrand crosslinks form preferentially (Fig. C.4).

Thus, upon bifuntional binding to DNA, the third Cl site can then bind to a protein, preferentially at Cys, His, or Met residues (Kloster et al. 2004). Platinum complexes are known to bind in the major groove of DNA and the ability of the dinuclear complexes to crosslink UvrA and UvrB suggests that the proteins contact the major groove of the DNA

helix within 4-4.5A (Van Houten et al. 1993). The flexibility of the dinuclear platinum adducts may be important in their crosslinking of Sp1 due to the DNA bending induced upon Sp1 binding (Kloster et al. 2004).

The results of these platinum crosslinking studies suggest that the formation of metal-mediated DNA-protein complexes may play a role in the cytotoxic properties of these compounds due to the irreversible crosslinking, and therefore sequestering, of repair proteins or transcription factors to DNA. The differences between mononuclear and dinuclear platinum complexes may also explain the different cytotoxic properties of the two classes of anticancer drugs. The differences in DNA adduct structure between mononuclear and dinuclear complexes may also be used to probe protein recognition of structurally different DNA crosslinks (Kloster et al. 2004).

C.7   Interaction of Platinum Molecules with Zinc Fingers

The demonstration of zinc finger crosslink formation by platinated DNA is fundamentally an example of coordination compounds acting as electrophiles toward the peptide cysteine residues. Small molecule platinum-metal agents have therefore been explored for their ability to target the HIV nucleocapsid retroviral protein NCp7. Figure C.5 shows the structures of the metal complexes studied as well as that of NCp7 nucleocapsid protein.

Again, *functionality* can be studied by use of structurally distinct compounds such as cDDP, *trans*-[PtCl (9-EtGua)(pyr)$_2$]$^+$, [PtCl(terpy)]$^+$, and [PtCl(dien)]$^+$ (Quintal et al. 2012). Further, the reactivity of the central metal ion may be altered by use of the general structure [MCl(chelate)] (M = Pt(II), Pd(II), or Au(III) and chelate = diethylenetriamine, dien or 2,2' ;6' ,2' -terpyridine, terpy). Interestingly, both Pt(II) and Pd(II)-dien species showed evidence of adduct formation on ZF by replacement of the M-Cl bond with zinc-bound thiolate. Eventual loss of the dien ligand, as well as zinc ejection, was observed. Due to the strong thiol affinity of gold drugs both Au(III) compounds reacted extremely fast

producing only "gold fingers". For all terpy compounds metal exchange occurred producing the product [Zn(terpy)]$^{2+}$. These results show that by modifying both the metal and ligand of the reacting compound, the chemical reactivity of zinc finger proteins can by altered (Quintal et al. 2011).
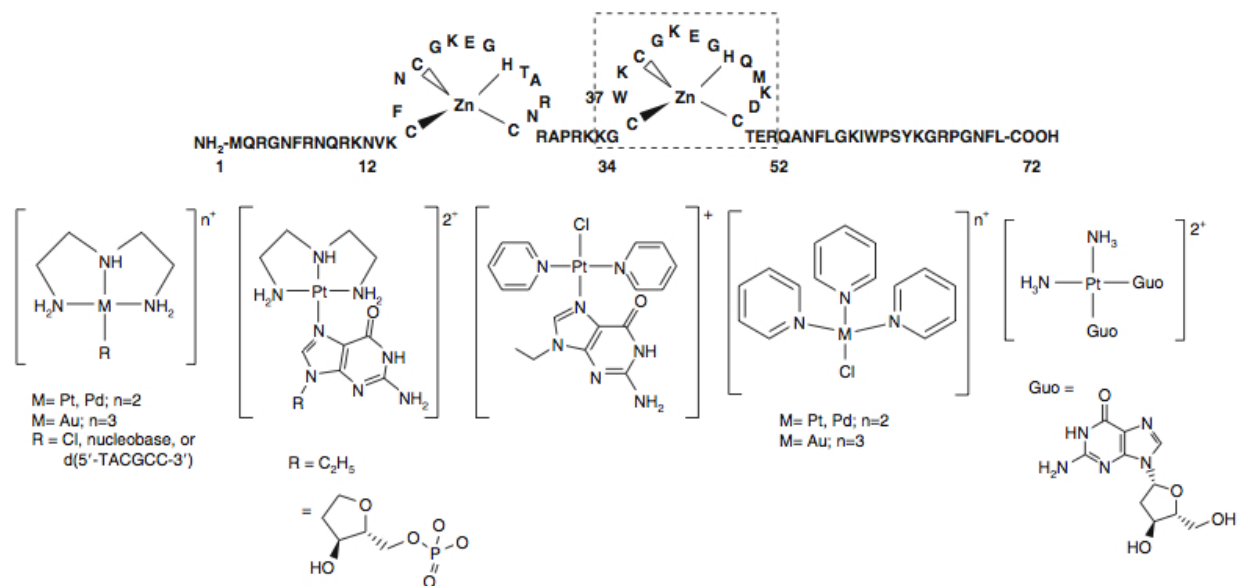
Figure C.5: Structures of HIV NCp7 nucleocapsid protein (ZF; C-terminal finger, ZF2 shown in dashed box) and the platinum-metal complexes studied for molecular recognition and electrophilic attack.

A major challenge for all small molecule electrophiles is selectivity. To enhance the selectivity of these druges, it is important to understand the details of the zinc finger-DNA interaction. The recognition of DNA or RNA by the HIV nucleocapsid protein NCp7 is dominated primarily by π-stacking between the purine nucleic acid bases and the planar aromatic amino acid residues, especially between guanine and tryptophan37 (Quital et al. 2011). Fluorescence quenching studies have shown that metallation of nucleobase compounds significantly enhances the π-π stacking interactions with L-tryptophan. Metallation modifies frontier molecular orbital properties, lowering the π-acceptor LUMO of the metallated nucleobase, thus improving the overlap toward the π-donor HOMO of the tryptophan.

Study of the biologically relevant C-terminal peptide (ZF2) of the HIV-NCp7 zinc knuckle showed that $[Pt(dien)(9EtGua)]^{2+}$ (9-EtGua = 9-ethylguanine) and $[Pt(dien)(5'-GMP)]$ (5'-GMP = guanosine 5'-monophosphate) quench tryptophan fluorescence with K_a, association constants, of 7.5 x 10^3 and 12.4 x 10^3 M^{-1}, respectively. Though there is little difference between their binding with the simple amino acid tryptophan, the extra phosphate group on the 5'-GMP causes a significant increase in binding with ZF2 (Anzellotti et al. 2006). ESI-MS of both $[Pt(dien)(9EtGua)]^{2+}$ and $[Pt(dien)(5'-GMP)]$ with ZF2 showed formation of a 1:1 adduct between the peptide and Pt-complex. It is most likely that this adduct formation is facilitated by the π-π stacking interactions between the tryptophan and the platinated nucleobase. Incubation of *cis*-$[Pt(NH_3)_2(Guo)_2]^{2+}$ (Guo = guanosine) with ZF2 showed significantly less formation of the 1:1 adduct, possibly due to steric hindrance from the mutually *cis*-oriented purines (Anzellotti et al. 2006).

The monofunctional *trans*-$[PtCl(9-EtGua)(pyr)_2]^+$ (pyr = pyridine) has high reactivity toward sulfur over nitrogen, and it has also been shown to cause Zn ejection in model chelates (see below). In the presence of a 1:1 stoichiometric ratio of *trans*-$[PtCl(9-EtGua)(pyr)_2]^+$, the ESI-MS of ZF2 showed numerous peaks consistent with multiple adduct formation. The peak corresponding to the adduct ($[ZF2(Pt[pyr]_2)_2]$-Zn) shows two $[Pt(pyr)]_2$ units bound to the protein with resultant loss of Zn. CD experiments revealed changes in the three-dimensional structure of the protein, consistent with the loss of tertiary structure due to Zn ejection. Therefore, the proposed mechanism for attack of Pt-nucleobase compounds on zinc fingers consists of two steps: (1) non-covalent recognition through π-π stacking of tryptophan with platinated nucleobase and (2) covalent interaction with Pt-S bond formation followed by zinc ejection (Anzellotti et al. 2006).

C.8 Platinated DNA Affects Zinc Finger Conformation

To expand on the studies of platinum-nucleobase complex - zinc finger interactions, the interaction of Pt(dien)6-mer (6-mer = d'(5'-TACGCC-3')) with the C-terminal finger of the HIV NCp7 zinc finger, ZF2, was studied by NMR Spectroscopy. In this case the Pt(dien) moiety was bound to the single guanine residue (C.6a). The solution structures of ZF2, the 6-mer/ZF2, and Pt(dien)6mer/ZF2 adducts were calculated from NOESY-derived distance constraints. For the 6-mer/ZF2 structure, stacking with tryptophan was observed as well as showed that there was an interaction between Trp37 and the ribose protons of the carbohydrate moiety of Gua4, confirming the carbohydrate-aromatic ring interaction as a key recognition site between NCp7 protein and oligonucleotides. The NMR spectrum of ZF2 in the presence of Pt(dien)6-mer showed weakening of the Trp37-Gua4 contact attributed by the steric effects caused by platination of Gua4. The aromatic ring of the tryptophan residue changes orientation (Fig. C.6b), causing the DNA to be in a completely different position than when platinum is absent.
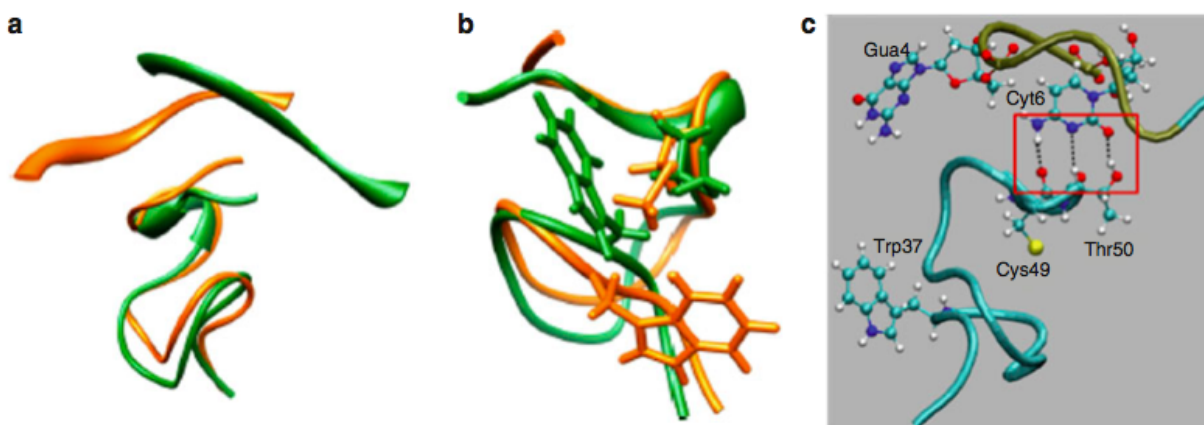

Figure C.6: (a) superposition of the minimized structures of the 6mer/ZF2 adduct (green) and Pt(dien)(6mer)/ZF2 adduct (orange) (b) change in conformation of Trp37 upon platination of Gua4 (c) stabilizing interactions of Cyt6 with the protein residues, Cys49 and Thr50, in the Pt(dien)(6mer)/ZF2 adduct (hydrogen bonding highlighted in red box)

Molecular dynamics calculations of the DNA-protein interactions showed that the π-stacking between Trp37 and Gua4 as well as the hydrogen bonding between the pentose and phosphate oxygen(s) of Cyt5 and Gua4 both help stabilize the interactions between the 6-mer and ZF2. Once platinum is bound, the 6-mer is less flexible and stays in one stable conformation on the surface of the zinc finger. The Gua4-Trp37 interaction is disrupted, resulting in hydrogen bonding interactions between Cyt6 and Cys49 and Thr50. Additionally, the backbone CH group is close to N3 of Cyt6. With the addition of this third hydrogen bond, the bonding mode imitates the three intermolecular Cyt-Gua base pair hydrogen bonds (Fig C.6c).

In conclusion, these results show for the first time structural characterization of platinated single-stranded DNA interacting with a zinc finger protein, resulting in conformational change of the peptide. These results further demonstrate the feasibility of using DNA-tethered coordination compounds to target specific zinc finger proteins (Quintal et al. 2012).

C.9 Small Molecule Models for Platinated DNA-Zinc Finger Interactions

To provide a small molecule model for the reactions of platinum complexes with ZFs, the chelate N,N'-bis (2-mercaptoethyl)-1,4-diazacycloheptanezinc(II), [Zn (bme-dach)]$_2$, was studied. Structures for model metal/DNA/protein crosslinks and zinc ejection were deduced from ESI-MS spectra of this [Zn(bme-dach)]$_2$ with $trans$-[PtCl(9-EtGua)(pyr)$_2$]$^+$, a model for a monofunctional adduct of platinum on DNA. The schematic of the reaction is shown in Fig. C.7.

The intermediate species [Zn(bme-dach)-Pt (9-EtGua)(pyr)$_2$]$^+$ was observed and after 20 h was identified as the major species present. This is considered to be the first heterodin-
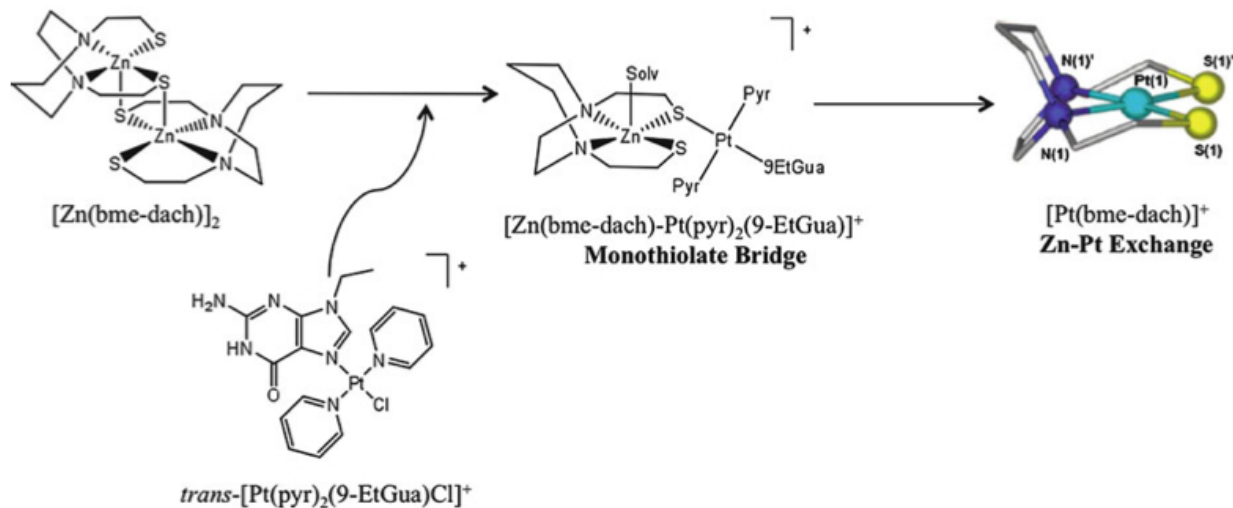
Figure C.7: Reaction pathway of [Zn(bme-dach)]$_2$ with *trans*-[PtCl(9-EtGua)(pyr)$_2$]$^+$ with formation of monothiolate bridges and metal exchanged species (Almarex et al. 2008)

uclear Pt,Zn monothiolate bridged species to be identified using biologically relevant species. MS experiments showed the final product to be [Pt(bme-dach)]$^+$, giving proof of Zn ejection followed by platinum replacement (Liu et al. 2005). Similar experiments were performed for [Pt(dien)Cl]Cl and [Pt(terpy)Cl]Cl. Results showed formation of mono- and dithiolate bridged intermediates as well as metal exchange and multimetallic aggregate species (Quintal et al. 2011). These results represent suitable models for the molecular structure of ternary DNA-protein complexes involving zinc finger proteins discussed above (Liu et al. 2005).

C.10   Acknowledgments

C.11   References

1. Almaraz E, de Paula Q, Liu Q, Reibenspies J, Darensbourg M, Farrell NJ (2008) Thiolate bridging and metal exchange in adducts of a zinc finger model and Pt(II)

complexes:biomimetic studies of protein/Pt/DNA interactions. J Am Chem Soc 130: 6272-6280

2. Anzellotti A, Liu Q, Bloemink M, Scarsdale J, Farrell N (2006) Targeting retroviral Zn finger-DNA interactions: a small-molecule approach using the electrophilic nature of *trans*-platinum-nucleobase compounds. Chem Biol 13:539-548

3. Darlix J-L, Gabus C, Nugeyre M-T, Clave F, Barre-Sinoussi F (1990) *Cis* elements and *trans*-acting factors involved in the RNA dimerization of the human immunodeficiency virus HIV-l. J Mol Biol 216:689-699

4. Harney A, Lee J, Manus L, Wang P, Ballweg D, LaBonne C, Meade T (2009) Targeted inhibition of Snail family zinc finger transcription factors by oligonucleotide-Co(III) Schiff base conjugate. Proc Natl Acad Sci USA 106:13667-13672

5. Hurtado R, Harney A, Heffern M, Holbrook R, Holmgren R, Meade T (2012) Specific inhibition of the transcription factor Ci by a Cobalt(III) Schiff baseâĽŠDNA conjugate. Mol Pharm 9:325-333

6. Kloster M, Kostrhunova H, Zaludova R, Malina J, Kasparkova J, Brabec V, Farrell N (2004) Trifunctional dinuclear platinum complexes as DNA-protein cross-linking agents. Biochemistry 43:7776-7786

7. Klug A (2010) The discovery of zinc fingers and their applica- tions in gene regulation and genome manipulation. Annu Rev Biochem 79:213-231

8. Lambert B, Jestin J-L, Brehin P, Oleykowski C, Yeung A, Mailliet P, Pretot C, Le Pecq J-B, Jacquemin-Sablon A, Chottard J-C (1995) Binding of the Escherichia coli UvrAB proteins to the DNA mono- and diadducts of *cis*-[N-2-amino- N-2-methylamino-2,2,1-bicycloheptane]dichloroplatinum (II) and cisplatin. J Biol Chem 270:21251-21257

9. Liu Q, Golden M, Darensbourg M, Farrell N (2005) Thiolate- bridged heterodinuclear platinum-zinc chelates as models for ternary platinum-DNA-protein complexes and zinc ejection from zinc fingers. Evidence from studies using ESI-mass spectrometry. Chem Commun 34:4360-4362

10. Louie AY, Meade TJ (1998) Isolation of a myoglobin molten globule by selective cobalt(III)-induced unfolding. Proc Natl Acad Sci USA 95:6663-6668

11. Quintal S, dePaula Q, Farrell N (2011) Zinc finger proteins as templates for metal ion exchange and ligand reactivity. Chemical and biological consequences. Metallomics 3:121-139

12. Quintal S, Viegas A, Erhardt S, Cabrita E, Farrell N (2012) Platinated DNA affects zinc finger conformation. Interaction of a platinated single-stranded oligonucleotide and the C-terminal zinc finger of nucleocapsid protein HIVNCp7. Biochemistry 51:1752-1761

13. Van Houten B, Illenye S, Qu Y, Farrell N (1993) Homodinuclear (Pt,Pt) and heterodinuclear (Ru,Pt) metal compounds as DNA-protein cross-linking agents: potential suicide DNA lesions. Biochemistry 32:11794-11801

Education

- PhD, Chemistry, May 2014, GPA: 3.714
  Dissertation: "Platinum Complexes and Zinc Finger Proteins: From Target Recognition to Fixation"
  Virginia Commonwealth University, Richmond, Virginia

- Bachelor of Science, Chemistry, May 2009; Cum Laude; Major GPA: 3.9
  Christopher Newport University, Newport News, Virginia

Honors and Societies

- Virginia Commonwealth University
  Teaching Assistantship scholarship
  Lidia M. Vallarino Scholarship, 2013-2014
  Altria Fellow, 2013-2014

- Christopher Newport University
  President's Leadership Program Scholarship
  Biology, Chemistry and Environmental Science Departmental honors
  Chemistry GPA 3.98

- American Chemical Society Member

Research Experience

- Virginia Commonwealth University
  Synthesis and characterization of Pt-amine-nucleobase complexes and study of their interaction with zinc finger proteins

- Christopher Newport University
  Analysis of water samples from tanks containing artifacts of the USS Monitor using Ion Chromatography in order to determine artifact stability - in partnership with the Mariner's Museum in Newport News, VA

Instrumentation and Techniques Experience

- Chemistry
  Ultraviolet-Visible Spectroscopy
  Nuclear Magnetic Resonance Spectroscopy

Fluorescence Spectroscopy
Inductively Coupled Plasma-Mass Spectrometry
Mass Spectrometry Data Analysis
Infrared Spectroscopy
Circular Dichroism Spectropolarimetry

- Biology
  MTT/WST Assay
  Cellular Uptake
  EMSA

PRESENTATIONS

- Tsotsoros, S.D.; Bate, A.B.; Farrell, N.P.; Use of platinum complexes to target zinc finger peptides. Poster Presentation at: VCU Chemistry Graduate Research Poster Session, 2013

- Tsotsoros, S.D.; Farrell, N.P.; Study of the interaction of platinum nucleobase complexes with zinc fingers. Poster Presentation at: VCU Chemistry Graduate Research Poster Session, 2012

- Tsotsoros, S.D.; Bayse, C.A.; Farrell, N.P.; Study of the interaction of platinum N-heterocycle and nucleobase complexes with biomolecules. Poster presentation at: SER-MACS 2011, Richmond, VA

- Tsotsoros, S.D.; Farrell, N.P.; Study of the interaction of platinum nucleobase complexes with biomolecules. Poster Presentation at: VCU Chemistry Graduate Research Poster Session, 2011

- Tsotsoros, S.D.; de Paula, Q.A.; Bate, A.A.; Bayse, C.A.; Farrell, N.P.; Complexes of substituted nucleobases and N-heterocycles. Poster presentation at: VCU Chemistry Graduate Research Poster Session, 2010

- Tsotsoros, S.D.; de Paula, Q.A.; Bate, A.A.; Bayse, C.A.; Farrell, N.P.; Complexes of substituted nucleobases and N-heterocycles. Poster presentation at: Gordon Research Conference, Metals in Medicine 2010, Andover, NH

PUBLICATIONS

- Tsotsoros, S.D.; Bate, A.B.; Dows, M.G.; Spell, S.R.; Bayse, C.A.; Farrell, N.P.; Mod-

ulation of the stacking interaction of MN4 (M= Pt, Pd, Au) complexes with tryptophan through N-heterocyclic ligands. J. Inorg. Biochem., 2014, 132, 2-5.

• Mangrum, J.B.; Zgani, I.; Tsotsoros, S.D.; Qu, Y.; Farrell, N.P.; Zinc finger peptide cleavage by a dinuclear platinum compound. Chem. Comm., 2013, 49, 6986-6988

• Spell, S.R.; Tsotsoros, S.D.; Farrell, N.P.; Metallated DNA-protein crosslinks as probes for zinc finger reactivity. In Encyclopedia of Metalloproteins; Kretsinger, R.H.; Permyakov, E.A.; Uversky, V.N., Eds., Springer Science and Business Media, LLC, 2013. (Spell, S.R. and Tsotsoros, S.D. contributed equally)

• de Paula, Q.A.; Tsotsoros, S.D.; Qu, Y.; Bayse, C.A.; Farrell, N.P.; Platinum-nucleobase PtN4 complexes as chemotypes for selective peptide reactions with biomolecules. Inorg. Chim. Act., 2012, 393, 222-229.

Publications In Progress

• Tsotsoros, S.D.; Farrell, N.P.; Investigation of the reaction of cDDP and tDDP with the C-terminal ZF of HIV1 NCp7. To be Submitted to J. Inorg. Biochem.

• Tsotsoros, S.D.; Daniel, A.G.; Peterson, E.J.; Bayse, C.A.; Farrell, N.P.; Modification of the $[Pt(dien)L]^{2+}$ coordination sphere to develop inhibitors of HIV1 NCp7. To be Submitted to J. Med. Chem.

• Tsotsoros, S.D.; Farrell, N.P.; A New Strategy in the Development of Antiviral Agents: Use of Platinum Complexes to Target Zinc Finger Proteins. To be Submitted to Accts. Chem. Res.

• Spell, S.R.; Tsotsoros, S.D.; Mangrum, J.B.; Peterson, E.J.; Fabris, D.L.; Farrell, N.P. A new class of HIV nucleocapsid protein (NCp7)-nucleic acid antagonists. To be Submitted to J. Inorg. Biochem.

Teaching Experience

• Virginia Commonwealth University, Richmond, VA
    General Chemistry Lab, Teaching Assistant, 2009-2010
        -Responsible for proctoring exams and grading quizzes and lab reports following grading key
        -Supervised students during lab period to ensure safety and successful completion of assignments
    Organic Chemistry Lab, Teaching Assistant, 2010-2013
        -Responsible for proctoring exams

-Wrote and graded quizzes, wrote key and graded lab reports

-Supervised students during lab period to ensure safety and successful completion of assignments

- College of William and Mary Summer Program for Gifted Children
  Teacher's Assistant, Summer 2005
  -Responsible for supervising students
  -Assisted with interactive experiments to ensure student success and safety

WORK EXPERIENCE

- United States Attorney's Office, Newport News, VA - Receptionist/Clerk, 2006-2009
  -Cleared an extensive background check and received Top Secret Security Clearance
  -Prepared subpoenas, filed important documents at the courthouse, closed cases and completed other -clerical duties to assist attorneys and legal staff
  -Processed expert witness contracts